Journal of Asian Earth Sciences: X 3 (2020) 100026

Contents lists available at ScienceDirect

Journal of Asian Earth Sciences: X

journal homepage: www.journals.elsevier.com/journal-of-asian-earth-sciences-x

Cambrian-Eocene pre-rift, pulsed rift, passive margin and emplacement processes along the northern margin of the Southern Neotethys: Evidence from the Antalya Complex in the Alanya Window (S Turkey)

Alastair H.F. Robertson[a,*], Osman Parlak[b,c], Tim C. Kinnaird[d], Kemal Taslı[e], Paulian Dumitrica[f]

[a] School of GeoSciences, University of Edinburgh, EH93JW Edinburgh, UK
[b] Çukurova Üniversitesi, Jeoloji Mühendisliği Bölümü, 01330 Balcalı, Adana, Turkey
[c] State Key Laboratory of Geological Processes and Mineral Resources, Center for Global Tectonics, School of Earth Sciences, China University of Geosciences, Wuhan 430074, China
[d] School of Earth and Environmental Sciences, University of St. Andrews, St Andrews, UK
[e] Mersin Üniversitesi, Jeoloji Mühendisliği Bölümü, Mersin, Turkey
[f] Dennigkofenweg 33, CH-3037 Guemligen, Switzerland

ARTICLE INFO

Keywords:
Antalya Complex
Alanya Window
Rifting
E Mediterranean
S Turkey
S Neotethys

ABSTRACT

Sedimentary rocks in the Alanya Window document pulsed Permian-Triassic rifting in a proximal basin setting, adjacent to the Tauride continental unit (Geyik Dağ). Late Cambrian-Early Ordovician clastic sediments accumulated along the north margin of Gondwana on a variable shallow-marine shelf. Above an unconformity related to rift-shoulder uplift, Late Permian facies document shallow-marine to evaporitic environments during regional tectonic subsidence (first main rift pulse). Above a second unconformity (both extension and sea-level controlled), Early Triassic carbonates and mudrocks accumulated on an unstable, gently subsiding shelf. Mudrocks, sandstones and lithoclastic debris-flows, derived from the underlying succession, accumulated during the Middle Triassic (Anisian-early Ladinian), implying strong tectonic subsidence and flank uplift (second main rift pulse). Radiolarian mudstones accumulated during late Middle Triassic-early Late Triassic in a well-oxidised, organically productive, but relatively quiescent, deep-water basin above the carbonate compensation depth (CCD). Thick (100s m) lithoclastic sandstone turbidites (commonly plant-rich) and localised debris-flows accumulated during the Late Triassic (Carnian), together with detached blocks of underlying lithologies (third main rift pulse), combined with regional uplift. Alkaline basaltic sills were intruded locally. Final continental break-up to create the Southern Neotethys took place regionally during the Late Triassic (Carnian). Latest Triassic-Late Cretaceous deposition records passive margin subsidence. Variable low-grade metamorphism and two-stage tectonic emplacement (southwards(?) then northwards) took place during latest Cretaceous and Eocene, respectively. The tectonic-sedimentary development of the Antalya Complex provides insights into rift/continental break-up processes that differ from the recently well-documented Alpine-North Atlantic region.

1. Introduction

Rifting and break-up of continents to form ocean basins is one of the most important processes on Earth and continues to be actively studied, especially the role of regional lithosphere extension versus magmatism (Şengör and Burke, 1978; Huismans et al., 2001; Buck, 2007). However, modern-day examples of continental rifting (unrelated to subduction) are sparse, with the Red Sea-Gulf of Aden being the best example (Cochran, 2005). Rift products are commonly very deeply buried beneath continental margins, as around the Atlantic Ocean. Well-documented magma-poor rifts, notably the Newfoundland-Iberia transect as studied by deep-sea drilling (e.g. Péron-Pinvidic and Manatschal, 2008), differ from magma-rich rifts such the East Greenland-Faroes transect (Reston and Manatschal, 2011), and variants exist (Franke, 2013). The processes of final continental break-up in the Red Sea are debatable, whether by mainly volcanic or non-volcanic processes (Stern and Johnson, 2018 vs. Stockli and Bosworth, 2019).

Studies of rifted margins on land provide useful insights. Notably, the rifted margins of the Alpine Tethys document non-volcanic rifting on all scales (Mohn et al., 2010). However, the rifted margins of the eastern Tethys appear to differ significantly from those of the western Tethys. In the eastern Mediterranean land outcrops there is little

* Corresponding author.
E-mail address: Alastair.Robertson@ed.ac.uk (A.H.F. Robertson).

https://doi.org/10.1016/j.jaesx.2020.100026
Received 23 October 2019; Received in revised form 27 January 2020; Accepted 15 February 2020
Available online 24 February 2020

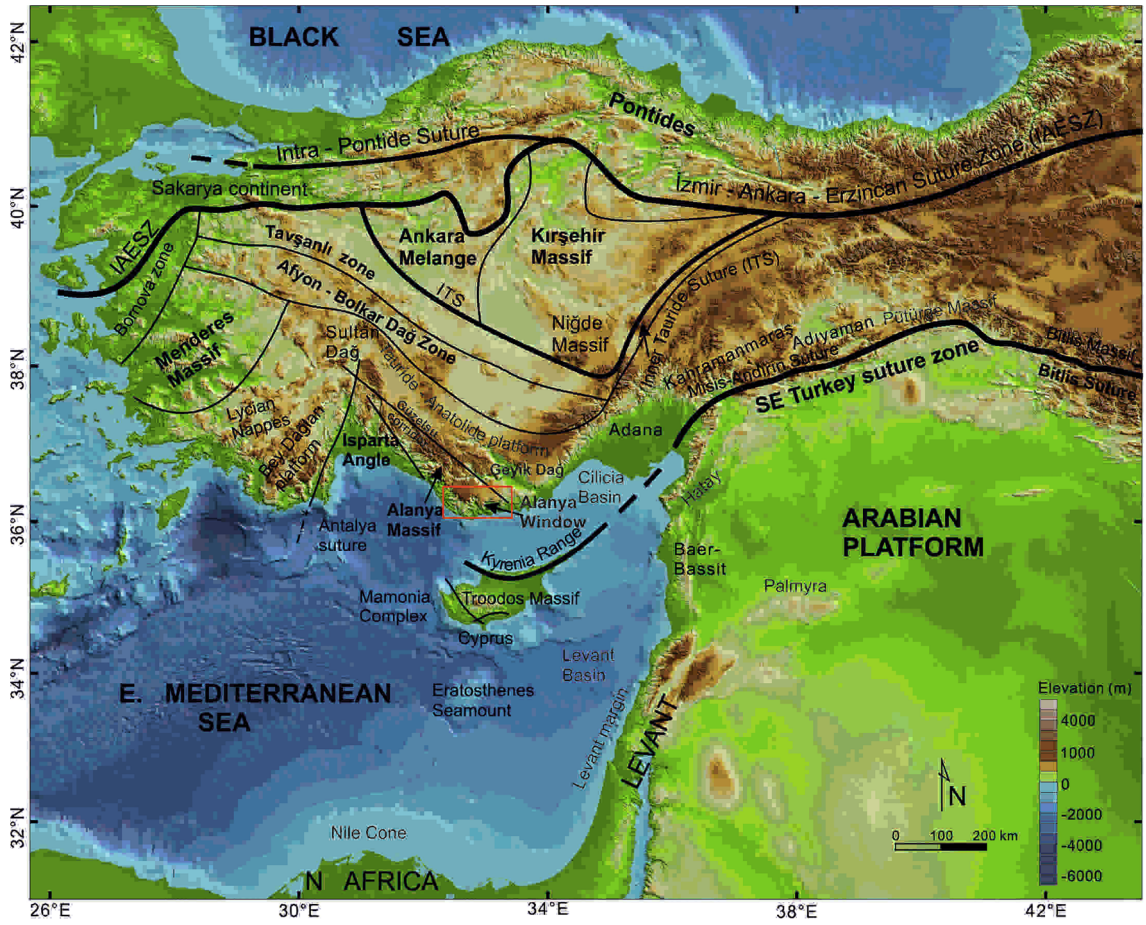

Fig. 1. Outline tectonic map of Turkey showing the location of the study area (red box) in relation to the major tectonic units of Turkey and Cyprus. Main data source MTA (2000); modified from Chen and Robertson (2020). Note the location of the Isparta Angle around which the Antalya Complex, discussed here, is exposed.

evidence of lithospheric-scale extensional detachment faulting or exhumation of sub-continental mantle lithosphere related to hyper-extension during continental break-up. In contrast, alkaline basaltic volcanism related to advanced rifting and continental breakup is relatively thick (hundreds of metres) and widespread, suggesting a comparison with plume-influenced volcanic-rifted margins (Robertson, 2007).

Here, we discuss a key area near to the northern coast of the easternmost Mediterranean Sea that provides insights into fundamental processes shaping the northern margin of the Southern Neotethys. We focus on the sedimentary and structural geology of the Antalya Complex, as exposed in the Alanya Window (Fig. 1). Rift-related successions making up the Antalya Complex were subsequently overthrusted by metamorphic rocks of the Alanya Massif.

The Alanya Window is exposed for c. 120 km NW–SE by up to 40 km NE–SW, between Gazipaşa (Antalya area) and Anamur (Mersin area) (Figs. 2 and 3).

Many authors have concluded that rifting and continental break-up to form the Southern Neotethys took place during the Permian-Triassic to form oceanic lithosphere, although opinions vary on the exact timing and tectonic processes (Garfunkel, 1998, 2004; Robertson, 2000; Stampli and Borel, 2002). Recent evidence from the Levant Basin, adjacent to the Levant continental margin (Fig. 1) suggests that its basement comprises deeply submerged continental crust (Gardosh and Druckman, 2006; Gardosh et al., 2010) and it is argued that the Southern Neotethys opened during the Cretaceous (Segev et al., 2018). However, this is debatable because the Southern Neotethys almost entirely subducted, leaving only fragments beneath the deep-marine Levant Basin in the south, and also emplaced on land along the northern margin of the Southern Neotethys, especially supra-subduction zone ophiolitic rocks (Robertson, 2002; Bağcı et al., 2008; Parlak et al., 2009) and also rift-related sediments and volcanics. The most extensive of these emplaced crustal fragments is the Antalya Complex (also known as the Antalya Nappes).

2. Previous research

During the 1970s–1980s there was much discussion of the Palaeozoic-Mesozoic Antalya Complex in the Isparta Angle of southwest Turkey (Figs. 1–3). For some, these units represented a sub-horizontal stack of thrust sheets known as the Antalya Nappes (Lefèvre, 1967, Brunn et al., 1970, 1971; Brunn, 1974) that were derived from an ocean basin and its margins to the north of the Mesozoic Tauride carbonate platform, known as the Bey Dağları in the west and the Geyik Dağ in the east (Ricou et al., 1984; Marcoux et al., 1989). For others, the Antalya Complex was viewed as a composite lithological assemblages that originated in a more southerly position, adjacent to the southern margin of the Tauride carbonate platform (Dumont et al., 1972; Woodcock and Robertson, 1977, 1982; Poisson, 1977; Monod, 1976, 1977; Delaune-Mayère et al., 1977; Şengör and Yılmaz, 1981; Hayward and Robertson, 1982). More information became available from regional mapping by MTA (Maden Tektik ve Arama) around the Isparta Angle (Şenel et al., 1992, 1996, 1998, 1999). Eventually the debate was largely if not completely resolved in favour of a southerly origin for the Antalya allochthon (Poisson et al., 2003; Vrielynck et al., 2003; Robertson et al., 2003; Stampli and Borel, 2002). Recent research has focused on basic volcanic rocks (Maury et al., 2008; Varol et al., 2007), the biostratigraphy of radiolarites and related deep-sea sediments and the biostratigraphy of Permian carbonate rocks (Tekin,

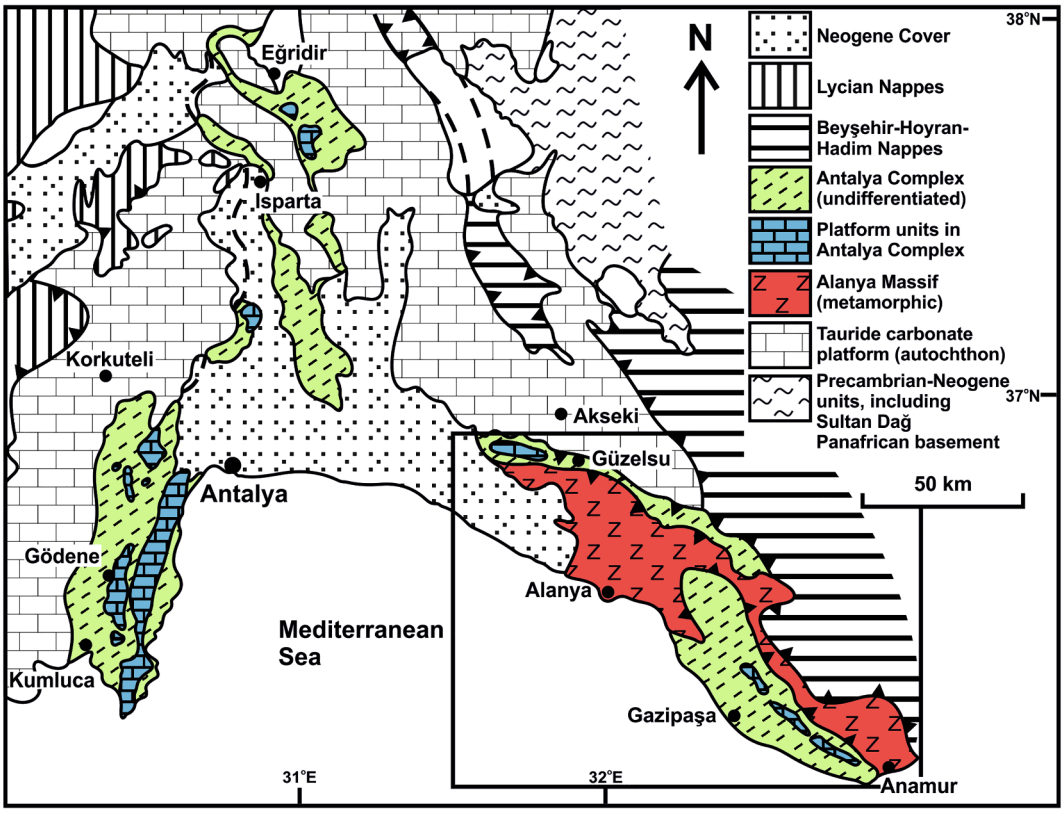

Fig. 2. Outline tectonic map of SW Turkey showing the outcrops of the Antalya Complex in relation to other major tectonic units in the region, based on Robertson and Woodcock (1984) and MTA (2000). The Antalya Complex is exposed in the east (Gazipaşa-Anamur area), within the large Alanya tectonic window through the metamorphic Alanya Massif.

1999; Tekin, 2002a, b, Moix et al., 2009; Tekin and Sönmez, 2010; Şahin et al., 2014; Şahin and Altıner, 2019). The regional palaeogeography is now better known, allowing comparisons and synthesis (Robertson et al., 2012; Barrier et al., 2018).

A large part of the Alanya Window was mapped at 1:25,000-scale by MTA during the late 1970s-early 1980s (Ulu, 1983), specifically map sheets P28-b2, P29-a1, P28-b4, P28-b3 & P29-a2), northeast of Gazipaşa. The results were later incorporated into the 1:500,000 geological map of Turkey (Konya sheet) (MTA, 2000), with some revisions (see also Şenel et al., 2016). An overall stratigraphy was first attempted by Ulu (1983, 1988) although this has since been strongly modified. An intact succession of Ordovician age was inferred, dominated by siliciclastic sediments (Çakmak Formation), based on the identification of conodonts: i.e. *Drepanoistodus forceps*, *Drepanodus homocurvatus*, *D. subrectus*, *Oistodus forceps* and *O. lanceolatus*. In one main area (e.g. 30 km NE of Gazipaşa; SE of Area C in Fig. 3), the succession was reported to pass, with apparent discordance, into a mixed siliciclastic succession of Early Devonian age (Narlıca Formation). This was dated based on the occurrence of the conodonts: *Icriodus brevis*, *I. woschmidti*, sp. and *Spathognathodus* (sp.) *steinhornensis eosteinhornensis*. This outcrop has since been re-mapped as a klippen of the Hadim Nappe which mainly crops out farther northeast (MTA, 2000). The existence of an Early Devonian transgressive succession has been confirmed in the Antalya Complex within the eastern limb of the Isparta Angle (i.e.Tahtalıdağ thrust sheet-Kavzan, Ovacık and Gündoğmuş sections (Göncüoğlu and Kozur, 2000a; see Şenel et al., 1992). Our recent fieldwork (in the type, Narlıca area) has revealed typical Late Triassic lithoclastic sandstone turbidites, overthrust by grey-green shales with lenticular up to thick-bedded micaceous sandstones (mapped as Devonian), in turn unconformably overlain by nodular Permian limestones.

Neritic carbonates of Late Permian age (Bıçkıcı Formation) were mainly dated by Ulu (1983, 1988) using a rich assemblage of large foraminifera, including *Paraglobivalvulina mira*, *Globivalvulina greace*, *G. vonderschmitti* and *Paradagmarita flabelliformis*. The overlying Early Triassic was determined mainly based on foraminifera including *Cyclogyra mahajeri*, whereas the Late Triassic (Carnian-Norian) was dated based on foraminifera including *Reophax* sp., *Ammobaculites* sp., *Trochammina* sp., *Meandrospira* sp., *Planiinvoluta* sp., *Opththalmidium* sp., *Galeonella* sp., *Triasina* sp., *Miliolipora* sp., *Endothyra* sp., *Earlandia* sp., *Duostomina* sp., *Variostoma* sp. and *Involutina* sp. The pelagic bivalve, *Halobia* sp. occurs towards the top of the succession.

Ulu (1983, 1988) reported that the Triassic succession is unconformably overlain by a heterogeneous succession of sandstones, shale, cherty limestone and debris-flow deposits, together with detached blocks of neritic limestone, radiolarite and pelagic limestone (Karaçukur Formation; e.g. near Karaçukur village in Area B and Beldibi Kayası in Area A; Figs. 3–5). This unit formed during the Late Cretaceous based on the occurrence of microfossils including *Globotruncana* sp. Blocks and pebbles of reef limestone were dated as Carnian-Norian based on the large foraminifera *Galeonella* sp., *Miliolipora* sp., *Opthtalmidium* sp., *Planiinvoluta* sp., *Endothyra* sp., *Reophax* sp., *Trochammina* sp., *Ammobaculites* sp., and *Duostominidae*. Pelagic limestones of Late Cretaceous age include the planktic foraminifera: *Globotruncana tricarinata* and *Globotruncana fornicata*, together with *Cuneolina* sp., *Siderolites* sp. and rudist fragments.

In addition to geological mapping, Ulu (1988) presented three N-S cross-sections, rose diagrams and stereonets to illustrate the structure of the Alanya Window. The bedding in the Ordovician is mainly E-W, extending more to c. NW-SE in the Late Permian, to again c. E-W in the Triassic, but c. NW-SE in younger units. Several km-scale anticloria, with rounded fold hinges, were mapped, for example in the Ordovician, based on changes in bedding orientation. Two main phases of deformation were inferred, the first c. E-W (e.g. trend 70°) and second more N-S (e.g. trend 15°) both within Ordovician lithologies. Mainly

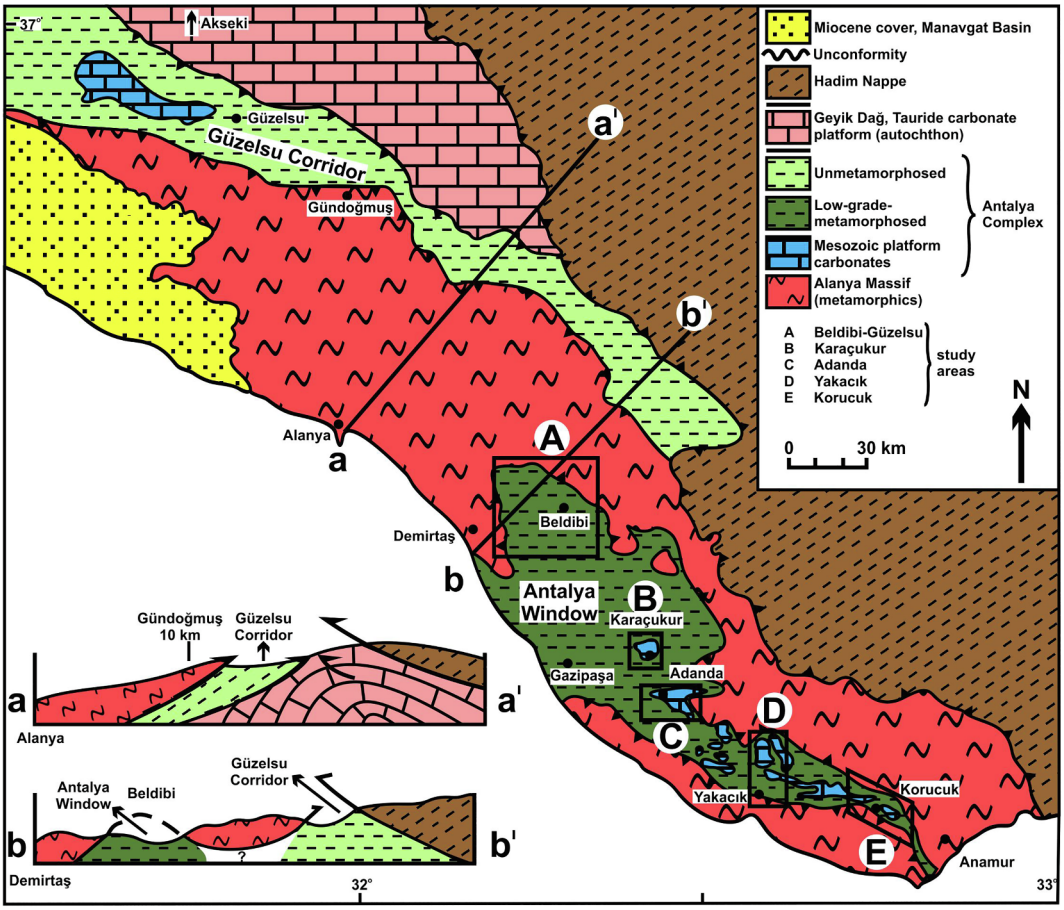

Fig. 3. Outline tectonic map of the southeastern segment of the Isparta Angle (see Fig. 2) showing the relationship of the Antalya Complex in the Alanya Window to other units including the overlying metamorphic Alanya Massif and an additional, outcrop of the Antalya Complex farther northwest and north (Güzelsu area). Inset: simplified cross-sections (assuming the preferred emplacement directions). Also shown are the present study areas within the Alanya Window. A. Beldibi-Gaziapaşa area; B. Karaçukur area; C. Adanda area; D. Yakacık area; E. Korucuk area. Main data sources: Özgül (1984b), Ulu (1983, 1988), MTA (2000).

northerly directions were recorded in the Late Permian (336° and 23°E), suggesting considerable structural variation both aerially and stratigraphically. Overall, bedding dips generally northwards, with common south-verging thrusts and both south and north-verging folds.

A well exposed (and easily accessible) area in the northwest (Beldibi area), mainly within map sheets P28-b1, P28-b4, P28-a2 and P28-a3, was mapped by Özgül (1984b). The lowermost siliciclastic succession, termed the Lordlar Formation, was constrained as Late Cambrian-Early Ordovician and an unconformity was recognised between this and an overlying Late Permian shallow-water succession, termed the Lordlar Formation. The Triassic (Sapadere Formation) unconformably overlies the Late Permian. A tectonic contact was reported between the top of the Triassic succession and an overlying Jurassic-Cretaceous succession (İnasar Formation). The olistostromal Karaçukur Formation described by Ulu (1983, 1988), although much reduced in the NE (Beldibi) area, was treated as an intact succession of latest Triassic and mainly Jurassic age. A late Cretaceous olistostrome was reported from the highest levels of the succession in Area A. Our mainly sedimentological and biostratigraphical results largely confirm the stratigraphy of Özgül (1984b), which is utilised here in slightly modified form (Fig. 6).

More recently, X-ray mineralogy was published for both whole-rock and clay fractions, together with determinations of crystallinity, illite and chlorite polytypes for shales from the Palaeozoic and Triassic successions in two areas in the Alanya Window, namely the northern part of the outcrop (Demirtaş-Alanya) and a more southerly part (Gazipaşa) (Bozkaya and Yalçın, 2005).

This is the first synthesis of the Antalya Complex in the Alanya Window.

3. Methods

The Antalya Complex in the Alanya Window was studied during four field visits (2015–2019) (Robertson et al., 2019). Our main study area was in the northeast of the window (Beldibi-Gazipaşa; Area A in Fig. 3). Places mentioned in the text are indicated on an outline topographic map (Fig. 4). An outline geological map of Area A is given in Fig. 5. Locally intact sections were measured and samples of neritic and pelagic limestone were dated, mainly using benthic and planktic foraminifera; some radiolarian cherts were also dated. The sedimentary lithologies were studied petrographically to help determine provenance. In addition, samples of rare intrusive microgabbro-diabase were chemically analysed to determine the tectonic setting of magmatism. Outcrop-scale structures were also studied, mainly in Area A in the northwest. For comparison, reconnaissance was carried out in four areas farther southeast, extending to near Anamur (Areas B-E in Fig. 3).

4. Results: Sedimentary successions

The NW part of the Alanya Window (Area A, Beldibi-Gazipaşa) is divisible into three tectonic units separated by thrust faults and, or high-angle faults. The first (lower) tectonic unit of Late Cambrian-Late Triassic age dominates the area and is itself structurally imbricated (e.g. c. E-W thrust south of Beslengiler and south of Lordlar) (Figs. 4 and 5). The second, intermediate, tectonic unit extends in age from Late Permian-Late Triassic. The lower and intermediate units are separated by a low-angle thrust which is well exposed on both sides of a N-S trending valley (east and west of both Lordlar and Kıllı) (Figs. 4 and 5). Farther

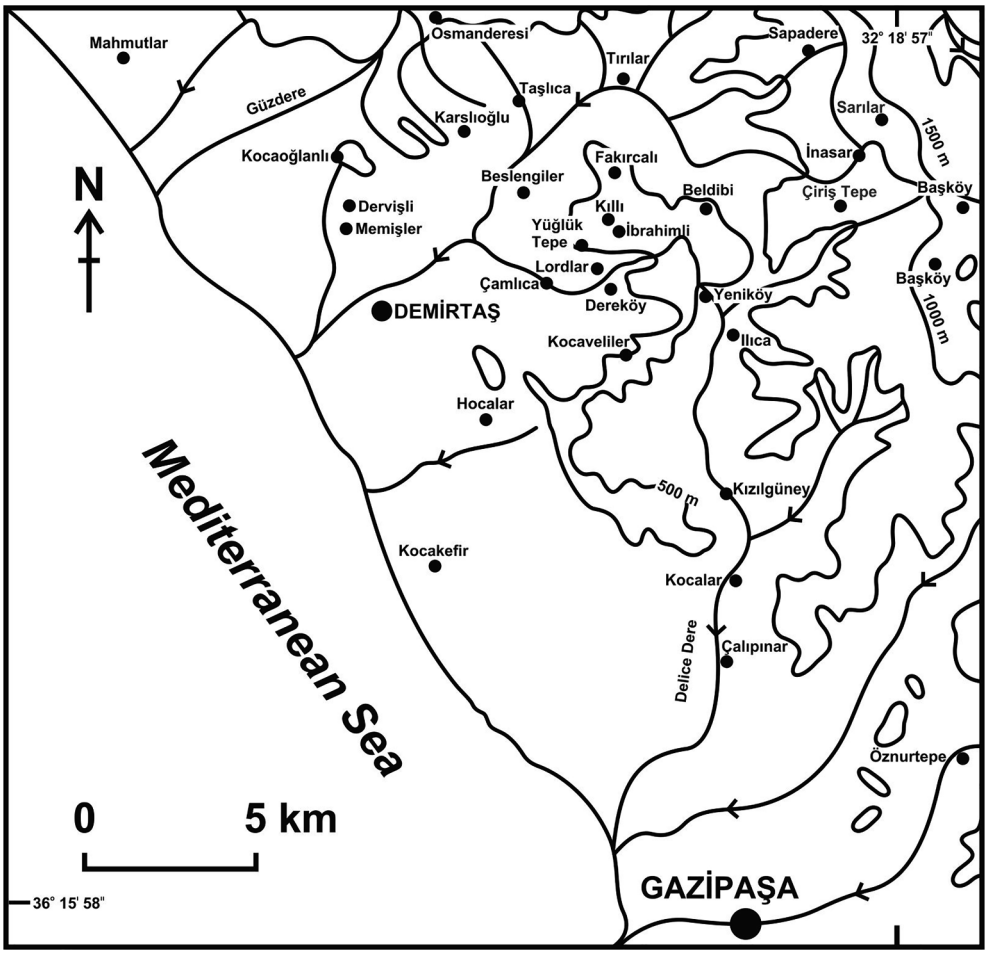

Fig. 4. Outline geographical map of the main study area in the north of the Alanya Window, showing the main places mentioned in the text. This area has a hilly landscape, deeply dissected by alluvium-floored valleys. Detailed geological correlation of units across valleys is difficult. Base map from Özgül (1984b). See Fig. 5 for outline geological map of the area.

south, this thrust contact is obscured by c. E-W or c. N-S faults or is not well exposed. The third tectonic unit occurs farther north-east (east of Beldibi) and comprises a dismembered succession of latest Triassic-Late Cretaceous age, together with broken formation and tectonic melange. This unit is separated from the intermediate unit by a poorly exposed tectonic contact.

Although internally faulted and folded, the three tectonic units in the northwest (Area A) can be restored as originally intact successions. The successions exposed in the two lower tectonic units do not differ significantly and so are described together (Fig. 6). In contrast, two different local successions are recognised in the upper tectonic unit here (İnasar Dere and Beldibi Kayası; Fig. 6).

We also take account of kilometre-scale outcrops of thick-bedded shallow-water-derived carbonate rocks of Jurassic-Cretaceous age that crop out extensively in the centre and southeast of the window (Areas B-E; Fig. 3).

4.1. Late Cambrian-Early Ordovician

The oldest confirmed rocks in Area A in the northwest (Figs. 5 and 7a) are sandstones, siltstones, shale and volumetrically subordinate nodular limestones (up to c. 150 m thick in total) of Late Cambrian-Early Ordovician age (Lordlar Formation; Fig. 6). The dating is based on trilobites, conodonts and brachiopods that mostly occur within pinkish nodular limestones. Key fossils are the conodonts *Furnishina furnishi* and *Onetodus* sp. of Late Cambrian age, and also *Scolopodus (a conodont)* and *Phycodes circinatum* (a trace fossil) of inferred Early Ordovician age (Özgül, 1984b). Late Cambrian and latest Cambrian-Early Ordovician (Early Tremadocian) conodonts include *Furnishina* sp., *F. furnishi, Phakelodus tenuis, P. terachimai and Gordylodus lindstromi* (Göncüoğlu and Kozur, 2000b). Elsewhere, Middle Cambrian conodonts have been identified from the Tahtalıdağ unit of the Antalya Complex along the western limb of the Isparta Angle (near Kemer) (Şenel et al., 2000). During this work, the presence of trilobite trace fossils and brachiopod shell fragments aided recognition of several of the Early Palaeozoic sections.

The Late Cambrian-Early Ordovician succession, as exposed in both the lower and intermediate tectono-stratigraphical units in Area A, is dominated by sandstone and shale, as observed in the type section, 300 m SW of Lordlar village (Figs. 4, 5, and 8a-1); also near Kocaoğlanlı (Figs. 4 and 8a-2) and NW of Yeniköy (Figs. 4, 7b, 8a-3). Neritic limestones of Cambrian-Ordovician age also occur locally as tectonic blocks (up to c. 100 m in size) (e.g. 1.5 km SW of Yeniköy) (Figs. 4, 5, 7d).

Most of the sandstones are regularly bedded and medium to thick-bedded, commonly with normal grading and shaly partings (Fig. 7f). The soles of some individual sandstone beds have well-developed flute casts (Fig. 7e). The upper part of the succession includes highly fossiliferous, reddish or pinkish-coloured micritic limestones, including microbial (stromatolitic) limestones, typically in depositional units up to several metres thick (Figs. 8a-1, 8a-2, 9a). In thin section, the Cambrian-Ordovician sandstones are quartzarenites, with relatively well-sorted, rounded to sub-angular grains, commonly with quartz overgrowths (Fig. 9b). In addition to quartz, muscovite and feldspar are common, together with grains of zircon and opaque minerals (e.g.

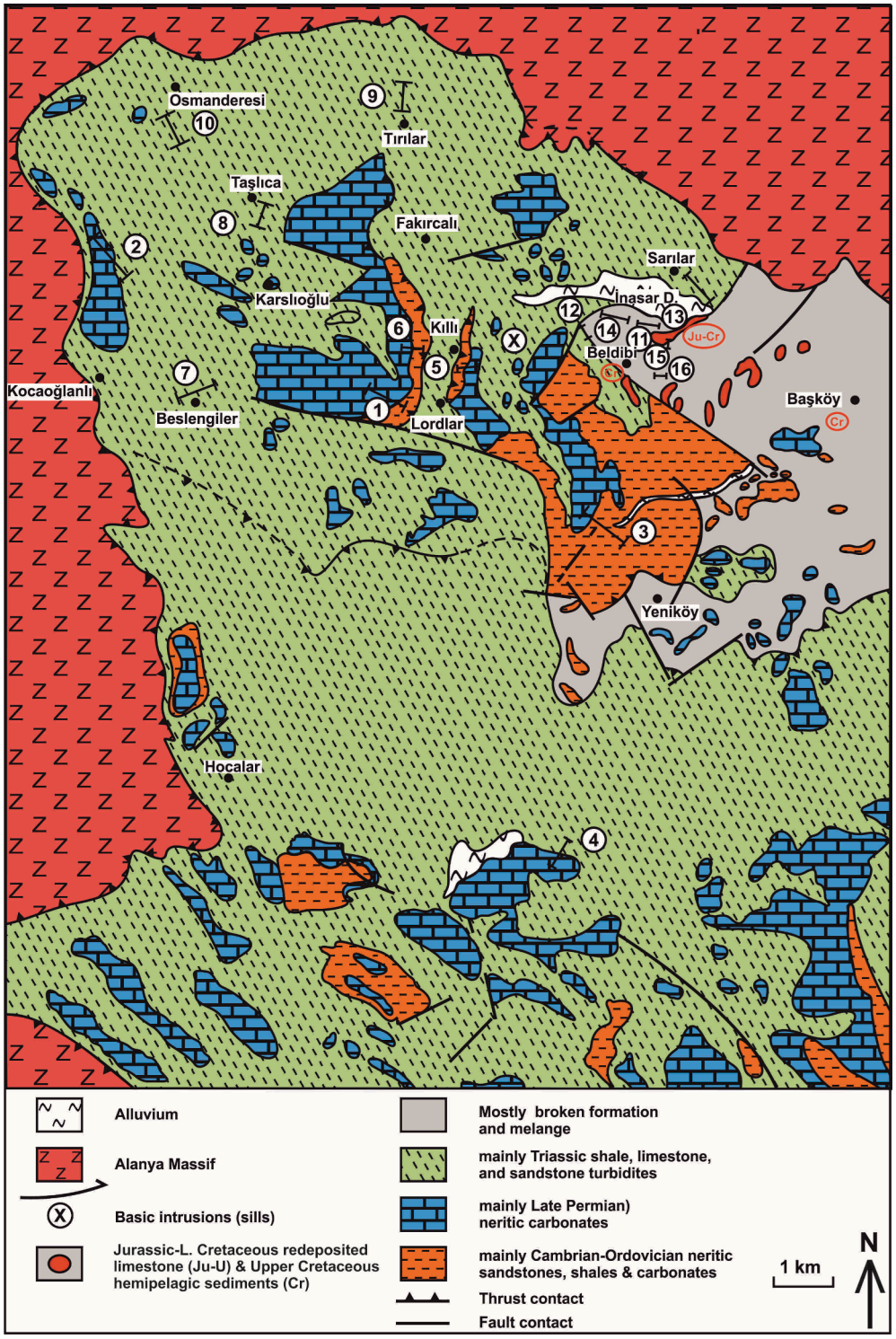

Fig. 5. Outline geological map of the best exposed outcrop of the Antalya Complex in the NW (Area A, Belbidi-Gazipaşa in Fig. 3), modified from Özgül (1984b), Ulu (1983, 1988), MTA (2000) and this study. The locations of logged successions are indicated. See text for explanation.

magnetite). Where the succession is strongly dismembered, Early Palaeozoic sandstones can be distinguished from Late Triassic sandstones, mainly based on their slightly paler colour, common muscovite (Fig. 9c) and well-sorted texture, commonly with well-rounded grains (Fig. 9d).

4.2. Late Permian

No base is exposed to the Permian succession in many outcrops (e.g. Delice Dere area; Fig. 8b-4). However, in places the Ordovician succession ends with a prominent low-angle unconformity (c. 15°) (e.g. İbrahimli (Kıllı)) (Fig. 8b-5; 7g), followed by the Late Permian succession (Yüğlük Tepe Formation; Fig. 6). Where locally well-exposed (e.g. near İbrahimli (Kıllı)) (Figs. 4, 8b-5, 7g), a lenticular basal conglomerate is developed above the unconformity surface (Fig. 7h). Neptunian fissures, infilled with rhombic dolomite crystals, penetrate downwards into the uppermost Ordovician sandstones beneath.

The Late Permian, which is up to 600 m thick, is dominated by shallow-water carbonates, some of which are dolomitic. The succession

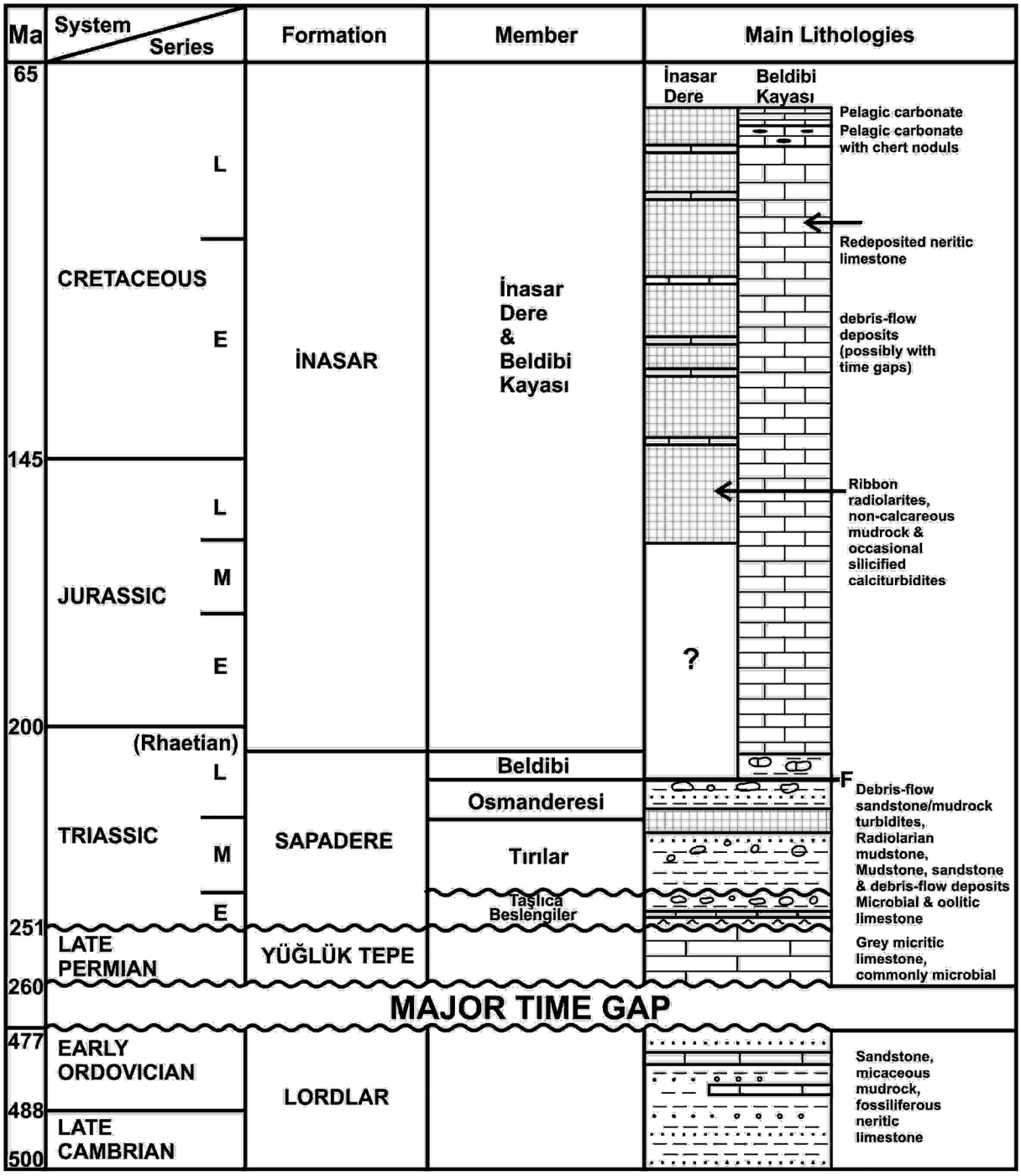

Fig. 6. Stratigraphy and lithological summary of the successions of the Antalya Complex exposed in the northern part of the Alanya Window (Area A, Belbidi in Fig. 3). Based on Özgül (1984b), with modification of the Jurassic-Cretaceous stratigraphy (see text).

is well-dated in Area A (Beldibi-Gazipaşa), mainly based on calcareous algae, benthic foraminifera and gastropods. Large foraminifera include: *Hemigordius* cf. *reicheli*, *Hemigordius* aff. *perimicus*, *Lunucammina post-carbonica*, *Eotuberitina reitlingezee*, *Dagmarita chanakchiensis*, *Paradagmarita monodi*, *Globivalvulina vondershmitti*, *Paraglobivalvulina gracilis*, *Paraglobivalvulina* sp., *Agathammina pusilla*, *Frondina permica*, *Lunucammina reporta*, *Pachypholia ovata*, and *Pachyphloia* sp.. In addition, calcareous algae include *Mizzia velebitana*, *Gymnocodium bellerophontis* and *Permocalculus* sp. (D. Altıner; in Özgül, 1984b) (Fig. 10a–e).

The Late Permian shows considerable local facies variation. Microbial (stromatolitic) carbonates, mostly biomicrite, and lenticular carbonate conglomerates (Fig. 7i) are abundant, for example in the İbrahimli (Kıllı) area (Fig. 8b-5). Elsewhere, neritic limestones alternate with fine-grained, very hard-weathering quartzose sandstones (quartzarenite) and shales, as seen at Lordlar (Fig. 8a-1) and Kocaoğlanlı (Fig. 8a-2). In thin section, the sandstones are dominated by angular to subrounded quartz grains (Fig. 9e). The neritic limestones are highly fossiliferous, with abundant mainly fragmented gastropods, bivalves and echinoderms (Fig. 7j, k; 9f-g).

4.3. Early-Middle Triassic

Above the Late Permian succession, the base of the Triassic

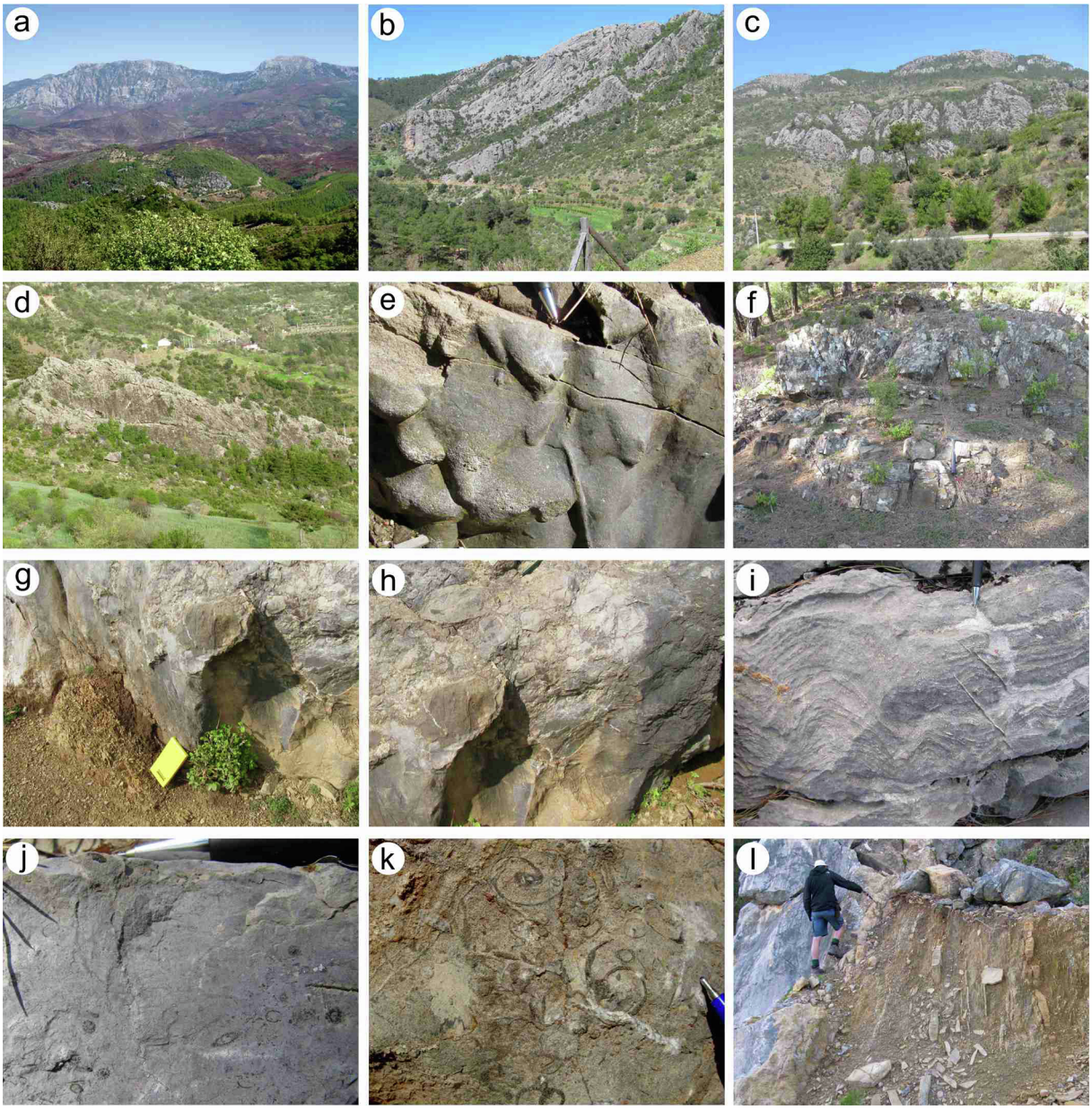

Fig. 7. Field photographs of lithologies in the southern (Gazipaşa) area (Late Cambrian-Early Triassic). **a,** View across the NW part of the main study area (Area A, Beldibi) showing the over-riding metamorphic Alanya Massif (escarpment in the distance); **b,** View NW from near Yeniköy across Early Ordovician sandstones (poorly exposed) to well-stratified Permian limestones, with Triassic above (forested area; upper left); **c.** En echelon, lenticular blocks of Palaeozoic limestone (grey), interspersed with Late Triassic sandstone turbidites (telegraph pole on left for scale); near Dereköy, SW part of Area A; **d,** Broken formation including Early Palaeozoic facies in a matrix of sheared and disrupted siliciclastic sediments; 1.5 km SW of Yeniköy (houses behind for scale); **e,** Large flute casts in Ordovician sandstone, near Kocaoğlanı, western edge of our main study area (Area A, Beldibi-Gazipaşa) (pen top for scale); **f,** Thick-bedded Ordovician sandstone with shaly partings (rarely well exposed), near Lordlar (hammer for scale); **g,** Steeply-dipping unconformable contact between Ordovician siliciclastic sediments and Late Permian limestone; near Ibrahimli, c.1 km NW of Lordlar (notebook for scale); **h,** Breccia-conglomerate at base of the Permian succession; detail of g (pen for scale); **i,** Wavy microbial lamination in Late Permian stromatolitic limestone, Kırıntı Tepe; c. 1 km NW of Kocaoğlanlı (pen for scale); **j,** Typical fossiliferous Late Permian limestone; 1 km west of İbrahamli (Kıllı), NW part of Area A (Beldibi-Gazipaşa) (pen for scale); **k,** Gastropod-rich Late Permian limestone, location as j (pen top for scale); **l,** Spectacular unconformity between steeply-dipping Late Permian limestone (left) and Early Triassic calcareous shales and thin-bedded limestones, 0.5 km NW of Kıllı (c. 1 km N of Lordlar).

(Sapadere Formation; Fig. 6) is characterised by a prominent unconformity, without an obvious angular discordance, as well exposed west of İbrahimli (Fig. 8b-6, 11a). Elsewhere, the contact is commonly faulted (near İbrahimli; Fig. 8b-5). In places, the succession begins with a thin package (c. 15 m) of oolitic limestone and/or microbial carbonate (stromatolite), with bivalves, gastropods and small foraminifera of inferred Early Scythian age (Beslengiler Member) (Fig. 6), as well exposed in the type section (Beslengiler Mah.) (Özgül, 1984b). Sedimentary structures include symmetrical wave ripples, asymmetrical current ripples, scour structures and concentrations of bivalve debris (shell hash).

Above a locally exposed karstic surface (Özgül, 1984b), the higher levels of the succession (Taşlıca Member) (Fig. 6) are dominated by alternations of thin-bedded, fine-grained limestone (calcilutite), with subordinate bioclastic limestone (calcarenite), quartzose sandstone, calcareous shale, marl and intraformational conglomerate, in total up to c. 200 m thick (e.g. Fig. 8b-4 to 8b-6). Calcareous lithologies include abundant pelagic bivalves (e.g. *Posidonia* sp.) and gastropods

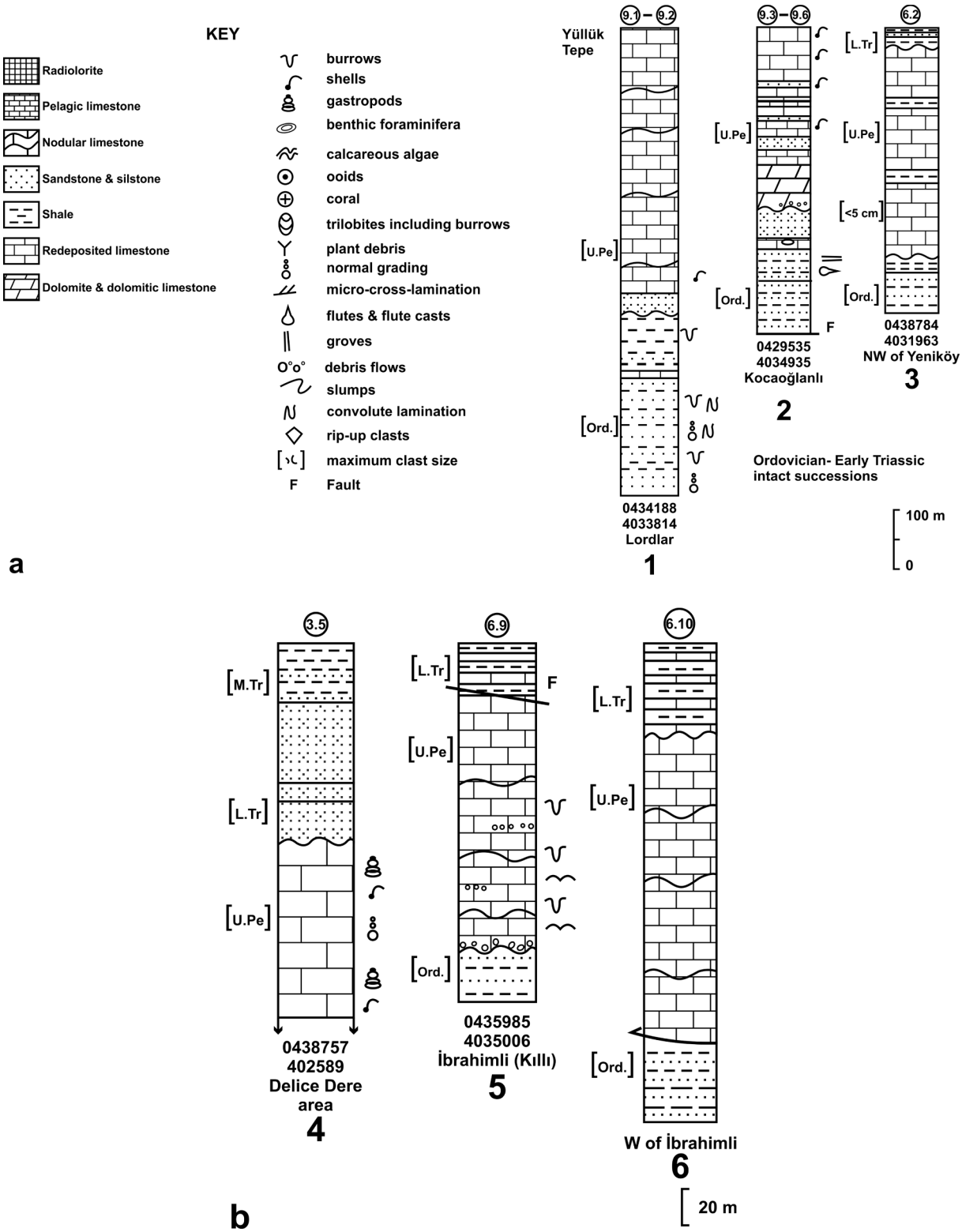

Fig. 8. Measured sedimentary logs of locally intact sections within the overall Early Ordovician-Late Cretaceous stratigraphy. The scales are appropriate to the thicknesses of the sedimentary units of different ages. **a,** 1–3 Logs of Early Ordovician-Early Triassic; **b,** 4–6 Logs of Late Permian-Early Triassic (larger scale); **c,** 7–12 Logs of Early Middle Triassic (further enlarged scale); **d,** 13–17 Logs of Early Jurassic-Late Cretaceous (further enlarged scale to highlight details). Ages in square brackets are based on lithological correlation with palaeontologically-dated exposures. GPS measurements are for domain 36S. For locations see Figs. 4 and 5. The numbers in circles are field sampling locations. GIS positioning of all sample locations is available from the authors on request.

(Fig. 9i–k), together with conodonts of Mid-Late Anisian (Middle Triassic) age (Özgül, 1984b). Shell fragments are commonly imbricated (Fig. 9i), indicating current reworking. Some intervals, for example at Delice Dere (Fig. 8b-4), are dominated by thin to medium-bedded, well-cemented white quartzarenites, with mainly sub-angular to sub-rounded quartz grains (Fig. 9h).

In some sections (e.g. Taşlıca; Fig. 8c-8), the succession passes upwards into a short interval (several tens of metres) of lenticular debris-

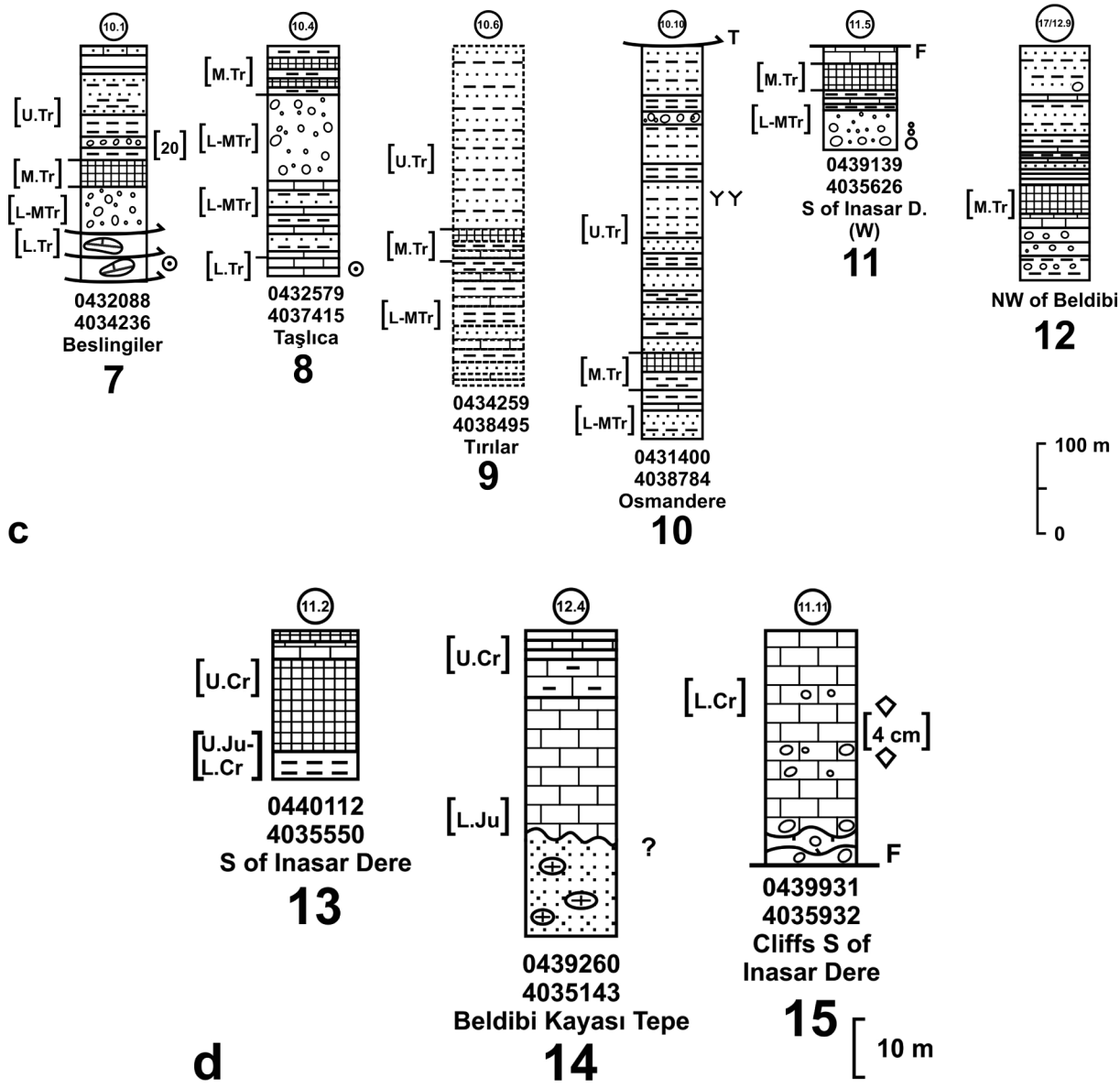

Fig. 8. (*continued*)

flow deposits that contain abundant poorly sorted clasts of Palaeozoic (Ordovician-Permian) limestone (Fig. 11b–d). Similar debris-flow deposits are exposed elsewhere in less complete sections (e.g. Beslengiler; Fig. 8c-7). Debris-flow deposits exposed north of Beldibi contain abundant detrital plagioclase, indicating a basic igneous source (Fig. 13a).

Debris-flow deposits, where present, thin and fine upwards and then pass into a distinctive unit of reddish-coloured, thinly bedded radiolarites (Figs. 9l and 11e) and radiolarian mudstones (Tırılar Member), up to c. 25 m thick (e.g. see Fig. 8c: Beslengiler, log 7; Taşlıca log. 8; Tırılar log 9; Osmandere log 10; south of İnasar Dere log. 11 & NW of Beldibi log 12). The type section near Tırılar is incomplete, whereas a deformed, overturned but more complete section is exposed farther southeast, near Sugözu (MTA topographic map Alanya P28-b2 E 30659 N 49070) (Tekin, 1999). Two local sections with overlapping radiolarian assemblages have been correlated there to infer a single succession, based on rich radiolarian assemblages that include *Mueller-itortis cochleata* and *Tritortis kretaensis* of late Ladinian to possibly early Carnian age (Tekin, 1999). During this work, one sample of chert from just beneath the basal thrust of the Alanya Nappe (GPS 36 S 0440634, 4036536; c. 2 km NW of Beldibi Kayası) was found to include almost entire specimens and age-diagnostic spines of *Tritortis dispiralis* and *T. kretaensis*, which are zonal markers of the uppermost Ladinian (upper Longobardian) and lowermost Carnian. The radiolarian mudstones are mainly calcareous and contain abundant fragments of pelagic bivalves including *Daonella indica* of Ladinian age (Özgül, 1984b). There are also sub-spherical, thin-shelled bivalves similar to protoconchs. The radiolarian sediments commonly contain thin (up to several cm-thick), laterally continuous, normal-graded, white siltstone partings that in thin section were found to be of quartzitic (detrital) origin.

Where well exposed, the radiolarian sediments pass upwards into alternating thin-bedded quartzose siltstones, micritic limestones, redeposited limestones and siliceous mudstone (shales), as well exposed NW of Beldibi and south of Inasar Dere (Figs. 8c-12, 8d-13).

4.4. Late Triassic

The succession grades upwards through shale and siltstone (c. 20 m) into relatively thick (>600 m) sandstone turbidites and shales (Osmanderesi Member; Figs. 6 and 11f–h). The succession is relatively intact in the lower tectonostratigraphic unit (Fig. 8c-7 to 8c-10). The sandstones are commonly rich in carbonised plant debris (e.g. twigs)

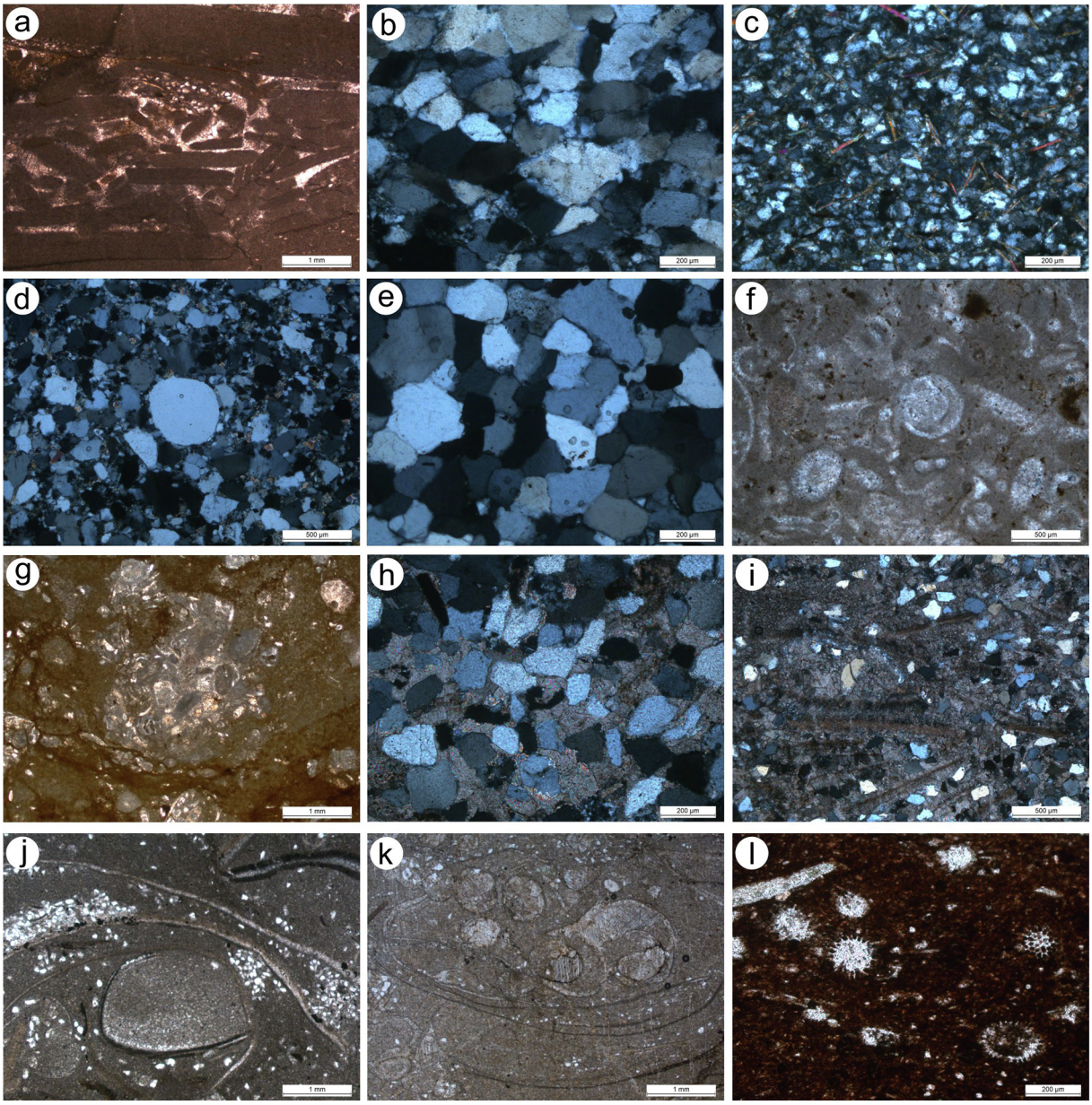

Fig. 9. Photomicrographs of sedimentary rocks from Cambrian-Triassic intervals of the Antalya Complex in the Alanya Window. **a,** Intraformational limestone microconglomerate composed of reworked microbial carbonate fragments, mixed with fine-grained quartzose siltstone; Late Cambrian-Early Ordovician; 2 km N of Yeniköy (NE part of Area A) (plane-polarized light); **b,** Quartzarenite with quartz overgrowths; well-sorted with minimal matrix; Late Cambrian-Early Ordovician; 1.5 km N of Çalıpınar (S part of Area A) (crossed polars); **c,** Well-sorted fine-grained sandstone with quartz and numerous randomly sorted muscovite laths; Late Cambrian-Early Ordovician; near Yeniköy (crossed polars); **d,** Well-sorted medium-grained quartzarenite. Mostly angular to subrounded grains of quartz, with minor quartz overgrowths and traces of diagenetic calcite spar; includes very well-rounded quartz grains, indicative of mixing of grains of differing textural maturity; Late Cambrian-Early Ordovician; near Karalar (S part of Area A) (crossed polars); **e,** Quartzarenite with originally angular to sub-rounded quartz grains, with minor quartz overgrowths; the grains are densely packed, with incipient sutured contacts; Late Permian; 1 km E of Kocaoğlanlı (W part of Area A) (crossed polars); **f,** Typical Late Permian neritic limestone rich in calcareous algae and shelly debris, in a fine-grained micritic matrix; 0.4 km E of Ibrahimli (Kıllı), 1.3 km NNE of Lordlar (NW part of Area A) (crossed polars); **g,** Reworked biomicrite, including benthic foraminifera and small shell fragments; affected by pressure solution cleavage in lower part of view; Late Permian; near Dervişli (W part of Area A) (plane-polarized light); **h,** Loosely packed quartzose sandstone with sub-angular to sub-rounded quartz grains, set in a calcite spar matrix; Early Triassic; 2 km E of Lordlar (crossed polars); **i,** Poorly sorted mixture of thin-shelled bivalves in a micritic matrix. The concentration of small quartz grains represent bioturbation; Early Triassic; Taşlıca Sr. (NW part of Area A) (crossed polars); **j,** Thin-shelled bivalves set in a silty micritic matrix with 'pockets' of quartz grains introduced by burrowing; Early Triassic; near Beslengiler (NW part of Area A) (plane-polarized light); **k,** Tightly imbricated thin-shelled bivalves in a micritic matrix; location as j (crossed polars); **l,** Recrystallised radiolarians set in a reddish coloured, iron-rich muddy matrix. The scattered nature of the radiolarians differs strongly from the packing typical of Late Jurassic-Early Cretaceous radiolarians in the study area; near Beslengiler (higher in the same succession as j); Early Triassic (plane-polarized light).

(Fig. 11i). Reworked Late Triassic benthic foraminifera (*Artrophicus* sp.) have been reported (Özgül, 1984b), and in addition Late Triassic microfossils (see previous work, above) and macrofossils (e.g. *Halobia* sp.) are known from elsewhere in the Alanya Window (Ulu, 1988). During this work, a Late Triassic age was mainly inferred by comparison with the better-dated fossiliferous interval stratigraphically below.

Individual sandstone beds of Late Triassic age range from thin, to medium, to thick-bedded, and are characterised by variably developed

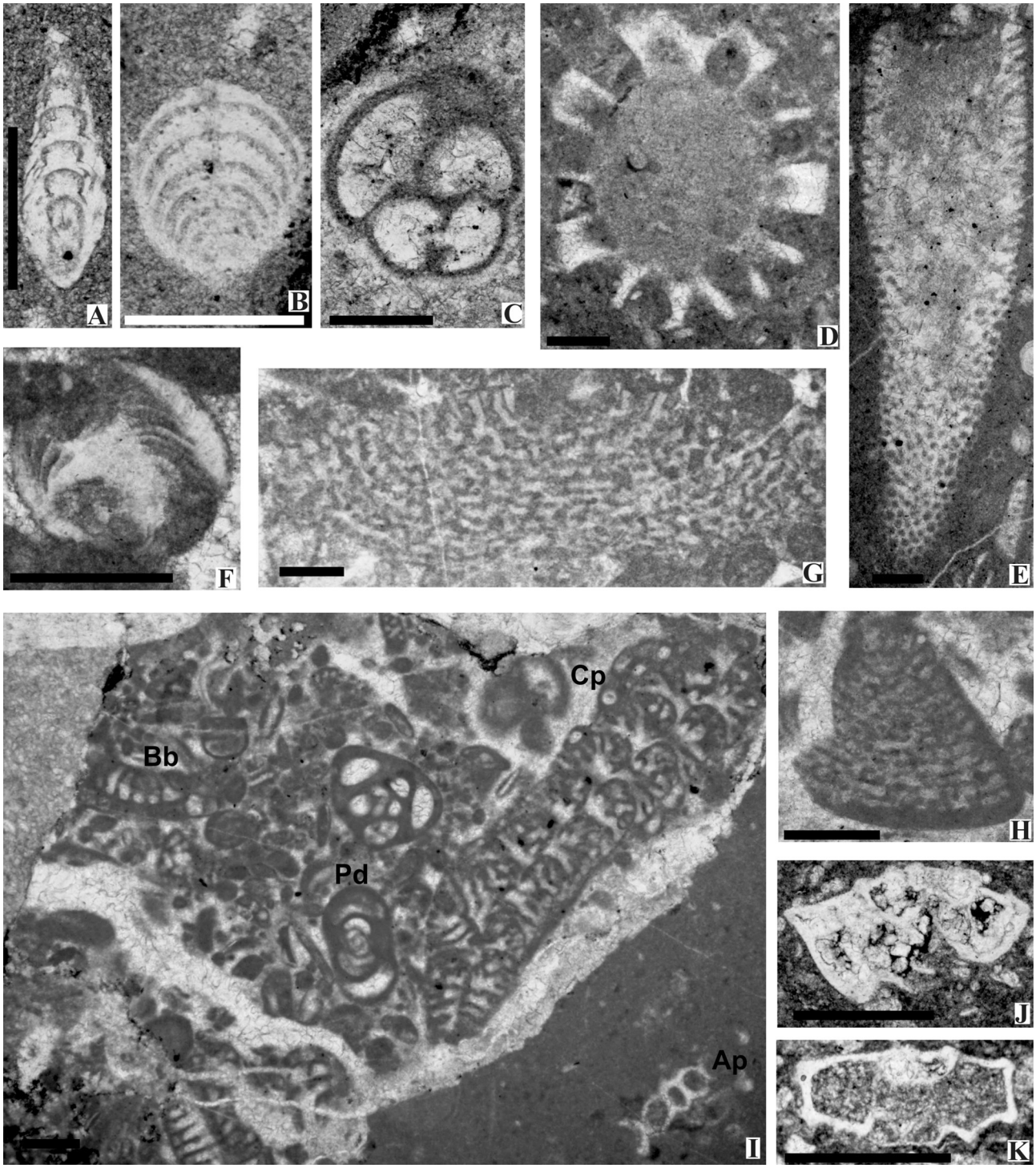

Fig. 10. Photomicrographs of calcareous fossils from the Alanya Window. **A-E:** Permian microfossils, **A.** *Pachphloia* sp., sample AN18-35; **B.** *Geinitzina* sp., sample AN18-55; **C.** *Globivalvulina* sp., sample AN18-55; **D.** *Mizzia* sp., sample AN18-9; **E.** *Gymnocodium* sp., sample AN18-35; **F.** Middle-Upper Jurassic, *Protopeneroplis striata* Weynschenk, sample AN18-117; G-H: Barremian-Aptian, **G.** *Palorbitolina lenticularis* (Blumenbach), sample AN18-122; **H.** *Paracoskinolina* sp., sample AN18-117; **I.** Cenomanian benthic foraminifera from reworked limestone clast: *Biconcava bentori* Hamaoui (Bb), *Pseudorhapydionina dubia* (De Castro) (Pd), *Cuneolina pavonia* d'Orbigny (Cp) and Lower Cretaceous dasycladalean alga *Actinoporella podolica* (Gümbel in Alth) (Ap), sample AN18-118; **J-K:** Campanian-Maastrichtian planktonic foraminifera, **J.** *Globotruncanita* sp., sample AN18-119; **K.** *Globotruncana linneiana* (d'Orbigny), sample AN18-121. Scale bars: 0.25 mm.

Bouma sequences (Fig. 8c; e.g. Tırılar log 9; Osmandere log 10). Finer-grained sandstone interbeds are commonly bioturbated (Fig. 12h).

A notable feature is the occurrence of well-bedded, lenticular, matrix-supported conglomerates, individually up to 2.8 m thick, which are interpreted as debris-flow deposits. Most of the debris-flow deposits are dominated by siltstone clasts, set in a grey, silty matrix. However, one prominent debris-flow deposit, c. 1.6 m thick (exposed along a track c. 0.8 km south of İnasar Dere) is composed of crudely-bedded, medium-coarse grained sandstone, with sub-angular clasts of siltstone and marl that increase in size upwards (i.e. reverse graded). The background sediments between the debris-flow intervals are thin to medium-bedded, medium to coarse-grained sandstone, together with parallel-

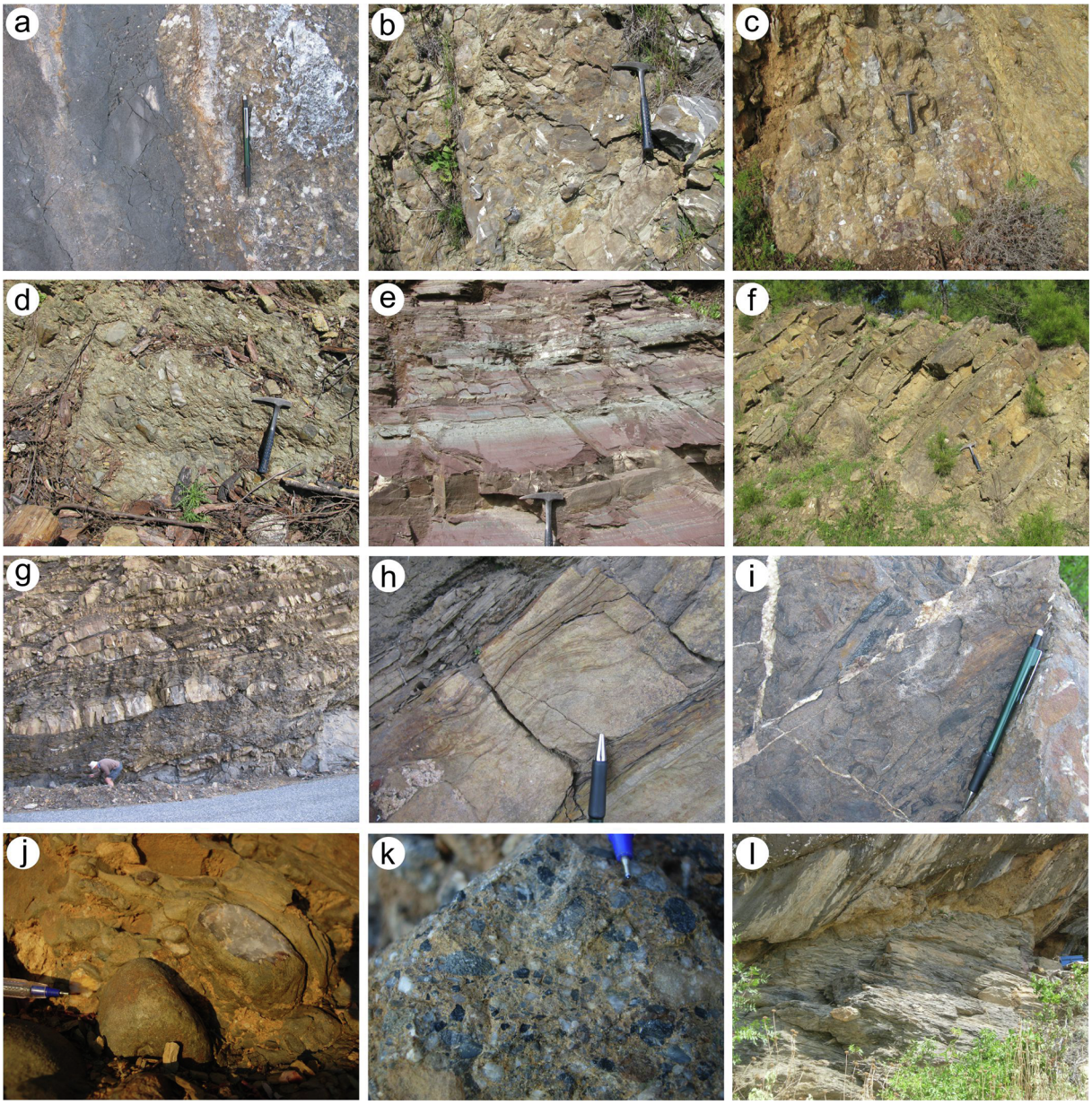

Fig. 11. Field photographs in the Alanya Window. **a,** Unconformity between Late Permian limestone (left) and Early Triassic pebbly facies (right), 0.5 km NW of Kıllı (pen for scale); **b,** Chaotic debris-flow unit composed of Palaeozoic limestone (grey) in an argillaceous matrix (Mid-Triassic); Taşlıca section (NW part of Area A) (hammer for scale); **c,** Stratiform debris-flow deposits, ranging from clast-rich (left) to clast poor (right) (Mid- Triassic); 1 km NW of Kızılgüney (near locality b) (hammer for scale); **d,** Weakly-cleaved debris-flow deposit with clasts of Palaeozoic sandstone in a sandy and argillaceous matrix; Middle Triassic; 0.5 km NW of Beldibi Kayası (1.7 km NW of Beldibi), (hammer for scale); **e,** Middle Triassic, impure (muddy) finely-laminated red radiolarian mudstone; patchy grey colour is the result of diagenetic reduction of iron; note also weakly developed inclined spaced-fracture cleavage; 1 km NNW of Kızılgüney, southern part of Area A (hammer for scale); **f,** Well-bedded, medium to thick-bedded sandstone turbidites, Late Triassic; near Osmanderesi; NW part of area A (hammer for scale); **g,** Thin-medium and thick-bedded sandstone turbidites, interbedded with dark, organic carbon-rich shale (affected by normal faulting); Late Triassic; 300 m ESE of Payamağacı, 1 km S of Başköy; NE part of area A; **h,** Thin-bedded sandstone turbidite showing normal grading, massive, wavy and planar lamination upwards; Late Triassic; Dereköy, SW part of Area A (pen for scale); **i,** Sandstone with abundant carbonised wood; Late Triassic; near Osmanderesi; NW part of area A (near locality f) (pen for scale); **j,** Unusual pebbly debris-flow deposit with well-rounded clasts of Palaeozoic(?) sandstone and vein quartz (broken pebble; pale grey), set in sandy matrix (pen for scale); Late Triassic; near Kocaveliler (SW part of area A); **k,** Unusual pebbly debris-flow deposit with numerous angular to sub-rounded clasts of Palaeozoic? black chert and more-rounded clasts of coarse quartzose sandstone, in a sandy matrix; Late Triassic; location as j; **l,** Sheared contact between pebbly debris-flow deposits below (Triassic?) and limestone above (Jurassic?); near Karaçukur köy (Area B).

laminated brown shale.

In thin section, the Late Triassic sandstones are mainly quartzarenites, with angular to subangular grains of quartz set in a fine-grained matrix, together with feldspar, muscovite, local biotite and opaque grains (Fig. 12g). This contrasts with the generally more rounded quartz grains and more abundant muscovite and/or biotite in the Cambrian-Ordovician sandstones. The debris-flow deposits include well-rounded clasts, set in a muddy or sandy matrix (Figs. 8c-7, 8c-10 and 11k). An exceptional debris-flow deposit includes clasts of metamorphic quartzite, schist, black (organic carbon-rich) mudrock, chert, phyllite, marble and sedimentary intraclasts (Figs. 11j-k and 12b-f). Many of the clasts are similar to the underlying Early Triassic, Late Permian and Cambro-Ordovician lithologies. There are also rare granitic clasts that are likely to have been derived from (unexposed) Precambrian

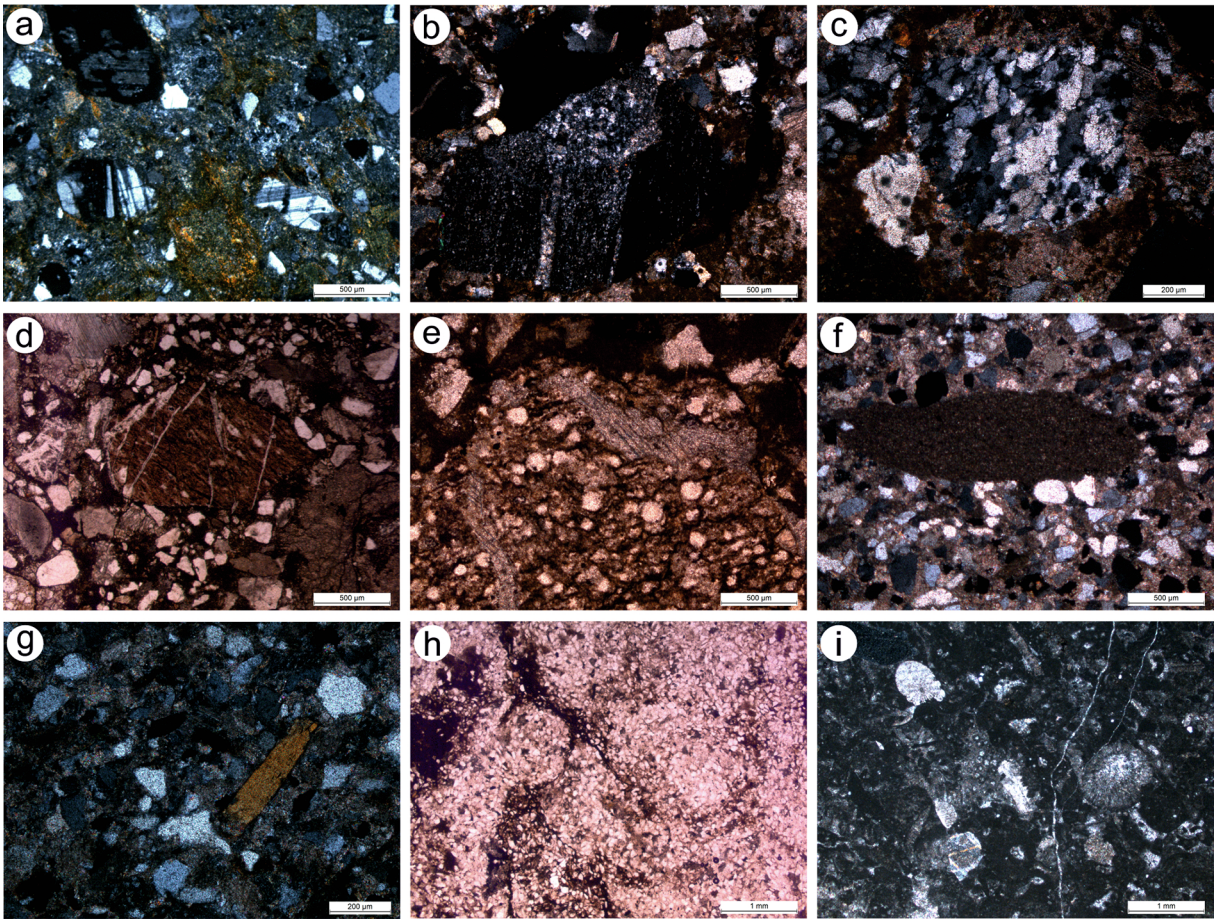

Fig. 12. Photomicrographs of Middle-Late Triassic sedimentary rocks. **a,** Bedded debris-flow deposit, rich in plagioclase crystals (fractured), quartz (including microcrystalline quartz) and meta-siltstone clasts, in a muddy matrix; Middle Triassic; 1.5 km N of Beldibi (crossed polars); **b,** Rounded grain of partly recrystallised finely-laminated black siltstone, set in medium-grained, calcite-cemented sandstone; from a 5 m-thick conglomerate lens (with well-rounded clasts); Late Triassic; near Kocaveliler (SW part of Area A) (crossed polars); **c,** Sub-rounded grain of metamorphic quartzite, set in calcite-cemented sandstone; Late Triassic; location as b (plane-polarised light); **d,** Rounded grain of highly cleaved, veined phyllite (possible mylonite), set in poorly sorted, matrix sandstone; Late Triassic; location as b-c (plane-polarised light); **e,** Sub-rounded grain of radiolarite (probably from the subjacent Mid-Triassic succession), partly replaced by calcite spar; Late Triassic; location as b-d (crossed polars); **f,** Calcareous siltstone rip-up clast (sub-rounded), set in typical calcite-cemented sandstone, rich in quartz grains; Late Triassic; 0.4 km N of Beldibi (crossed polars); **g,** Typical Late Triassic sandstone with mostly angular quartz grains, cemented by calcite spar; includes biotite crystals; 0.5 km N of Tırılar (NW part of area A) (crossed polars); **h,** Bioturbated calcite-cemented quartzose siltstone within Late Triassic succession; c. 2 km E of Memişler (west part of Area A) (plane-polarised light); **i,** Redeposited micritic limestone; rich in fragments of calcareous algae, with in addition echinoderm and bivalve debris; 2 km NE of Beldibi; Jurassic (crossed polars).

(Cadomian) basement.

In places, the Late Triassic sandstone turbidites contain exotic blocks and lenses, up to tens of metres thick and several 100 m long, that are made up of Palaeozoic lithologies, similar to those exposed stratigraphically beneath. In some areas, the blocks and disrupted lenses form elongate, c. E-W trending trails, notably south and south-west of Lordlar. The exotic units have been interpreted as olistoliths; i.e. emplaced by gravitational processes (Özgül, 1984b; Ulu, 1988) (Fig. 7c). The blocks and lenses have sheared and brecciated margins indicating a tectonic influence on their formation. An origin purely related to tectonic emplacement is unlikely, however, because the exotic units are restricted to within the Late Triassic deep-water turbidites.

4.5. Latest Triassic-Cretaceous

Two contrasting successions are exposed in the third, uppermost tectonic unit in the north-east (east of Beldibi), separated by a tectonic contact (Figs. 4 and 5). The first succession, termed the İnasar Dere Member (new name) (Fig. 6), is dominated by radiolarites and pelagic carbonates. Similar facies are exposed several kilometres farther east, near Başköy, although additional facies are present. The second succession begins with reef limestone blocks in mudrock (Beldibi Member; Sapadere Formation). This is followed by redeposited carbonate, then pelagic carbonates (Beldibi Kayası Member; İnasar Formation) (Fig. 6). The two contrasting successions are separated by a (probable) poorly exposed thrust contact.

The structurally lower succession (İnasar Dere Member) was studied in two local sections, as follows:

The first section is well-exposed along a track, c. 300 m south of İnasar Dere and 400 m NNW of Beldibi Kayası (Fig. 8d-14). Ribbon radiolarites, up to 30 m thick, pass upwards into pinkish pelagic limestones with chert nodules (c. 8 m thick). One sample of radiolarite from this section yielded *Emiluvia*? sp., *Favosyringium*? sp. and *Podocapsa*? sp. of Late Jurassic or Early Cretaceous age. The likely presence of *Emiluvia* suggests an age no younger than late Valanginian/earliest Hauterivian. A sample from higher in the radiolarite interval contains a better preserved assemblage including *Alievium gallowayi* (White), *Patellulla planconvexa* (Pessagno), *Patellulla verteroensis* (Pessagno) and *Patulibrachium* sp. of Early Campanian age. Another sample contains a well-developed assemblage, including *Dictyomitra kozlovae* (Foreman) and *Pseudoaulophacus* sp. of probable Early Campanian age. The radiolarites

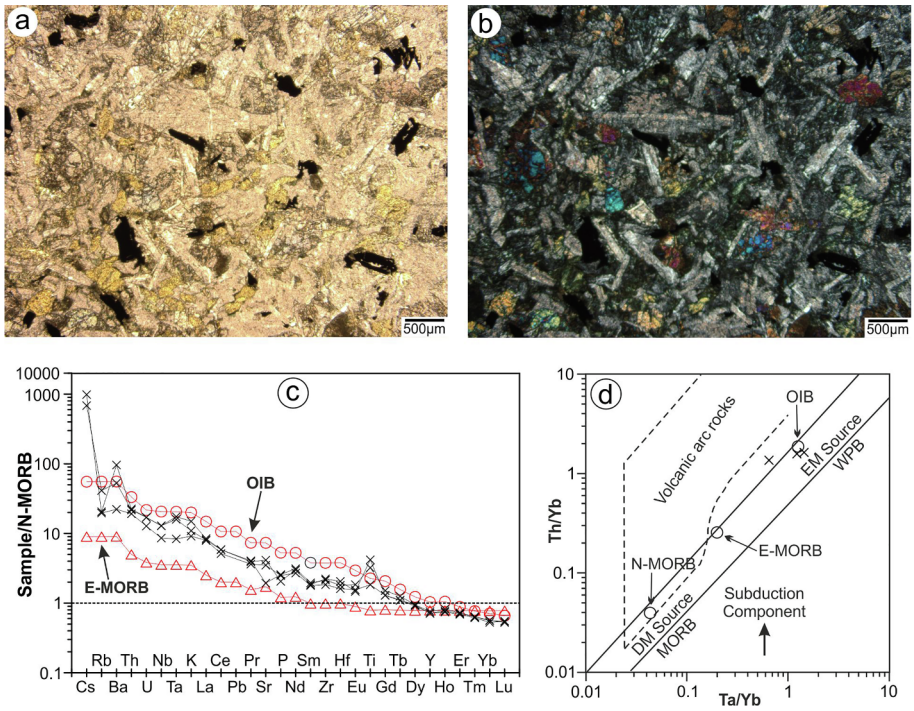

Fig. 13. Basaltic sills cutting the Triassic succession. **a-b** Photomicrographs of microgabbro-diabase with abundant plagioclase, clinopyroxene and interstitial opaque oxide; **c,** MORB-normalised spider plot of three samples of the microgabbro-diabase sills compared with E-MORB (enriched MORB) and OIB (ocean island basalt); **d,** Th/Yb vs. Ta/Yb plot of the same samples showing their enriched chemical composition which is compatible with a rift setting. See text for discussion.

include spasmodic, thin (< 25 cm) interbeds of normal-graded calcarenites, interpreted as calciturbidites, that are dominated by neritic bioclastic material including the benthic foraminifera *Protopeneroplis striata*, *Valvulina lugeoni*, *Mesoendothyra* sp. and *Trocholina* sp. (Özgül, 1984b).

The second local section is located c. 1.5 km farther east, several hundred metres southwest of Başköy (Figs. 4 and 5) (GPS 36S 0441967 4034600). Although too sheared and faulted to log effectively, the succession begins with alternations of ribbon radiolarite and pelagic carbonate (c. 60 m thick). There are then alternations of calcareous shale, lithoclastic sandstone (quartz-poor), dark coloured marl/pelagic limestone and pebbly debris-flow deposits. The pelagic limestones contain very poorly preserved Cretaceous planktic foraminifera (e.g. heterohelids). The radiolarites, although poorly preserved, are inferred to be Cenomanian-Turonian (or younger) based on the presence of *Alievium* cf. *superbum* (Squinabol) and, more specifically, Turonian based on *Crucella cachensis* (Pessagno). The sandstones are lithoclastic and contain abundant subrounded grains of radiolarian chert, pelagic limestone (mostly recrystallised) and shale/claystone. Many of the grains were still unlithified when reworked and fused during sub-sea-floor compaction. The Late Cretaceous lithologies in this section were gravitationally disturbed or reworked as debris-flows, probably during latest Cretaceous time.

The second, contrasting succession begins with sheared dark-coloured mudrock (Beldibi Member), as exposed along İnasar Dere (0.6 km NE of Belbdibi Kayası Tepe). This is overlain by well-bedded, brownish-coloured, quartz-rich muddy siltstones (up to c. 60 m thick), as exposed on a steeply sloping hillside (0.6 km NE of Belbibi Kayası Tepe). The siltstones (Fig. 8d-14) contain scattered blocks of reef limestone (up to c. 2 m in size) (see supplementary material for illustrations). Individual bocks are sub-rounded, with abraded and altered margins; many are fractured and calcite-veined. The reef blocks are scattered throughout massive siltstone without finer-grained, re-deposited carbonate interbeds. The interiors of the blocks contain well-preserved coral, sponges, brachiopods, bivalves and conodonts, of inferred Norian (Late Triassic) age (Özgül, 1984b; this study). Ulu (1988) dated similar blocks of reef limestone from a wider area as Carnian-Norian. Some of the individual blocks preserve primary growth fabrics.

Above a poorly exposed contact (possible low-angle unconformity) the section continues with thick-bedded limestones, estimated as 60 m thick (Beldibi Kayası Member). The outcrop is lenticular (c. 1 km long), folded and dissected by high-angle faults. The limestones were studied on the northeast flank of Beldibi Kayası Tepe (Fig. 8d-14), extending northeastwards for c. 600 m as far as İnasar Dere (Fig. 8d-15) (see also supplementary information). The limestone succession begins with lenticular calcirudites (c. 25 m) composed of rubbly, stylolitic and nodular limestone, with angular limestone clasts (up to 8 cm in size), set in a reddish calcareous matrix. Many of the clasts are grey micritic limestone with radiolarians, sponge spicules and ostracod fragments; other clasts include reworked neritic carbonate with echinoderm debris and nodosarid foraminifer (Özgül, 1984b). Carbonates from near the base of the exposed section (Fig. 12i) include common reworked benthic foraminifera; e.g. *Galeanella panticae*, *Tetrataxis inflata*, *Sigmolina* sp., *Spiriamphorella* sp. the *Agathammina austroalpina* and Duostominidae, and also Microproblematica (*Muranella sphaerica*), together indicating a Rhaetian-Liassic age (Özgül, 1984b); i.e. slightly younger than the underlying Carnian(?)-Norian reef limestone blocks (Beldibi Member). During this work, well-bedded grey calcarenites (Fig. 10f, h, i) from a cliff-section directly south of İnasar Dere (Fig. 8d-15) were found to include benthic foraminifera of both Middle-Late Jurassic age (Fig. 10f) and Early Cretaceous (Barremian-Aptian) age (Fig. 10g, h), Dasycladalean algae of Early Cretaceous age (Fig. 10i) and also reworked Cenomanian-aged benthic foraminifera (Fig. 10i), together with corals, bryozoans and echinoderms. All of the lithologies studied are redeposited.

The succession (Beldibi Kayası Member) (Figs. 8d-14, 8d-15) grades upwards into grey, medium-bedded hemipelagic limestones (c. 7 m thick), with lenticular chert formed by carbonate replacement. Microfossils include the benthic foraminifera *Ophthalmidium* sp., *Endothyra* sp. and Vernuilinidae, and also the incertae sedis *Thaumatoporella* sp. (Özgül, 1984b). The siliceous limestone is transitional upwards (over several tens of cm) into pink pelagic carbonate (c. 10 m thick), as well-exposed near the crest and on the SW-facing dip slope of Beldibi Kayasıtepe. The pelagic carbonates contain relatively well-preserved planktic foraminifera, including *Globotruncana lapparenti*, *G. bulloides*, *G.* cf. *coronata*, *G. stuarti*, *G. linneiana* and *Siderolites* sp. of Campanian-Maastrichtian age (Özgül, 1984b). In addition, several species of planktic foraminifera of late Cretaceous age were identified during this

study (Fig. 10j and k). Red pelagic limestones, exposed in a fault-bounded unit c. 450 m farther northeast (near and to the north of the Beldibi road), contain abundant echinoderm debris and Late Cretaceous Globotruncanidae.

The intact succession (Beldibi Kayası Member) ends with a major fault (exposed along the road to Beldibi), characterised by a c. 10 m-wide zone of shearing, brecciation, carbonate veining and chert re-crystallisation. Southwards along the road there is an intact (c. 60 m thick) succession of radiolarian chert alternating with shale, although the original stratigraphic position is uncertain. A sample of grey argillaceous and calcareous chert from near the top of this interval yielded the planktonic foraminifera Hedbergellidae, Heterohelicidae, Radiolaria and ostracod fragments of (imprecise) Cretaceous age. On the hillside several hundred m to the east (Çiriş Tepe; GPS: 36S 0439894 4034988), a similar, but strongly folded chert interval was found to include rare radiolarians i.e. *Cryptamphorella conara* (Foreman), *Dictyomitra duodecimporata* Squinabol, *Praeconocaryomma* sp. of late Campanian-Maastrichtian age. This chert-dominated section is interpreted as the uppermost part of the İnasar Dere Member (see above) that immediately predated thrust-related emplacement of the Antalya Complex.

5. Results: Intrusive igneous rocks

Basic igneous rocks are rare in the Alanya Window. However, a working quarry c. 2.5 km WNW of Beldibi (GPS: 36S 0436659 4235328), exposes a sill-like body of microgabbro-diabase, estimated as c. 60 m thick. Several diabase sills, up to 3 m thick, which are probably related to the same intrusion, are exposed along the main road c. 2 km northwest of Beldibi. The small sills exhibit well-developed chilled margins against Triassic shale and sandstone.

In thin section (Fig. 13a and b), the microgabbro exhibits micro-granular to sub-ophitic textures, mainly comprising plagioclase and clinopyroxene. Plagioclase is altered to albite, related to low-grade metamorphism or late-stage hydrothermal activity. Clinopyroxene occurs either as euhedral to subhedral grains surrounded by plagioclase, or as infill of the interstices between feldspars, and is surrounded by reaction rims of green hornblende. Secondary phases include chlorite, epidote and opaque minerals.

Three samples of microgabbro were analysed at the ACME laboratory, Vancouver, Canada. Major element contents were determined from $LiBO_2$ fusion by ICP-ES using 5 g of sample pulp. Other elements (including rare earth elements) were determined by ICP-MS. The major and trace element contents of the samples are given in Table 1.

The diabase sills are classified as alkaline basalt based on Zr/Ti (0.005–0.01) versus Nb/Y (1–1.5) ratios. Incompatible trace element ratios such as Y/Ta (8.7–18.3), Y/Nb (0.7–1), Zr/Nb (5.3–6.8), Ti/Nb (698–1061), Sm/Yb (2.8–3) and Ce/Sm (8.2–9) for the sills suggest that they were derived by melting of an OIB (ocean island basalt)-like 'enriched' mantle source. The REE concentrations of the diabase sills display significant light REE enrichment with respect to HREEs (La_N/Yb_N = 8.3–9.4). Relatively high TiO_2 (2.3–5.3 wt%), P_2O_5 (0.2–0.3 wt %) and Zr (136–164 ppm) suggest derivation from an 'enriched' mantle source. N-MORB normalized spider diagram for the diabase sills with E-MORB and OIB for comparison (Fig. 13c), are highly-enriched and exhibit a close similarity to OIB. The Th/Yb versus Ta/Yb ratio-ratio plot (Fig. 13d), discriminates between depleted mantle (MORB) and enriched mantle (intraplate) sources (Pearce, 1982). The addition of a subduction chemical component (associated with slab-derived fluids/melts) results in an increase in Th/Yb in the mantle source (arrow in Fig. 13d). The diabase-microgabbro plots in the enriched mantle source/within plate basalt region, consistent with a continental rift-related setting.

Possibly related to the same Triassic magmatic event, Ulu (1988) mentions an occurrence of sub-alkaline tholeiitic pillow lava, supported by a photomicrograph (but without locality information).

Table 1
Major, trace and rare earth element data for microgabbro-diabase intrusions from the Triassic succession in the northeast part of the Alanya Window (area A, Beldibi-Gazipaşa). See text for discussion.

Sample	AN17-157	AN17-158	AN17-159
Rock Type	Diabase	Diabase	Diabase
Location	Beldibi Mine	Beldibi Mine	Beldibi Mine
GPS Location	36S 0436659E/ 4035328N	36S 0436659E/ 4035328N	36S 0437648E/ 4035650N
SiO_2	45.64	44.88	47.98
TiO_2	4.08	5.31	2.33
Al_2O_3	14.45	14.57	15.86
FeO*	14.44	13.00	10.66
MgO	4.64	5.88	6.26
CaO	8.36	7.74	7.03
Na_2O	4.39	4.31	4.68
K_2O	0.79	1.08	0.66
P_2O5	0.30	0.24	0.29
MnO	0.17	0.15	0.15
Cr_2O_3	<0.002	0.013	0.014
LOI	2.4	2.5	3.8
Sum	99.77	99.72	99.77
Ni	<20	99	56
Sc	25	31	23
Ba	604	333	140
Be	2	<1	<1
Co	36.5	44.5	37.6
Cs	<0.1	4.8	6.9
Ga	21.5	16.7	16.7
Hf	3.7	4.2	3.3
Nb	30.1	30.0	20.0
Rb	11.5	23.1	11.0
Sn	3	1	2
Sr	174.3	372.5	315.2
Ta	2.1	2.3	1.1
Th	2.7	2.6	2.3
U	0.8	0.8	0.6
V	391	364	219
W	0.8	<0.5	<0.5
Zr	158.1	164.8	136.0
Y	21.2	19.9	20.1
La	20.1	21.1	19.8
Ce	43.8	43.9	38.5
Pr	5.34	5.19	4.78
Nd	22.8	21.8	19.7
Sm	5.14	4.87	4.70
Eu	1.88	1.50	1.58
Gd	5.55	4.77	4.75
Tb	0.84	0.74	0.73
Dy	4.31	4.28	4.14
Ho	0.83	0.75	0.78
Er	2.16	2.05	2.11
Tm	0.29	0.28	0.29
Yb	1.73	1.61	1.71
Lu	0.24	0.25	0.25

Total Fe is indicated as FeO*. < means below detection limit.

The second occurrence of intrusive igneous rock is a single known block of partially recrystallised granitic rock that could be a fragment of Cadomian basement (see supplementary information for details and illustration). Radiometric dating and geochemical studies are needed to test this. Felsic intrusive rocks, including aplitic dykes of Late Precambrian age, dated to 950–1000 Ma, are reported from beneath the Palaeozoic succession within the Alanya metamorphic massif (Sarıağaç unit), and to the southeast of the Alanya Window in the Anamur (Mersin) area (Çetinkaplan et al., 2010; Çetinkaplan, 2018). Comparable Late Precambrian felsic intrusive rocks are also reported from elsewhere in the Taurides-Anatolides.

6. Results: Sedimentary evidence from more southerly areas

To aid interpretation of the well-exposed area in the northwest of the Alanya Window (Area A; Beldibi-Gazipaşa), reconnaissance was

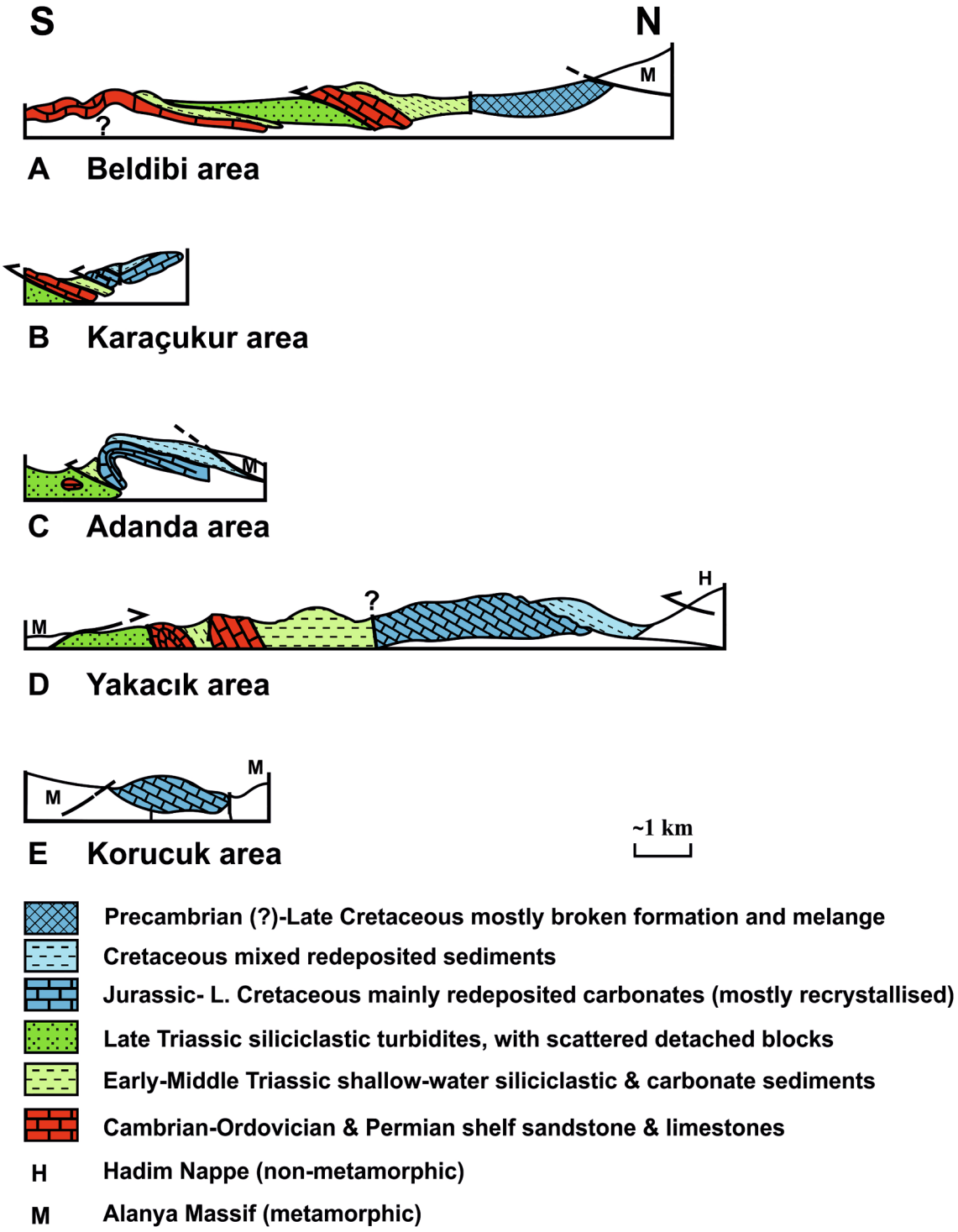

Fig. 14. Outline cross-sections of the local study areas (see Fig. 3). **A.** Beldibi area in the NW (part of main study Area A); **B.** Karaçukur (Area B); **C.** Adanda (Area C); **D.** Yakacık (Area D); **E.** Korucak (Area E). See text for explanation.

carried out of four outcrops further southeast (Areas B-E) (Figs. 3 and 14), with particular reference to Mesozoic limestones that are mainly exposed in northerly, structurally high parts of the outcrop (Ulu, 1983, 1988; MTA, 2000; *this study*). These limestones were originally mapped as exotic blocks in a regional-scale Late Cretaceous olistostrome (Karaçukur Formation of Ulu, 1988). However, they are re-interpreted here as complexly deformed but otherwise coherent successions of Jurassic-Cretaceous age.

6.1. Karaçukur area

The first comparative outcrop is located c. 35 km to the SW of Area A, near Karaçukur village (Area B; Figs. 3 and 14b). The local outcrop (i.e. SE of Karaçukur) begins with thick-bedded carbonate rocks of probable Late Permian age (Yüğlük Tepe Formation), overlain by Triassic sandstone and shale (Sapadere Formation). The locally exposed succession begins with dismembered and folded varicoloured shales, thin-bedded siltstones, quartzose sandstones and limestone of inferred Early Triassic age. Reddish shales and occasional radiolarites above this

are assumed to be Mid-Triassic age. Lenticular debris flow-deposits, of probable Early-Mid Triassic age, contain clasts of neritic limestone (Permian?) and rarely of micaceous sandstone, probably derived from the underlying Cambrian-Ordovician succession (Lordlar Formation). Above this, Late Triassic sandstone turbidites include isolated detached limestone blocks (c. typically 3–5 m in size) of probable Permian age, several of which are mantled by angular clasts composed of lithologically similar limestone. Another block (c. 20 m across) comprises alternating purple siltstone and thick-bedded, medium-grained sandstone of probable Early-Middle Triassic age. The blocks are similar to those in Area A (see above).

The above Permian-Triassic succession is overlain by a northward-dipping, carbonate succession, locally up to c. 150 m thick, of Jurassic-Cretaceous age (Ulu, 1983, 1988). The main limestone exposure (up to 3 km E-W by 2 km N-S) is directly underlain by debris flow-deposits (Triassic?), with clasts of grey recrystallised limestone (up to 25 cm across) in a matrix of brownish shale and sandstone (near Karaçukur) (see supplementary material for illustration). The field relations hint at a near-primary depositional relationship between the Permo-Triassic succession and the overlying Jurassic-Cretaceous succession, prior to tectonic emplacement, which resulted in a sheared contact (Fig. 11i).

Although largely recrystallised, the Jurassic limestone are mainly redeposited and retain recognisable bivalve, echinoderm, benthic foraminifera and calcareous algal fragments. The higher levels of the succession, comprising Late Cretaceous-aged redeposited and hemipelagic facies are exposed in a fault-dissected syncline (Karaçukur Formation of Ulu, 1988). Smaller limestone outcrops (< 300 m across) farther east represent disrupted remnants of the same Jurassic-Cretaceous stratigraphy, which is inferred to have been laterally continuous prior to tectonic emplacement. The succession can also be correlated with the Jurassic-Cretaceous Beldibi Kayası Member to the NE in Area A.

6.2. Adanda area

The second comparative outcrop (Area C, Adanda) is located c. 10 km farther southwest (Figs. 3 and 14c). The section begins (in the south) with folded and sheared sandstone turbidites of inferred Late Triassic age (Sapadere Formation). The Late Triassic sandstones are overlain northwards, above a deformed but possibly originally stratigraphic contact, by a strongly folded and fault-dissected succession of Jurassic limestones (c. 80 m thick) (see supplementary material for illustrations). The lowest limestone unit, composed of fine-medium grained calcarenite, is deformed into a large generally south-verging anticline, with fine sandstone and siltstone, stratigraphically above. The thick-bedded limestones are followed, stratigraphically above, by a variably deformed succession (> 100 m thick) of alternating hemipelagic marls, calcareous shales, calcareous siltstones/sandstones, quartzose sandstones and thin-bedded redeposited limestones (calciturbidites), as exposed along the road to, and near Adanda castle. Occasional debris-flow intercalations contain isolated limestone blocks (25 × 35 cm) of dark bivalve shell-rich limestone set in a shaly matrix. Interbedded pelletal limestone includes reworked clasts of limestone with the benthic foraminifera, Orbitolinidae and *Tubiphytes* sp.; also, bryozoans, coral, echinoderm and rudist bivalve fragments that, together, suggest a Late Cretaceous age (see supplementary material). Interbedded hemipelagic marls include poorly preserved planktic foraminifera and calcified radiolarians.

6.3. Yakacık area

The third comparative outcrop (Area D, Yakacık) is located c. 50 km farther southeast, to the north of the coastal town of Yakacık (Figs. 3 and 14d). The section is dominated in the south by Triassic sandstone turbidites (Sapadere Formation). Northwards, there is a strongly folded and faulted succession of thick-bedded, recrystallised Late Permian(?) limestones, in turn overlain by a mixed carbonate-siliciclastic succession of inferred Early-Middle Triassic age. Northwards, there is an exceptionally thick (up to c. 1000 m), mainly north-dipping succession of thick-bedded, relatively fine-grained limestones, mapped as Jurassic-Early Cretaceous in age (Ulu, 1983, 1988). The basal contact could not be observed. The limestones pass upwards into an intact succession of thin to medium-bedded calcareous sandstones, dark-coloured shales, thin-bedded limestones and debris-flow deposits with clasts of micritic limestone, similar to the Late Cretaceous succession in Area C (Adanda) farther west. The outcrop is terminated by the Hadim Nappe (see supplementary material for illustrations).

6.4. Korucuk area

The fourth comparative outcrop (Area E, Korucuk) is near the southeast termination of the Alanya Window, to the northeast of Anamur (Figs. 3 and 14e). Jurassic-Early Cretaceous thick-bedded limestones extend unbroken (although folded and faulted) for > 50 km E-W before pinching out towards the coast (Ulu, 1983, 1988). The outcrop near Anamur is exceptionally schistose and recrystallised. Where observed (W of Korucuk), N-dipping, calc-schist is overlain by well-bedded marble (> 80 m thick) (see supplementary material for illustrations). The marble dips northwards and is in high-angle fault contact with well-bedded, south-dipping, meta-clastic sedimentary rocks (calc-schist, shale, quartzose sandstone and siltstone) of the Alanya Massif, as widely exposed further north.

In summary, our reconnaissance of Areas B-E show that the stratigraphy described from the NW (Area A) is broadly applicable to the Alanya Window as a whole. However, the Jurassic-Cretaceous neritic-derived to pelagic limestones that are only locally exposed in the NW area (Beldibi Kayası Member), however, form an important component of the succession mainly in the higher structural levels of the window.

7. Discussion of sedimentary and magmatic development

The following stages of development can be recognised based on the evidence from the Alanya Window:

7.1. Pre-Permian: pre-rift platform deposition

The lowest part of the succession accumulated prior to the initial rifting of the Southern Neotethys. Although undated (Cadomian?) the oldest rocks in the Antalya Window may be represented by partially recrystallised granitic rocks, now represented by one or more detached blocks (see supplementary material).

Cambrian-Early Ordovician sandstones, shales and limestones, similar to those in the Alanya Window, accumulated extensively along the northern margin of the Arabian continent (Göncüoğlu et al., 2004; Göncüoğlu and Kozlu, 2000), following tectonic assembly of the Cadomian basement (Avigad et al., 2016). Terrigenous sediments of similar age are exposed in both autochthonous units, for example the Sultandağı Massif, central-southern Anatolia (MTA, 2000), and the Geyik Dağ in the Seydişehir area (Seydişehir Formation; Dean et al., 1999), and also in allochthonous units including the Alanya Massif (MTA, 2000; Çetinkaplan, 2018), the Antalya Complex (e.g. near Kemer) (Marcoux, 1979; MTA, 2000) and the Hadim Nappe (e.g. near Silifke) (Demirtaşlı, 1983). The more northerly facies are relatively fine grained (siltstone and shale), consistent with a relatively distal (northerly) setting on the Gondwana margin. The source rocks included mica-rich metamorphics, similar to some of the meta-sedimentary rocks, as locally exposed in the Alanya Massif (e.g. Sarıağaç schist, near Anamur) (Çetinkaplan et al., 2010; Çetinkaplan et al., 2016a, 2016b). Similar lithologies are exposed in Cadomian basement, as exposed in the Sultandağı Massif (MTA, 2000), the Menderes Massif (Zlatkin et al., 2013), the Afyon zone, the Karacahisar dome in south-central Anatolia (Abbo et al., 2015) and elsewhere. The ultimate source is interpreted to

be north-east Gondwana (NE Africa/Arabia) (Ustaömer et al., 2019).

Alternative depositional settings are: first, the sands accumulated from turbidity currents within intra-platform basins, or, secondly, they accumulated from high-energy surges (storms) on a shallow-water platform. The fauna and trace fossils are consistent with a relatively shallow-water depositional setting (Dean et al., 1999; Ghienne et al., 2010). The locally intercalated reddish-pinkish micritic limestones are suggestive of periodically condensed (slow) deposition, perhaps during relative sea-level highs when clastic input from land diminished.

Transgressive Late Palaeozoic sediments (Early Silurian and/or Early Devonian) are documented locally within the Antalya Complex, notably in the Güzelsu area in the east of the Isparta Angle (NW of the Antalya Window) and the Kemer area in the west of the Isparta Angle (Şenel et al., 1992; Göncüoğlu and Kozur, 2000c). In contrast, sediments of this age range are absent from our main study area in the Alanya Window (area A, Beldibi-Gazipaşa). Either they were never deposited in this area, or they were eroded as a result of Permian rift-related uplift. The eustatic sea level rise following the Ordovician-earliest Silurian glaciation (Göncüoğlu and Kozur, 2000c) is likely to have resulted in regional marine transgression and sediment deposition, such that rift-related Permian uplift is the likely explanation of why Permian sediments directly overlie Ordovician, as in our main study area.

7.2. Late Permian: First major rift phase

The angular unconformity (locally up to c. 15°) between the Late Cambrian-Early Ordovician succession and the Late Permian succession in our main study area (Area A, Beldibi) indicates marked tilting, followed by shallow-marine transgression. The Mid-Late Permian is widely recognised as the time of initial rifting of the Southern Neotethys (Poisson, 1977; Robertson and Woodcock, 1982; Robertson, 1993; Stampli and Borel, 2002; Mackintosh and Robertson, 2012; Şahin et al., 2014). In places along the eastern limb of the Isparta Angle, dolomites are dated as early as Middle Permian (Şenel et al., 1992). Active crustal extension in our area is suggested by the development of neptunian fissures on the unconformity surface.

Microbial carbonates (stromatolites) commonly accumulated above the unconformity in a marginal-marine, lagoonal setting. This was followed by accumulation of shallow-marine carbonates with a diverse fauna, similar to the Late Permian of the Taurides generally, which include invertebrates, dasycladacean and gymnocodiacean algae, and also small benthic foraminifera (Altıner et al., 2000; Şahin and Altıner, 2019). The moderately sorted quartz-rich sands are likely to have been reworked from underlying Early Palaeozoic sandstones and/or directly from Cadomian basement. The sandstone-limestone alternations represent some combination of rift-induced tectonic subsidence and/or eustatic sea-level change during the latest stages of southern hemisphere glaciation (Rygel et al., 2008).

Recent study of the Antalya Complex in the Güzelsu outcrop to the northeast of the Alanya Window (Fig. 2) suggests that rifting began as early as the Capitanian (late Middle Permian), based on reported local intercalations of alkaline basalt (Şahin et al., 2014). Further studies of Permian facies of the Antalya Complex around the Isparta Angle suggest that, in places, rifting began as early as the mid Early-early Late Permian (Late Artinskian-Roadian) (Şahin and Altıner, 2019). After relative quiescence during the early Capitanian, further extension and basaltic volcanism is reported locally (Güzelsu area) during the late Middle Permian (mid-late Capitanian), followed by further tectonic quiescence during the Late Permian (Şahin and Altıner, 2019) until the Griesbachian (earliest Triassic) (Şahin and Altıner, 2019). The Late Permian outcrops in the Alanya Window lack evidence of volcanism or proximal rift-related facies (e.g. rift-related breccias) and are likely to have accumulated during a period of gradual tectonic subsidence and glacio-eustatic sea-level change.

7.3. Early Triassic: Increased tectonic subsidence

The prominent unconformity between the Late Permian and Triassic successions in the Alanya Window represents a period of erosion and/or non-deposition. Elsewhere in the Taurides, notably in the Aladağ unit of the Hadim Nappe and the Kütahya-Bolkardağ Belt, the Permian-Triassic boundary is also characterised by an unconformity, in places followed by rift-related volcanism (Ünal et al., 2003; Göncüoğlu, 2011; Robertson et al., 2009; Mackintosh and Robertson, 2012). This unconformity could be explained by on-going rifting, although a low stand in eustatic sea-level could also explain the break in deposition.

Relatively stable neritic carbonate deposition during the Late Permian was replaced by varied, more terrigenous accumulation during the Early Triassic, probably representing rift-related subsidence and marginal uplift and erosion. Latest Permian low-latitude climate warming and global mass extinction (Erwin et al., 2002; Joachimski et al., 2012) also resulted in a marked change in facies and a switch from a diverse fauna during the Late Permian to an impoverished benthos during the earliest Triassic. This was largely restricted to primitive organisms that deposited microbial carbonate, together with a few species of bivalves, gastropods and small benthic foraminifera. During the Early Triassic, shoals of ooids formed in warm hypersaline lagoons, probably during a time of reduced biogenic carbonate production after mass extinction (Groves and Altıner, 2005). The local development of a karstic surface (Özgül, 1984b) reflects either continuing sea-level fluctuation or on-going rifting. Probably related to gradual tectonic subsidence and/or a rising sea level (Haq et al., 1988), open-shelf conditions developed during the Mid-Triassic (Mid-Late Anisian), with frequent alternations of relatively fine-grained terrigenous sediments (mudrocks) and bioclastic carbonate. Current activity is indicated by reworking of terrigenous sediment, concentrations of bivalve shells and occasional intraformational conglomerates.

7.4. Mid-Triassic (Ladinian): Second major rift phase

The upward passage from Early Triassic shelf sediments to muds, sands and debris-flow deposits indicates increasing sediment accommodation space as a result of further rift-related subsidence. This took place during a period of eustatic sea-level fall (Haq et al., 1988). The presence of debris-flow deposits indicates relatively steep and unstable depositional slopes. Clasts at least as old as early Palaeozoic (sandstone and limestone) indicate that underlying strata, hundreds of metres lower in the stratigraphy, were exhumed and eroded related to this phase of crustal extension. The combined evidence, therefore, indicates a second major rift phase during the Mid-Triassic.

7.5. Late Mid-early Late Triassic: deep-water rift basin

The overlying radiolarian sediments accumulated during the uppermost Ladinian (upper Longobardian) and lowermost Carnian, a time interval estimated as, at most, 4.5 Ma. The reddish brown colour indicates a well-oxidised depositional setting. Where commonly greenish or greyish, this relates to influx of reducing fluids during diagenesis or tectonic emplacement. The impure, muddy composition of the radiolarian sediments and the well-laminated mudstone partings indicate a continuing terrigenous influence, albeit very fine grained. The thin (several cm) laterally continuous, normal-graded quartzose siltstones are interpreted as low-density turbidity current deposits. The fine-grained and uniform nature of the background clastic material suggests a period of relative tectonic stability. Alternative controls on radiolarian deposition were either formation below the CCD or high productivity related to nutrient upwelling (Jenkyns and Winterer, 1982; De Wever et al., 1994). The presence of interbedded bivalve-rich calcareous mudstones and of overlying limestones (see below) indicate deposition above the CCD. High radiolarian productivity is therefore preferred. Water depths are likely to have remained modest (several

hundred metres). Radiolarites that encompass the uppermost Ladinian-lowermost Carnian time interval are reported from farther west, especially the Meliata-Maliac (Vardar) unit of the Eastern Mediterranean region, where, in contrast, they accumulated on oceanic crust. Similar, but more long-ranging, radiolarites are reported from the eastern Tethys in Oman (Hawasina) and Tibet (Yarlung-Tsangpo), again mainly above oceanic crust (De Wever et al., 1994).

In several areas (e.g. Slovenian and Pindos-Budva units of the Adria continental margin), Mid-Triassic radiolarian deposition ended before the Late Anisian, pointing to local variability in the timing of radiolarite accumulation (although this could be an artefact of variable terrigenous input). The reddish, well-oxidised nature of the radiolarian sediments indicates that the rift basin in the Alanya Window experienced an unrestricted open-ocean connection, probably with an already established deep-water seaway bordering North Africa (Robertson et al., 1991; Barrier et al., 2018).

After radiolarian-rich sedimentation ended there was a return to more diverse sedimentation, with alternations of radiolarian-bearing terrigenous muds, quartzose silts and impure limestones (marls), mainly deposited by low-density turbidity currents. A possible explanation for the end of the radiolarian deposition is simply increased dilution by terrigenous material. However, in many other continental margin settings (e.g. Adria, as above) Mid-Triassic radiolarian deposition was followed by the accumulation of pelagic chalks with chert nodules. This suggests that the Middle (to earliest Late) Triassic radiolarites relate to a specific Tethys-wide period of enhanced climate and/or current controlled upwelling. The Mid-Permian is recognised as one of five periods when the global oceans were nutrient-rich, related to climate change or tectonics (uplift). During this time, there was increased weathering and continental run-off of silica to adjacent marine basins (Large et al., 2015).

7.6. Late Triassic (Carnian): Third major rift phase

The mainly fine-grained sediments were succeeded by coarser-grained sandstone turbidites, interspersed with localised debris-flow deposits and, in places, with exotic lenses and blocks (olitostromes). Their thickness (several hundred metres), lithoclastic composition and scarcity of fossils point to rapid deposition without a significant break. Where present, benthic foraminifera are contemporaneous but reworked (Özgül, 1984b; *this study*). Derivation from a tropically forested landscape is indicated by the abundance of plant detritus. The metamorphic rock debris and rare granitoid rock clasts point to widespread exhumation and erosion of metamorphic basement, similar to the Cadomian of the Alanya Massif (i.e. Anamur area) (Çetinkaplan, 2018) and the Tauride continent generally (e.g. Sultandağ Massif; see above). The relatively lithoclastic and mica-poor composition of the Late Triassic turbidites points to rapid sediment transport/deposition with little reworking. The well-rounded clasts within the lenticular mass-flow conglomerates are likely to have originated from a river or beach environment, followed by transport and accumulation within deep-marine channels. The clast composition suggests that all parts of the underlying succession (e.g. Cambrian-Ordovician sandstone; Permian carbonate rocks) shed detritus to the deep-water rift basin.

Rift blocks that previously supplied lithoclasts to the underlying Mid-Triassic debris-flow deposits are likely to have been reactivated during the Late Triassic. However, the source area appears to have increased by the Late Triassic because, amongst the clasts present, black chert is characteristic of at least Silurian and Carboniferous-aged deep-water successions, as exposed in allochthonous Palaeotethyan units along the northern margin of the Tauride-Anatolide continental unit (e.g. Konya Melange and Çataloturan unit (Afyon Zone)) (Göncüoğlu et al., 2007; Robertson and Ustaömer, 2009). Black chert, typically as well-rounded grains, is a minor constituent of Late Triassic turbidites throughout the Antalya Complex (Gutnic et al., 1979; Robertson and Woodcock, 1982; Waldron, 1984b).

The exotic blocks and lenses are suggested to represent rift fault blocks that were exhumed during the Late Triassic third major rift phase, resulting in exposure at, or near, the sea-floor, where they became unstable and collapsed into the deep-water rift basin. Comparable collapsed material is well known from extensional rift basins elsewhere, including the Dolomites (N Italy) (Bosellini et al., 1977), southern Italy (Bosellini et al., 1993) and central Greece (Johns, 1978).

7.7. Late Triassic rift magmatism

Elsewhere in the Antalya Complex, the latest Triassic (middle-late Carnian) was characterised by extensive deep-water eruption of alkaline, OIB-type basalts (Marcoux, 1970; Monod, 1977; Robertson and Woodcock, 1981c; Robertson et al., 1991; Varol et al., 2011). In the Güzelsu outcrop to the northwest (Fig. 2), basaltic rocks are locally overlain by pelagic sediments dated as late Carnian-early Norian in age (Varol et al., 2007).

The basaltic eruptions in the Antalya Complex can be interpreted in three ways: first, as a major phase of crustal extension, followed by tectonic quiescence (i.e. a failed rift (aulacogen)); secondly, extension leading to final-continental break-up to form oceanic lithosphere; or, thirdly, as plume-influenced magmatism (with or without crustal extension). Latest Triassic enriched mid-ocean ridge basalt (E-MORB) to normal mid-ocean ridge basalt (N-MORB), together with deep-water sediments (e.g. radiolarites; Halobia limestones) occur elsewhere in the easternmost Mediterranean, including the SW segment of the Antalya Complex (Antalya-Kumluca) (Robertson and Waldron, 1990), the Adıyaman area (Uzunçimen et al., 2011; Robertson et al., 2016), and western Cyprus (Malpas et al., 1993). The combined evidence suggests that some sea-floor spreading took place within the South Neotethyan region during latest Triassic-earliest Jurassic time (Robertson and Woodcock, 1982; Marcoux, 1979, 1995; Robertson et al., 2012, 2016). Final continental break-up appears to have taken place during the latest Triassic (middle-late Carnian) in the Antalya Complex and was possibly plume-influenced. However, Late Triassic rift-related magmatism in the Alanya Window is mainly restricted to rare sills of alkaline basalt cutting Triassic deep-marine sediments. The probable explanation is that these successions formed in a proximal (near-continental) setting well away from the locus of extensional magmatism.

7.8. Jurassic-Cretaceous post-rift subsidence

The Jurassic-Cretaceous successions in the Alanya Window and elsewhere in the Antalya Complex relate to regional passive margin subsidence. Two contrasting Jurassic-Cretaceous successions are recognised in the northeast of Area A (Beldibi Kayası-Başköy). One succession is fine-grained, mainly made up of radiolarites and micritic limestones of Late Jurassic-Late Cretaceous age (Fig. 15a); the other encompasses a similar time range but with Early Jurassic-Early Cretaceous redeposited neritic carbonates, overlain by Late Cretaceous pelagic carbonate (without radiolarites) (Fig. 15b).

Comparison with other units of the Antalya Complex, notably the Hocaköy section in the Güzelsu area to the northwest (Tekin, 2002), and elsewhere in the Antalya Complex (Robertson and Woodcock, 1981a, 1981b; Robertson and Woodcock, 1982; Vrielynck et al., 2003) suggests that background radiolarian deposition persisted regionally throughout Early Jurassic-Early Cretaceous time in distal-margin settings.

In many south-Tethyan areas, including the Isparta Angle and the Adria continental margin farther west, earliest Jurassic (Hettangian-Sinemurian) successions are mainly mudstone/shale or siliceous limestone and chert, whereas ribbon radiolarites predominate from late Early to early Middle Jurassic (Bajocian in Antalya), to the early Late Cretaceous (Cenomanian) (*De Wever et al., 2014*). The radiolarian accumulation in the Antalya Complex, as elsewhere, can be explained by high plankton productivity in a deep-water basin along a rifted passive

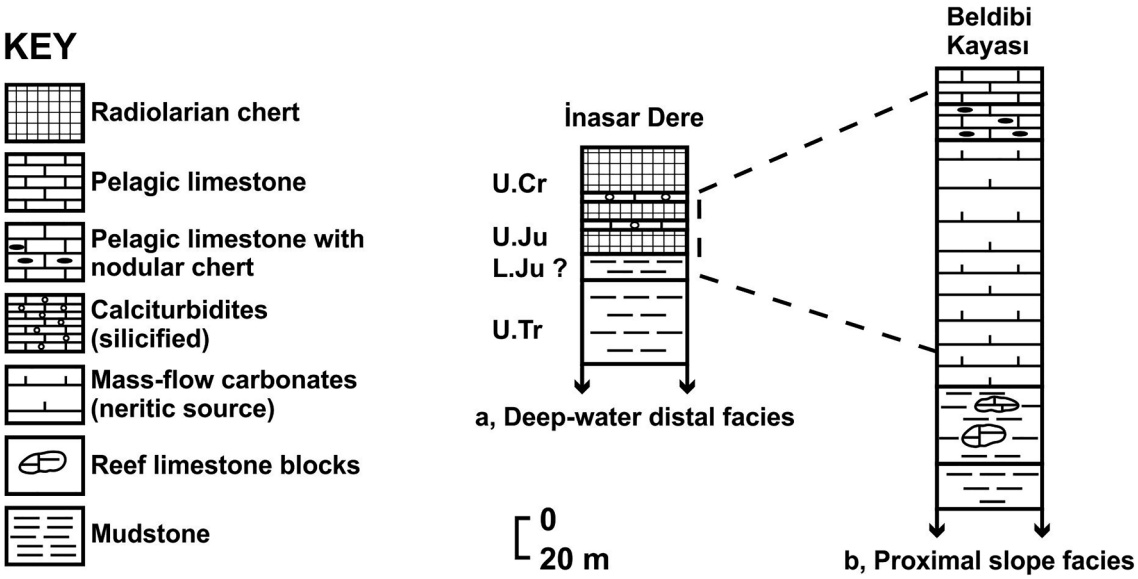

Fig. 15. Summary of the Late Triassic-Late Cretaceous successions exposed in the northwest of the Antalya Window in the İnasar Dere and Beldibi Kayası areas (NE part of Area A). The İnasar Dere succession represents relatively distal deep-water facies (also exposed near Başköy), whereas the partially contemporaneous succession at Beldibi Kayası (within several kms.) is interpreted as carbonate platform margin/slope facies, overlain by hemipelagic/pelagic carbonates.

margin or in an oceanic setting (Jenkyns and Winterer, 1982). The normal-graded, commonly silicified, interbeds represent calciturbidites that were derived from a contemporaneous shallow-water carbonate platform; they accumulated below the CCD where they underwent diagenetic replacement by silica.

Where present (Başköy section), the pinkish/greyish-coloured micritic to sandy carbonate interbeds with calcified radiolarians (up to several metres thick) are interpreted as redeposited periplatform ooze that accumulated in a deep-water relatively distal setting, adjacent to a carbonate platform. These deposits are comparable with some 'drift' deposits, as reported from modern carbonate platforms, including the Bahamas (Betzler et al., 1999), the Maldives, and ancient platform margins in the Alpine-Mediterranean Tethyan region (Eberli et al., 2019).

The exposed base of the second, more proximal succession (Beldibi Member) (Fig. 15b) is dated as no younger than latest Triassic (Norian) at its base by the presence of the reef limestone blocks of this age (Özgül, 1984b). Similar reef blocks characterise relatively proximal facies of the Antalya Complex around the Isparta Angle, notably in the Güzelsu area to the northwest and north (Monod, 1977; our unpublished data), in their type area (i.e. Tilkideliği Formation of the Çatal Tepe Group) in the SW segment of the Antalya Complex (Antalya-Kumluca), and in the apex of the Isparta Angle (e.g. Eğridir area), where similar reef blocks are dated as late Carnian and early Norian (Poisson, 1977; Robertson and Woodcock, 1981b, 1984; Robertson, 1993; Şenel et al., 1996, 1998, 1999).

The abundance of colonial coral, some of it in life position, points to rapid growth and then collapse of the reef edge during the Norian. This could be explained by tectonic disturbance, relative sea-level change, or a regional to global biotic crisis. Coral reefs expanded and diversified during the Mid-Late Triassic and were then strongly affected by the latest Triassic global mass extinction (*Flügel et al., 2001*). However, the input of reef blocks appears to predate this biotic crisis. Tectonic subsidence during late-stage rifting and inferred continental break-up during the Mid-Carnian are likely to have stimulated reef-growth and subsequent collapse. On the other hand, the Late Triassic was characterised by a major eustatic sea-level fall (Haq et al., 1988) which could also have triggered collapse of the platform margin.

The mudrocks containing latest Triassic (Norian) reef blocks are directly followed by carbonate mass flow-deposits, with a Rhaetian to Early Jurassic shallow-water biota (Beldibi Kayası Member). The presence of benthic foraminifera and calcareous algae, in particular, indicate continuing carbonate redeposition from a neighbouring carbonate platform during Early Jurassic-Early Cretaceous time. Neritic carbonate input eventually gave way to silica-rich micritic carbonate deposits that were diagenetically reconstituted to form nodular (replacement) chert. The overlying pelagic limestones of Campanian-Maastrichtian age accumulated during a time when parts of the Tauride carbonate platform (e.g. Bey Dağları in the SW) were drowned and undergoing pelagic carbonate deposition (Poisson, 1977; Hayward and Robertson, 1982; Sarı and Özer, 2002; Sarı, 2009), reflecting some combination of regional tectonic subsidence or eustatic sea-level rise. In contrast, shallow-water deposition continued in some areas into the late Maastrichtian, including the northern part of the Mesozoic carbonate platform (Geyik Dağ) in the Central Taurides, to the north and northwest of the Alanya Window (Solak et al., 2017, 2019).

The two contrasting Jurassic-Cretaceous successions in the northwest (Area A) are interpreted as distal deposits (Fig. 15a) versus more proximal (Fig. 15b) that both accumulated during passive margin subsidence. The localised, lenticular redeposited limestone-dominated succession could represent a platform-margin (distal) sediment lens or channel, explaining the co-existence of similar-aged, more pelagic facies in a small area. Comparable-scale platform-margin channels are known from modern carbonate platforms such as the Bahamas (e.g. Eberli et al., 2019), and from emplaced Tethyan units, as documented in the Oman Mountains (Watts and Garrison, 1986; Cooper et al., 2016) and Ladakh (N India) (Robertson and Degnan, 1993).

7.9. Jurassic-Cretaceous carbonate platform slope development

The mainly Jurassic carbonate rocks carbonate rocks forming the higher levels of the tectono-stratigraphy in the central and eastern outcrop of the Alanya Window (Areas B-E) are interpreted as the emplaced remnants of a single carbonate platform or proximal slope unit, at least 60 km long from NW to SE and up to c. 1 km thick. The Jurassic-Cretaceous carbonate facies thinned westwards and are preserved only a localised lens or channel in the NW of Area A (Beldibi Kaysı Member (Fig. 15b).

One possible interpretation is that the Jurassic-Cretaceous lithologies represent carbonate platform or proximal slope facies of the

Mesozoic carbonate platform (Geyik Dağ) to the north, mainly based on the following: 1. The limestones include slope facies rather than entirely in situ platform facies as would be expected for an off-margin carbonate build-up (e.g. coral reefs), similar to those represented by the Tahtahlı Dağ unit in adjacent ourcrops of the Antalya Complex, for example the SW segment of the Antalya Complex (Kemer area) and in the Güzelsu outcrop (to the northwest) (Poisson, 1977; Monod, 1977, 1979; Marcoux, 1979; Robertson and Woodcock, 1982; Şenel et al., 1996); 2. The Jurassic-Cretaceous limestones are not floored by a regional-scale thrust, as reported for the Tahtahlı Dağ unit (upper Antalya nappe) as in some other area (e.g. Güzelsu outcrop) but instead preserve hints of an original stratigraphic relationship with the underlying Triassic succession; 3. The limestones occur above deep-water Triassic facies, whereas the upper Antalya nappe (e.g. Güzelsu outcrop) commonly includes pre-rift Palaeozoic lithologies; 4. The latest Triassic facies in Area A (Beldibi Member) are very similar to the Tilkideliği Formation of the Çatal Tepe Group elsewhere, which is interpreted as (thrust-emplaced) proximal facies of the autochthonous carbonate platform (e.g. Bey Dağları) (Poisson, 1977; Robertson and Woodcock, 1982); 5. Similar carbonate platform slope deposits, correlated with the Geyik Dağ, are recognised to the northwest in the Güzelsu outcrop (Monod, 1977; Şenel et al., 1980). Specifically, the Karasay unit overlies Late Triassic sandstones and is dominated by Early Jurassic-Late Cretaceous redeposited, platform-derived carbonates. The succession ends with Late Cretaceous *Globotrunca*-bearing pelagic limestones and marls, silts and limestone mass-flow deposits, similar, for example, to the well-exposed facies in Area A. However, further study of the biostratigraphy and facies of the upper limestone unit in the Antalya Window is still needed to test this alternative.

The succession in the northeast of Area A (Başköy section) includes a mixed assemblage of radiolarian sediments of Cenomanian and/or Turonian age, redeposited fine-grained to sand-sized carbonate, lithoclastic sandstone, shale and occasional pebbly debris-flow deposits. The lithoclastic sands were reworked from the directly underlying succession while still not fully consolidated. These sediments can be compared with the Late Cretaceous redeposited carbonates, lithoclastic carbonates, hemi-pelagic carbonates and debris-flow deposits that form the higher stratigraphical levels of the upper limestones units, as observed in areas B-D (Karaçukur Formation of Ulu, 1988). These sediments are also similar to the Late Cretaceous Yavça-type facies, as well exposed in the uppermost levels of the Tauride carbonate platform (Bolkar Dağ) farther east (Parlak and Robertson, 2004).

7.10. Latest Cretaceous emplacement-related foredeep

Late Cretaceous pelagic limestones in the autochthonous Tauride platform succession (e.g. Bolkar Dağ), in places, pass upwards into calciturbidites, debris-flow deposits, lithoclastic muds, sand/silt turbidites and detached blocks (olistoliths). This heterogeneous succession records the collapse of the carbonate platform, probably related to regional flexural loading, associated with the emplacement of allochthonous rocks. Similar facies occur between the Tauride carbonate platform (Geyik Dağ) and the over-riding Antalya Complex along the eastern limb of the Isparta Angle (Robertson, 1993; Şenel et al., 1996, 1998, 1999). The Late Cretaceous pelagic and redeposited facies in Area A (Başköy section) and more widely in Areas B-D are interpreted as the result of tectonic destabilisation of the source carbonate platform as a precursor to tectonic emplacement of the Antalya Complex.

8. Results: Structural evidence for emplacement

The evidence is mainly from the nature of broken formation and tectonic melange, and from structures of up to several kilometre-scale.

8.1. Broken formation and melange

The highest structural levels of the NW outcrop (Area A), NW of Beldibi i.e. along the road to Beldibi and around Çiriş Tepe c. 250 m farther west (Figs. 4, 5) are characterised by a distinctive body of highly sheared sandstone and shale, with strongly elongated (phacoidal) blocks. The exposure includes shear-bounded units of cleaved shale (individually up to tens of metres thick), with clasts of silicified limestone (up to 25 cm in size), ribbon chert (with locally N-verging folds), silicified calciturbidites (in units up to c. 40 m thick), dark grey-black organic carbon-rich limestone (strongly tectonised and calcite-veined), indurated coarse-grained grey sandstone, and also blocks (up to c. 20 m in size) of coarsely crystalline dolomite and reddish marble. Previously, this lithological assemblage was interpreted as an olistostrome (i.e. sedimentary debris-flow deposits), stratigraphically above Late Cretaceous pelagic limestones (Çiriş Tepe Member of Özgül, 1984b). Units of the subjacent Palaeozoic-Mesozoic succession are indeed present, one of which contains *Orbitoides* sp. of indeterminate late Mesozoic-Cenozoic age (Özgül,1984b). However, the blocks and lenses are separated by sheared tectonic contacts without any sedimentary matrix or sedimentary interbeds. The units with locally semi-coherent sections are instead interpreted as broken formation and the block-like units as tectonic melange. The deformation is attributed to the emplacement of the Antalya Complex during the latest Cretaceous, post-dating the youngest, Late Cretaceous part of the underlying intact succession (i.e. İnasar Dere and Beldibi Kayası Members).

8.2. Structural evidence

Small to large-scale structures in the Antalya Complex were investigated mainly in Area A (Beldibi-Gazipaşa), with additional reconnaissance data from Areas B-E further southeast. The number of measurements made of different structures are summarised in Table 2, whereas the location numbers, geographic co-ordinates, inferred age, lithology and other details of the structural measurements are listed in the supplementary material. In addition, Google satellite images marking the sample locations are available from the authors on request.

8.2.1. Antalya Complex-Alanya Massif contact relations

The contact between the Antalya Complex and the metamorphic Alanya Massif is a variably dipping thrust, with metamorphic rocks above (Okay and Özgül, 1984; Özgül, 1984b; MTA, 2000). In some areas, there is a clear lithological contrast between very low-grade-metamorphosed (anchizonal-diagenetic grade) lithologies of the Antalya Complex below, and greenschist facies schist and marble of the Alanya Massif above (e.g. NE of Beldibi). Near the coast (e.g. between Gazipaşa and Demirtaş; loc. 5.1) the uppermost c. 10 m of the Antalya Complex is highly strained with a pervasive low-angle crenulation cleavage and crenulation folds that are north-verging and trend subparallel to sedimentary bedding (locs. 5.3 & 5.4; e.g. Kocakefir; GPS 36S

Table 2
Summary of measurements made of different outcrop-scale structures in the Antalya Complex in the Antalya Window. Further details are given in the supplementary material.

	Planes	Lineations
Bedding	227	12
Cleavage	80	8
Schistosity/tectonic fabric	115	24
Shear/Thrust	193	13
Fold	257	212
Quartz Vein	14	3
Penetrative Fault	50	21
Joints	12	
Fracture	6	

0429761 4021941). Where, rarely, the thrust contact is well exposed (e.g. loc. 5.2; GPS 36S 029761 021941) there is a local c.10° angular discordance between highly sheared and recrystallised dark (Permian?) limestone and mylonitically deformed marble marking the base of the Alanya Massif above. The Antalya Complex in the east (near Anamur) is also highly deformed and recrystallised, similar to the adjacent Alanya Massif.

North of Gazipaşa (c. 4 km inland, near Hocalar; loc. 5.10; GPS 36S 0431235 2028310), Triassic pebbly debris-flow deposits of the Antalya Complex and overlying thick-bedded pale-grey marble of the Alanya Massif both include small-scale folds and C-S fabrics that are indicative of local top-to-the north displacement. Top-to-the north fabrics were also observed further northwest, between Gazipaşa and Demirtaş. However, elsewhere (i.e. N of Yakacık; loc. 8.1; GPS 36S 0462822 3997762) the lowest levels of the Alanya metamorphic rocks close to the Antalya Complex include well-developed C-S fabrics indicative of local top-to-the south movement, suggesting a complex deformation history.

8.2.2. Outcrop-scale deformation style

The generally thick-bedded Late Permian, mainly carbonate rocks, are relatively undeformed (e.g. Fig. 16a). However, in places they have undergone large-scale semi-ductile folding (Fig. 16b) and/or brittle-style upright, to inclined folding (Fig. 16c). More thinly bedded, commonly shale-rich lithologies, for example Early Triassic thin-bedded limestone-shale and Mid-Triassic ribbon radiolarites commonly show complex and locally variable deformation. Most folds are of cylindrical type with bed thickness remaining relatively constant around fold hinges and limbs (e.g. Fig. 16d). However, some folds, especially those towards the south, where the metamorphic grade is higher (see below) exhibit fold hinge-thickening/limb-thinning and axial planar cleavage, with mineral-filled tension gashes on some fold limbs (Fig. 16e). Mid-Triassic ribbon radiolarites are commonly deformed into trains of chevron folds (Fig. 16f). Some folds are dissected by high-angle faults (Fig. 16g). Outcrop-scale reverse-faults and thrusts are locally present (Fig. 16h). Intense deformation in the form of crenulation folding and strain-slip cleavage were rarely observed (Fig. 16i-j). In places, Triassic debris-flow deposits are strongly deformed by shearing and layer-parallel extension to form phacoidal fabrics (Fig. 16k). The broken formation and tectonic melange in the highest levels of the tectonostratigraphy, east of Belbidi Kayası (Fig. 16l) and also east of Yenişehir, have complex and variable structural fabrics indicative of high-stain conditions, including locally developed trains of asymmetrical folds with top-to-the north vergence.

8.2.3. Outcrop-scale structural geometry

Measurements were routinely made of sedimentary bedding, schistosity (or related tectonic fabric), reverse fault/thrust planes, shear planes, cleavage, quartz veins, penetrative faults, joints and fractures (all as dip and dip directions; see Supplementary material). Folds were measured as dip and dip direction of fold axial planes and as trend and plunge of fold hinges. Structural asymmetry (e.g. fold vergence and/or fold facing) was noted in relation to stratigraphical way-up, where possible. The data for bedding, cleavage/schistose fabric, shear planes and fold axial planes proved to be the most useful for interpretation of kinematics.

The structural data were initially plotted for the Antalya Complex as a whole, revealing an overall dominance of c. E-W orientated structures. To increase resolution, the area as a whole was divided into the main study area in the northwest (Area A, Beldibi-Gazipaşa Fig. 3), and areas farther east (Areas B-E; Fig. 3), where only reconnaissance data were collected.

The main study area (Area A) was further subdivided into a southerly segment (S of Lordlar) (Fig. 5) and two more northerly segments in which the structures were analysed in terms of the stratigraphic units in which they occur. Structures in the southerly segment (Fig. 17a) have the following main features: 1. Bedding orientation is relatively coherent within the Cambrian-Ordovician succession striking WNW-ESE, whereas there is no preferred orientation in the Permian-Triassic succession; 2. Shear planes and folds cutting the Cambrian-Ordovician and Triassic successions have dominantly E-W and NW-SE orientations; 3. Limited kinematic evidence suggests top-to-the-SW displacement.

The northerly part of Area A was subdivided into northeasterly and northwesterly sub-regions. Both sub-regions show less coherence than the southern segment (Fig. 17b). The north-westerly sub-region has the greatest structural complexity, as there is no preferred orientation of bedding or tectonic fabrics, although folds are mainly orientated N-S to NNE-SSW. The north-easterly sub-region shows slightly more structural coherence, with Palaeozoic and Triassic successions showing dominantly E-W trends to bedding (e.g. around Lordlar). Shear orientations are again mainly E-W, although with subordinate NW-SE and NE-SW trends. Some folds trend parallel to tectonic fabric/shears, although with subordinate NW-SE and NE-SW trends. Other folds have axes that trend at right angles to the main E-W tectonic fabric. Data from farther east (e.g. around Yeniköy) for Palaeozoic-Triassic lithologies have relatively more consistent NW-SE bedding orientations and structural fabrics.

For the central and easterly areas of the Alanya Window (Areas B-E), structural data were subdivided into those from the mainly Permian-Triassic lower tectono-stratigraphic levels in the south, and those from the higher tectono-stratigraphic levels in the north, dominated by Jurassic-Cretaceous lithologies. The mainly Triassic strata have an E-W to WSW-ENE structural grain, with E-W to WSW-ENE trending folds, shears (with m to 10 s m offsets) and schistosity. In contrast, the Jurassic-Cretaceous strata have complex and heterogeneous structures of commonly ductile and semi-ductile character. The Jurassic is preferentially aligned E-W to WNW-ESE, whereas the Cretaceous is orientated NW-SE. The Jurassic and Cretaceous are cut by both NE-SW and NW-SE shears (with m to 10 s m offsets) and deformed by E-W and NW to c. N-S trending folds.

In summary, the outcrop-scale structures have a complex and variable pattern which largely reflects the presence of large, km-scale structures.

8.2.4. Larger structures observed on satellite images

Satellite images were examined to shed light on larger-scale structures (100 s of m to kms). The most obvious large-scale structures are observable on well-exposed (but relatively inaccessible) mountainous outcrops. However, these features cannot be easily correlated with the outcrop-scale data that were mainly collected from road sections in topographically lower areas.

In the south of Area A (i.e. N of Gazipaşa) the mainly Palaeozoic stratigraphy (e.g. Permian limestones) is relatively continuous on a c. WNW-ESE trend, consistent with the observed outcrop-scale structures. The stratigraphy is highly folded, commonly with variably orientated recumbent folds (up to km-sized) (e.g. Fig. 18a). In Area C (Adanda), high-angle faults are orientated at high-to low angles relative to bedding, with evidence of extension (or transtension) parallel to bedding (Fig. 18b). Along strike farther southeast (i.e. NE of Öznurtepe) (Fig. 18c) and also north of Yakacık (Area D; Fig. 18d), several folds exhibit semi-ductile fabrics and are variably c. NW to SW-vergent.

The northwest part of Area A is dominated by a km-scale SE-vergent recumbent fold (S of Fakırcalı) that has been refolded into an upright anticline with a local NNE-SSW axis (Fig. 18e). The area farther south (around Lordlar) is dominated by the southward continuation of the same anticlinal structure. This has an irregular c. N-S to NNW-ESE trend which hints at later-stage N-S compression (Fig. 18f). The c. N-S anticline deforms a limb of the pre-existing SE-verging recumbent anticlinorium (Fig. 18g). In the far northeast of Area A (Beldibi area) there is a c. NW-SE trending antiform with steeply dipping limbs (Fig. 18h). Locally (e.g. near Ilıca) an open NW-vergent anticline is imaged (Fig. 18i).

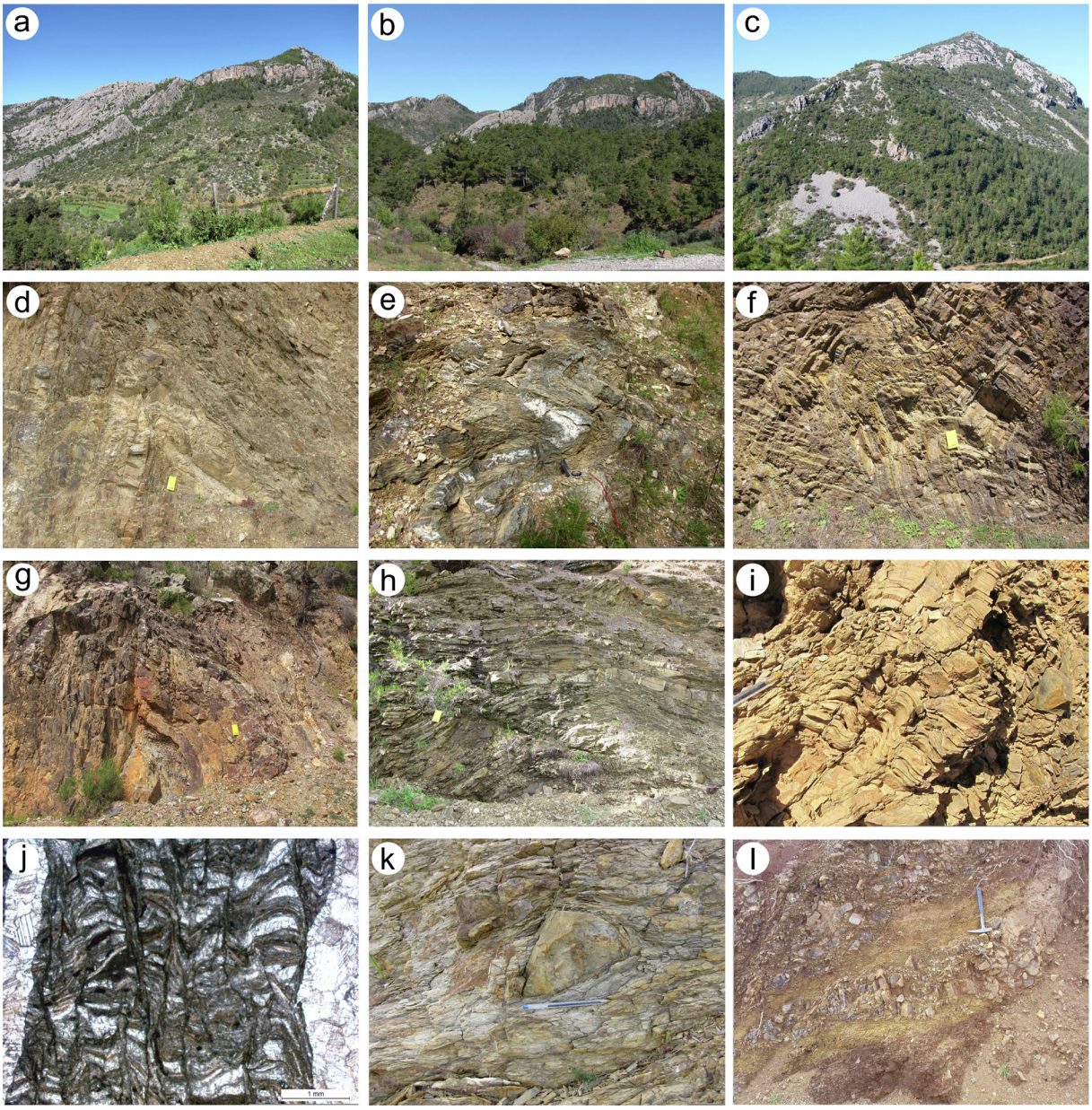

Fig. 16. Field photographs and photomicrograph of structures in the Alanya Window. **a,** Relatively intact Ordovician-Permian succession, viewed to the NW; 1 km N of Yeniköy (loc. 6.2). Ordovician strata (lower, central) are soft-weathering, whereas overlying Permian carbonates are erosionally resistant; note recumbent folding to the east; **b,** Wider-scale view of the structure shown in a, also showing the overlying Triassic succession dipping regularly westwards (upper left); **c,** Structure shown in a and b viewed to the west, showing refolding into a large upright anticline (truncated by a high-angle fault; hence the scree in the foreground); **d,** Tightly folded Late Triassic sandstone turbidites; 1.5 km NNE of Karalar (loc. 4.6; GPS 36S 0438849 4024187); **e,** Recumbent fold in Late Triassic sandstone turbidites with axial planar cleavage development and tension gashes on limbs (loc. 4.1); **f,** Inclined chevron folds in Mid-Triassic radiolarite; Taşlıca area (loc. 10.4; GPS 36S 0432579 4037415); **g,** Early Triassic limestone-shale, folded (axial plane 242/20) and later dissected by a high-angle fault (plane 082/22, slickenlines 70/084); 2 km NW of Karalar (loc. 3.3; GPS: 36S 0437806 4022124); **h,** Low-angle reverse fault cutting Ordovician sandstones and shales; 0.5 km N of Lordlar (loc. 6.8; GPS: 36S 0435972 4033277); **i,** Crenulation folds with spaced fracture cleavage in Triassic calcareous shale; Adanda area (Area C; loc. 10.8; GPS: 36S 04510228 4010190); **j,** Photomicrograph (crossed nicols) showing strain-slip cleavage dissecting bedding in Early Triassic bioclastic limestone at a high angle. Both margins are cut by later-stage veins of calcite spar. Calcite veins (on both sides) indicate later-stage dilation; near İnasar Dere (Area A) (near 36S 0438825 4035667); **k,** Triassic pebbly debris-flow deposit affected by layer-parallel extension and related small high-angle fault; c. 1 km E of Yeniköy (loc. 3.11; GPS: 36S 0440513 4030667); **l.** Highly sheared and disrupted thin-bedded silicified limestone and shale (broken formation) from the highest structural levels of the tectono-stratigraphy; Çiriş Tepe area (near 36S 0439894 4035323).

The Jurassic-Cretaceous succession exposed in Areas B-E, has a NW-SE trend that can be traced for tens of kilometres laterally. In places, the limestones are isoclinally folded about c. NW-SE axes. The stratigraphy is commonly dissected into lenses or blocks by oblique normal faults that range from a high-angle to bedding, to bedding sub-parallel (e.g. N of Korucuk; Fig. 18j). Some tight to isoclinal folds have a southerly vergence (e.g. road to Adanda castle; see Supplementary Fig. 2). Some open, concentric structures tend to be more north-vergent (e.g. NE of Karaçukur; Fig. 18k). A good example of high-angle brittle faulting that affects the window as a whole is exposed in the northwest (N of Çamlıca; Fig. 18l) where offsets indicate local right-lateral shortening.

Overall, the combined outcrop and satellite image data indicate dominantly NW-SE to E-W structural trends, commonly with relatively early isoclinal, recumbent folding. In places, semi-ductile-type

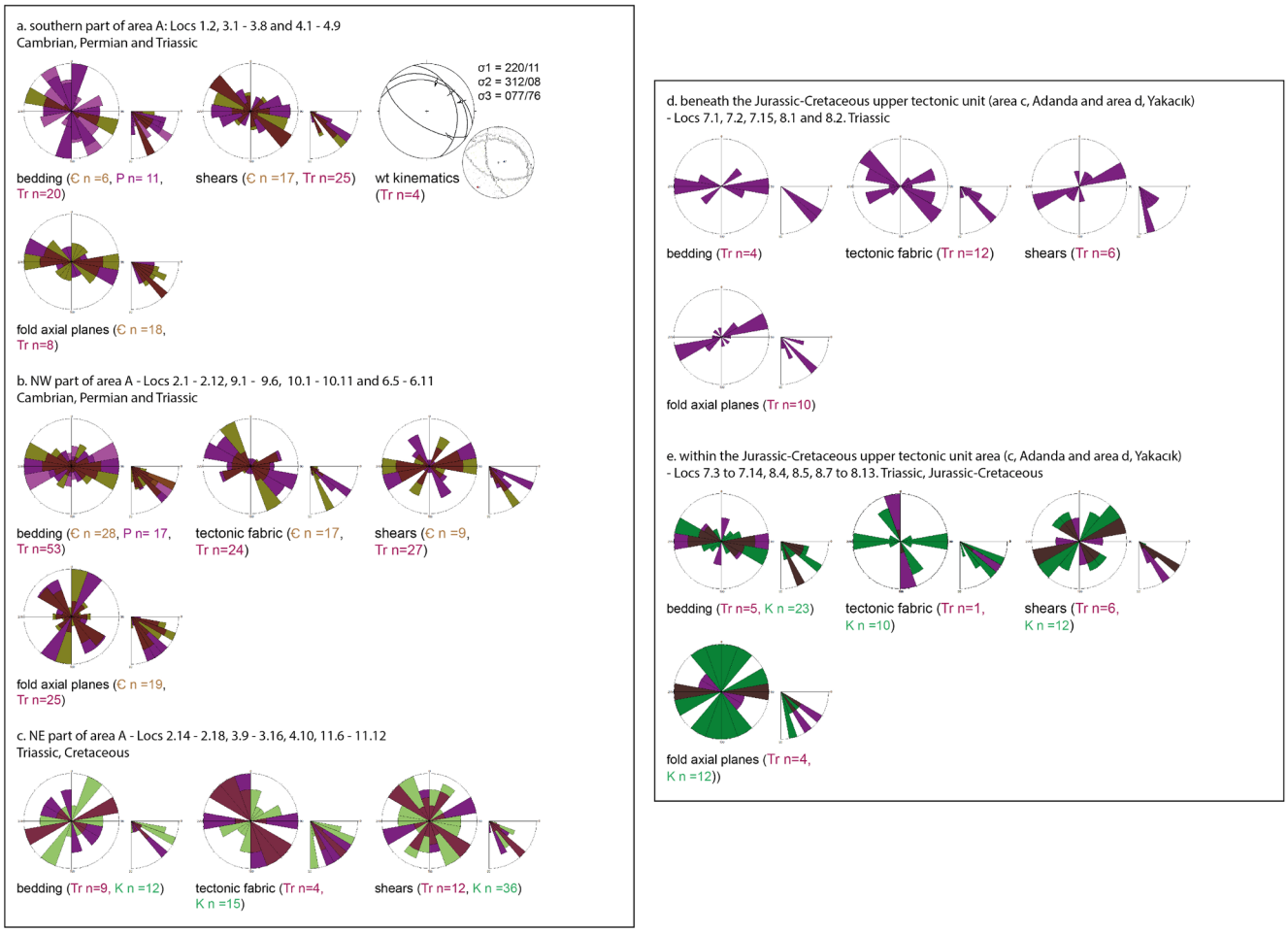

Fig. 17. Structural data mainly collected from the westerly outcrop (area A) of the Antalya Complex in the Alanya Window, together with a pilot study of several areas farther SE. **a,** Southern part of area A; **b,** NW part of area A; **c,** NE part of area A; **d,** Beneath Jurassic-Cretaceous carbonates in area C (Adanda) and area D (Yakacık); **e,** Within the Jurassic-Cretaceous upper tectonic unit in area C (Adanda) and area D (Yakacık). The data are plotted as rose diagrams for azimuths (directions) and rose diagrams for dip measurements. Data from different-aged units are indicated in different colours. See text for explanation. The locations (numbered) are shown on satellite images, available from the authors on request.

structures have been deformed into NW-SE to N-S upright to inclined, relatively open folds. The area as a whole is cut by several generations of faults which range widely in trend from c. N-S to c. E-W, with local evidence of compression/transpression and extension to form tectonic blocks or lenses in some areas.

8.3. Metamorphism

The Antalya Complex in the Alanya Window has undergone very low-grade metamorphism, in places reaching greenschist facies (Ulu, 1983, 1988; Özgül, 1984b). The metamorphic grade of the Antalya Complex is higher near the coast (e.g. Demirtaş in the NW; Figs. 3 and 4) than in most places further inland (Özgül, 1984b), as supported by X-ray diffraction data (Bozkaya and Yalçın, 2004, 2005), and also appears to be relatively high in the southeast near the southern contact with the Alanya metamorphics (near Anamur). A possible cause of the variation of metamorphism is increased depth of burial, generally southwards, related to regional northward subduction during latest Cretaceous time.

9. Discussion of structural evidence

The outcrop-scale structural data (Fig. 17) indicate dominantly compressional deformation, with a N-S to NE-SW principal axis; however, folds with E-W, N-S, S-N or variable vergence are all locally present. Satellite images (Fig. 18) confirm the presence of up to several km-sized, semi-ductile-type isoclinal to recumbent, folds. In places, these relatively early structures are deformed by more open c. N-S brittle style folds. The outcrop-scale measurements do not confirm a unique sense of displacement, probably owing to variable degrees of flattening and lateral extrusion. However, the mapping and cross-sections (Ulu, 1988), satellite images, and some small-scale structures provide some evidence for relatively early-stage semi-ductile, generally southward displacement. The later upright c. N-S trending (or oblique) anticlines and synclines resulted from c. E-W compression (or transpression) with a tendency towards northward vergence. Later-stage high-angle brittle-style faults, variably oblique to bedding, in places dissected competent lithologies (e.g. Permian limestones) into blocks or lenses, probably in response to strike-slip/transpression. The kinematic information from the contact zone (10s of metres) between the Antalya Complex and Alanya Massif is mainly suggestive of northward overthrusting.

10. Palaeogeography and tectonic development

10.1. Regional tectonic restoration

In the widely accepted interpretation of the Antalya Complex as having a southerly derivation related to the Southern Neotethys (Özgül, 1984a, b; Monod, 1976, 1977, 1979; Poisson, 1977; Woodcock and Robertson, 1977; Şengör and Yılmaz, 1981; Robertson and Woodcock, 1982, 1984; Yılmaz, 1984; Yılmaz and Maxwell, 1984; Robertson,

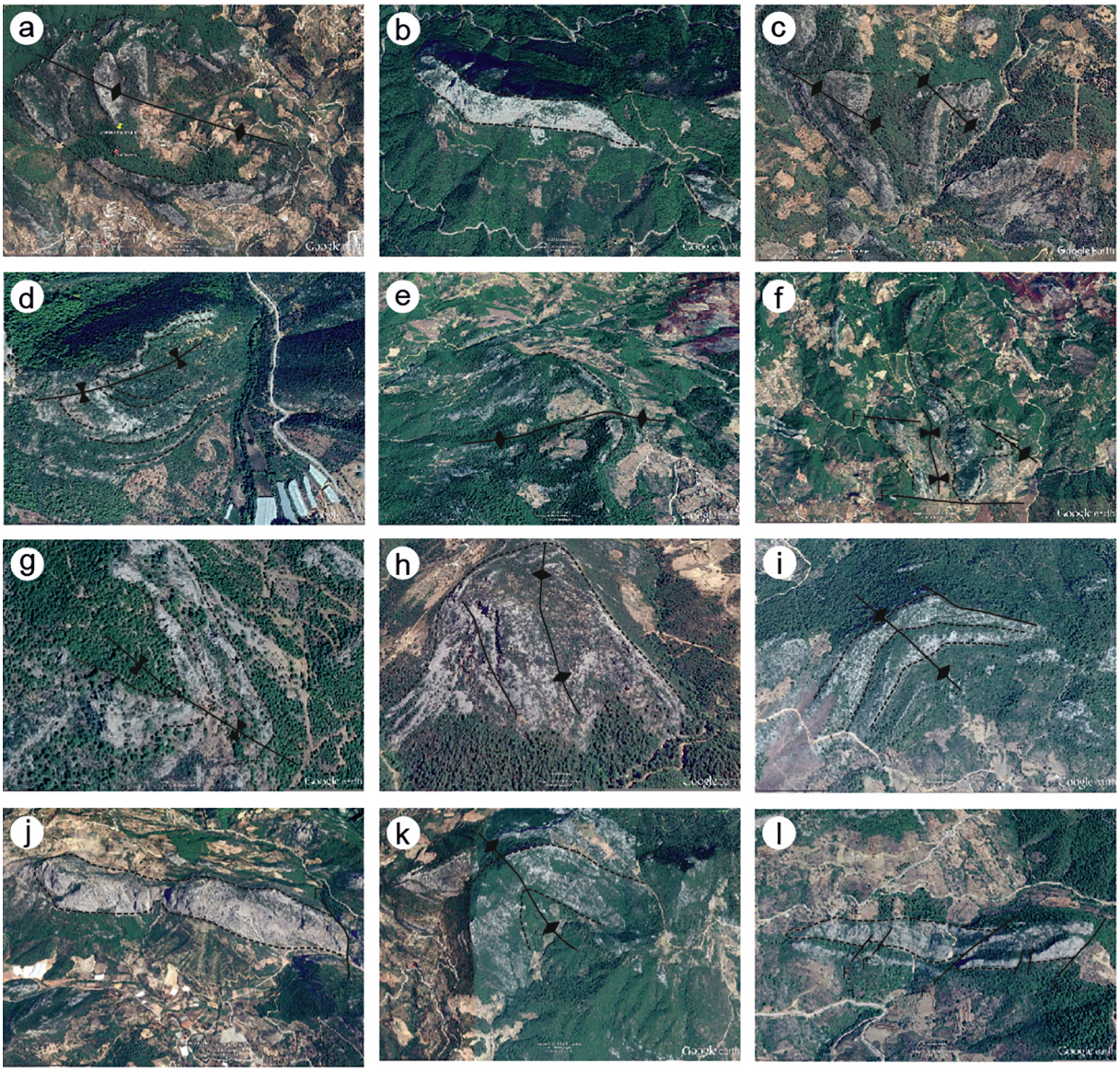

Fig. 18. Satellite images of large-scale structures exposed within the Antalya Window. **a,** WNW-verging recumbent fold deforming Palaeozoic limestone (fault-disrupted); N of Gazipaşa, N of Kızılgüney (area B; 36°22′24.78″N, 32°17′37.89″E); **b,** Mainly N-dipping Permian neritic limestone showing large-scale fault-controlled lateral extension to form semi-detached slabs/blocks; area c, Adanda; 36°14′13.41″N, 32°26′38.47″E); **c,** NW-verging fold in Paleozoic limestone; NW of Öznurtepe (SE of area A; 36°22′19.64″N, 32°23′4.37″E); **d,** WSW-verging recumbent fold deforming Palaeozoic limestone; limbs affected by strain-slip; north of Yakacık (area D; 36° 7′50.52″N, 32°35′4.80″); **e,** E-verging recumbent anticline (faulted) with hint of open-refolding along c. N-S axis; Palaeozoic limestone; just south of Fakırcalı area (NW part of area A; 36°27′52.86″, 32°16′16.72″E); **f,** Approximately N-trending anticline cored by Early Palaeozoic (incompetent) sediments. The structure is folded about c. E-W axes in the north and south and may be part of a larger-scale structure which is truncated in the south by a c. E-W high-angle fault; area around Lordlar (NW part of area A; 36°26′6.69″N, 32°18′13.46″E); **g,** Locally SE-closing syncline within larger-scale E-verging recumbent anticline; SW of Beldibi (NE part of area A; 36°26′20.65″, 32°18′46.04″E); **h,** Local c. NW-SE trending, upright anticline in Palaeozoic limestone; W of Ilıca (NE part of area A; 36°24′11.68″, 32°21′1.50″E); **i,** Inclined open anticline, verging to NW (fault-disrupted), E of Öznurtepe (SE of area A;36°21′28.83″N, 32°25′49.09″E); **j,** North-dipping Mesozoic limestone in southeast of the Window. The limestone is truncated at both ends by oblique extensional faults; N of Korucuk (near area E; 36°13′10.33″N, 32°26′48.00″E); **k,** NW-verging inclined fold deforming Mesozoic limestone; NE of Karaçukur (near area B; 36°17′23.07″N, 32°25′20.84″E); **l,** Steeply dipping Late Palaeozoic limestone; offset and truncated by obliquely-trending high-angle faults. The main fault in the centre-right is offset as a result of right-lateral transpression; c. 1 km N of Çamlıca, northern part of area A.

1977; Robertson et al., 1991; Stampli and Borel, 2002; Şahin and Altıner, 2019), the lithologies exposed in the Alanya Window originated to the south of the Tauride carbonate platform (Geyik Dağ).

Some authors (Göncüoğlu and Kozur, 2000b; Şenel et al., 2000) have argued that the Antalya units were derived from the north of the Tauride carbonate platform mainly because of the Palaeozoic sediments within the Antalya units have a relatively distal aspect, based on facies and palaeontological evidence, compared to exposures within the Tauride continental unit (e.g. Geyik Dağ). This assumes a simple south to north, proximal to distal trend within the northern margin of Gondwana in this region. However, the Cadomian basement of the Tauride continental unit is a mix of different tectono-stratigraphical units of different crustal type and thickness (e.g. arc; back-arc) (Avigad et al., 2006) that could have resulted in a variable palaeogeography during the Palaeozoic, potentially with relatively deep-water basinal settings in both northerly and southerly areas.

In the Güzelsu area (Fig. 3), directly to north and northwest of the Alanya Window, a sizeable outcrop of the Antalya Complex is

sandwiched between the autochthonous Tauride carbonate platform beneath (to the north) and the metamorphic Alanya Complex above (to the south) (Blumenthal, 1951; Monod, 1976; Monod, 1977; Okay and Özgül, 1984; Demirtaşlı, 1987; Şenel et al., 1998, 1999; MTA, 2000). Unlike the Antalya Window, the Antalya Complex in the Güzelsu area is dominated by high-level-type brittle-style thrusting and folding, which also characterise most other outcrops of the Antalya Complex around the Isparta Angle (e.g. Antalya-Kumluca, SW segment) (Woodcock and Robertson, 1977, 1982). Also, the Güzelsu outcrop includes abundant Late Triassic deep-marine basaltic lavas, Jurassic Cretaceous deep-sea pelagic/ hemipelagic sedimentary rocks (e.g. radiolarites) and also some ophiolitic rocks, in contrast to the Alanya Window.

The Late Cretaceous higher levels of the sedimentary succession in the southernmost Geyik Dağ, structurally beneath the Güzelsu outcrop, include abundant detritus from the Antalya Complex (e.g. basalt, chert, sandstone) that is, however, absent from similar-aged successions further north (Monod, 1977). The sediments containing Antalya Complex detritus are dated as Campanian-Maastrichtian, and in one unit (Pirnos block), reliably as Danian (Şenel et al., 1998).

Recent biostratigraphic work confirms that shallow-water carbonate deposition persisted along the northern margin of the Tauride carbonate platform (to the north of the Alanya Window and Güzelsu outcrops) until the Late Maastrichtian, followed, above a major unconformity, by Early Eocene conglomerate (Madenli section) (Solak et al., 2019). Comparable shallow-marine facies existed until the late Maastrichtian-Danian? farther west in the Tauride carbonate platform (Anamas-Akseki area; Kuyucak area) (Solak et al., 2017). The highest levels of the pelagic succession farther east (6 km west of Geyik Dağ) are dated as Danian in age (Özer and Karıman, 2019). There is, therefore, no sedimentary evidence from the Tauride carbonate platform (Geyik Dağ) to support southward emplacement of the Antalya Complex during latest Cretaceous time to provide the observed detritus in the south. The regional evidence suggests instead that the Antalya Complex was emplaced generally northwards onto the Tauride carbonate platform during latest Cretaceous time (Monod, 1976, 1977, 1979, Özgül, 1976, 1984a,b; Demirtaşlı, 1983, 1987; Robertson et al., 1991; Robertson, 1993). In addition, the Eocene, uppermost levels of the intact succession in the Geyik Dağ, directly beneath the Antalya Complex in the Güzelsu area, are dominated by coarse-grained, angular, poorly sorted metamorphic rock debris, including blueschist that was derived from the Alanya metamorphic massif (now exposed several kilometres to the south). This evidence suggests that the Alanya metamorphics were emplaced to their final (present-day) position in response to generally northward emplacement during the Eocene (Monod, 1977; Özgül, 1984a, b; Robertson et al., 1991).

10.2. Restoration as a proximal rift

In general, the Antalya Complex outcrop in the Alanya Window represents a relatively proximal, near-margin part of the Antalya Complex, whereas the Güzelsu outcrop can be interpreted as a more distal, more oceanward part of the same rifted continental margin (Fig. 19). Two alternatives are, first: because the Güzelsu outcrop is the more northerly of the two outcrops, the Alanya Window could restore further south, suggesting a link with the Alanya Massif. However, the Güzelsu outcrop is an imbricated pile of thrust sheets, including broken formation and melange that has clearly been emplaced a substantial distance (many kms) onto the southern margin of the Tauride carbonate platform. In contrast, the Alanya Window successions are folded but more stratigraphically intact, and may have undergone less tectonic transport. Secondly, the Alanya Window outcrop restores to a proximal position close to the Geyik Dağ carbonate platform where, by implication, it was overthrust by the Güzelsu outcrop during its late Cretaceous emplacement. There are no obvious remnants of the Güzelsu outcrop in the Alanya Window beneath the Alanya metamorphic massif (e.g. basaltic volcanics), although these might have been cut out related to erosion or northward emplacement of the Alanya Massif.

Several lines of evidence favour the second interpretation (i.e. proximal rifted margin of Tauride continent): 1. The succession of latest Triassic shales with reef blocks (Beldibi Member) is very similar to the Tilkideliği Formation of the Çatal Tepe Group and its facies equivalents, which characterise the most proximal (continentward) of the allochthonous units emplaced onto the Tauride carbonate platform all around the Isparta Angle (Poisson, 1977; Robertson and Woodcock, 1981b, 1984; Robertson, 1993; Şenel et al., 1996, 1998, 1999); 2. The paucity of magmatic rocks, mainly restricted to rare alkaline basaltic sills, is consistent with a proximal setting away from the rift axis where alkaline volcanism predominated, as best exposed in the SW (Antalya-Kumluca) segment of the Antalya Complex (Marcoux, 1970; Şenel, 1980; Robertson and Woodcock, 1981c); 3. Ophiolitic rocks are absent in contrast to most other outcrops of the Antalya Complex; 4. The Antalya Window successions are relatively intact structurally, consistent with a proximal (continentward) setting compared to the imbricate thrusting experienced by relatively distal units of the Antalya Complex, as exposed in the SW (Antalya-Kumluca) segment of the Antalya Complex (Woodcock and Robertson, 1982) and the NE segment of the Antalya Complex (Waldron, 1984a; Vrielynck et al., 2003).

We, therefore, propose that the Alanya Window outcrop of the Antalya Complex restores to a proximal (northerly) position adjacent to the southern margin of the Tauride carbonate platform (Fig. 20). Similar facies probably accumulated all around the southern periphery of the Tauride continent but, elsewhere, were concealed by Late Cretaceous overthrusting of more distal sedimentary and ophiolitic units. The Jurassic-Cretaceous upper limestones (areas B–E) and facies equivalent to the northwest (Area A) (Beldibi Kayası Member) are tentatively interpreted as Tauride platform and/or upper slope facies that prograded over the proximal margin of the Triassic rift basin. The intermediate tectono-stratigraphic unit in the northwest (Area A) restores to a slightly more distal, southerly position, followed southwards by the lowest tectono-stratigraphic unit which includes the detached blocks and lenses (olistoliths) of pre-rift lithologies near the rift axis.

10.3. Emplacement setting

Radiometric dating of blueschists of the Alanya Massif indicate that HP-LT metamorphism, and also exhumation both took place during latest Cretaceous time, probably related to northward subduction/collision of an Alanya microcontinent beneath the Tauride carbonate platform (Geyik Dağ) to the north (Okay and Özgül, 1984; Okay, 1989; Çetinkaplan et al., 2010, Çetinkaplan et al., 2016a, 2016b). Garnet–glaucophane–phengite schist within eclogitic lenses is dated at c. 85–82 Ma (Santonian–Campanian) and, elsewhere, phengites within schist gave an age of 80–82 Ma (Campanian), implying first, deep-level HP-LT metamorphism (at up to 14–18 kbar), followed by rapid exhumation (Çetinkaplan et al., 2010, Çetinkaplan et al., 2016a, 2016b). The Antalya Complex in the Alanya Window, as elsewhere around the Isparta Angle, was emplaced during latest Cretaceous time. Regional evidence (Anamur area) indicates that the Alanya metamorphic rocks were subaerially exposed during the Late Palaeocene-Early Eocene (Özgül, 1983a, b). The Antalya Complex is likely to have experienced similar exhumation, such that significant erosion may have taken place prior to overthrusting by the Alanya Massif. During the Eocene, the partly eroded Alanya metamorphic massif (several km thick) was emplaced northwards over the Antalya Complex, represented by both the Alanya Window and Güzelsu outcrops (Monod, 1977; Okay and Özgül, 1984; Özgül, 1983, 1984a; Robertson et al., 1991, 2013; Şenel et al., 1999; Çetinkaplan et al., 2010, Çetinkaplan et al., 2016a, 2016b, Çetinkaplan, 2018). The localised broken formation/melange in the uppermost levels of the tectono-stratigraphy (Area A; E of Beldibi) may be a surviving remnant of originally more extensive overthrust units, possibly including relatively distal sediments (e.g. radiolarian chert) and ophiolitic rocks, as exposed in the Güzelsu area.

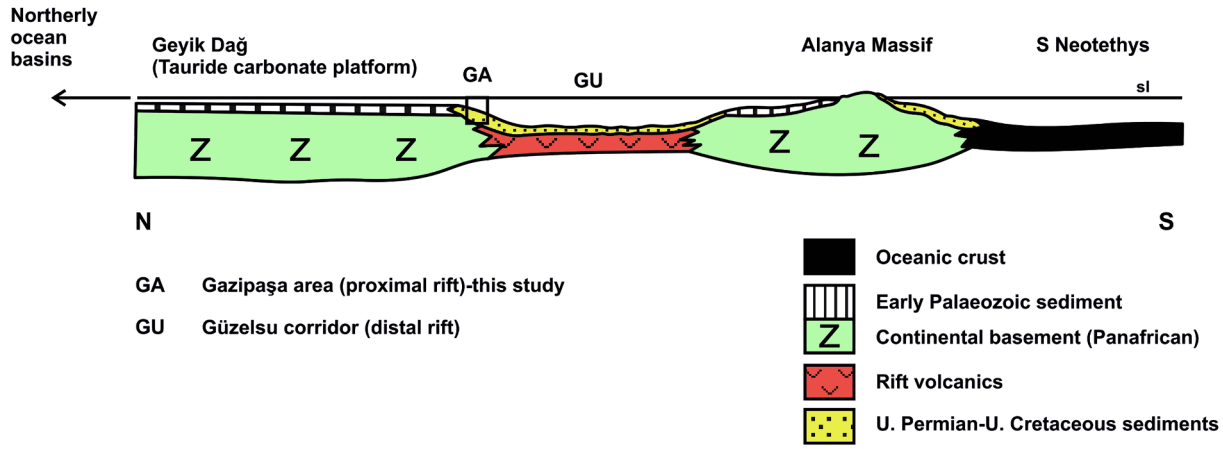

Fig. 19. Reconstruction of the Early Palaeozoic-Late Cretaceous successions in the Alanya Window and adjacent areas. The outcrop is restored as the proximal southerly rifted margin of the Tauride continental unit (Geyik Dağ). The Güzelsu area is represented by a narrow corridor outcrop between the Geyik Dağ (below) and the Alanya Massif (above), which is interpreted as a microcontinent (see Fig. 3).

The low-grade metamorphism (locally up to greenschist) in the Antalya Complex in the Alanya Window (Bozkaya and Yalçın, 2005) and large-scale semi-ductile deformation of the Antalya Complex in the Alanya Window increase in intensity to the SE, in general structurally downwards. The up-to-greenschist-facies metamorphism is likely to be Late Cretaceous, as in the over-riding Alanya metamorphic rocks. Metamorphism of the Antalya Complex during the Late Triassic (Bozkaya and Yalçın, 2005) is unlikely as we have not identified any stratigraphical or structural evidence within the Antalya Complex of high heat flow or basin inversion (reverse faulting/thrusting) during the Late Triassic-Early Jurassic. As a proximal rifted margin, the Antalya Complex in the Antalya Window could have been sandwiched between the northward-subducting Alanya microcontinent to the south and the over-riding Tauride microcontinent (Geyik Dağ) to the north, where it underwent low-grade metamorphism and southward-verging large-scale semi-ductile folding.

During the Eocene, the exhumed Antalya Complex in the Alanya Window was overthrust, northwards by the Alanya metamorphic massif producing the common north-vergent structures along, and close to, the thrust contact between the two units, and evidence of generally northward-verging folding and thrusting locally in the higher structural levels of the Antalya Complex (e.g. around Çiriş Tepe, Area A). The Eocene northward thrusting and folding in the Alanya Window and the Alanya Massif are likely to have been driven by the final-stage suturing of the İzmir-Ankara-Erzincan ocean farther north (i.e. regional back-thrusting). Eocene re-thrusting (of variable vergence) also affected the eastern limb of the Isparta Angle elsewhere (Monod, 1977; Waldron, 1984a; Şenel et al., 1998). The high-angle faulting, including both bedding-oblique extension and bedding-oblique compression could represent late-stage transtension/transpression in different local areas of the Alanya Window. Sedimentary and structural evidence from the Neogene sedimentary cover of the Antalya Complex to the southwest of the Güzelsu outcrop (Manavgat basin) (Flecker et al., 1995, 2005; Karabıyıkoğlu et al., 2000) suggests that Neotectonic faulting to form the Cilicia basin offshore (Aksu et al., 2005) is also likely to have affected the Alanya Window.

11. Implications for rift processes

This study emphasises the importance of rifting during the Permian-Triassic related to the formation of the Southern Neotethys and, in particular, highlights the requirement for an open-ocean connection as early as the Middle Triassic to explain the extensive radiolarian facies. The exposures in the Alanya Window represent an excellent example of pulsed rifting over c. 30 Ma, prior to continental break-up during Late Triassic (Carnian) time, as summarised in Fig. 20a–f. In most other outcrops of the Antalya Complex (e.g. Antalya-Kumluca, SW segment), equivalent rift-facies are absent or not well exposed. It is, therefore, likely that the Alanya Window outcrop represents part of the proximal rifted margin that remains buried beneath the allochthon elsewhere around the Isparta Angle.

Recent support for opening of the Southern Neotethys during the Cretaceous rather than the Permian-Triassic (Segev et al., 2018) mainly applies to the Levant basin, to the south of the Eratosthenes Seamount (Fig. 1). Oceanic crust further north, of at least partially Late Triassic age, was largely subducted, other than for tiny emplaced fragments mainly in western Cyprus, southern Turkey and northern Syria. There is some evidence that regional rifting was followed by spreading during the latest Triassic-earliest Jurassic along the northern margin of the Southern Neotethys (Malpas et al., 1993; Robertson et al., 2012).

The rift development of Antalya Window also suggests that attempts to classify modern and ancient rifts in terms of non-volcanic versus volcanic-related end members may be artificial. The rift history of the Antalya Complex is similar in many ways to that of the Red Sea, where rifting was long-lived and pulsed, with the earlier history suggesting a non-volcanic rifted setting (Bosworth and Stockli, 2016) but the later history, arguably, being akin to a volcanic-rifted margin immediately prior to continental break-up (Stern and Johnson, 2018). The Antalya Complex outcrops provide insights into what the axial Red Sea rift might look like in terms of facies and depositional processes. There is no evidence of the hyper-extension in the rift-related Antalya Complex, specifically the Alanya Window, in contrast to the West Mediterranean (Alpine)-North Atlantic region (e.g. Newfoundland-Iberia transect).

12. Conclusions

- The Antalya Complex in the Alanya Window includes a remarkably intact Late Cambrian-latest Cretaceous succession that documents three main stages of rifting related to continental break-up to form the Southern Neotethys. Rifting was pulsed for c. 30 Ma, prior to final continental break-up during the Late Triassic (Carnian), coeval elsewhere along the northern margin of the South Neotethys (e.g. SE Turkey).
- The first stage of rifting in the Middle-Late Permian represented low-degree crustal extension. This was characterised by modest uplift and erosion, then non-marine to shallow-marine deposition in a gently subsiding basin, with only rare, localised volcanism (outside the study areas);
- The second phase of rifting, of Middle Triassic (early Anisian) age, records more intense rifting to form a deeper-water marine basin,

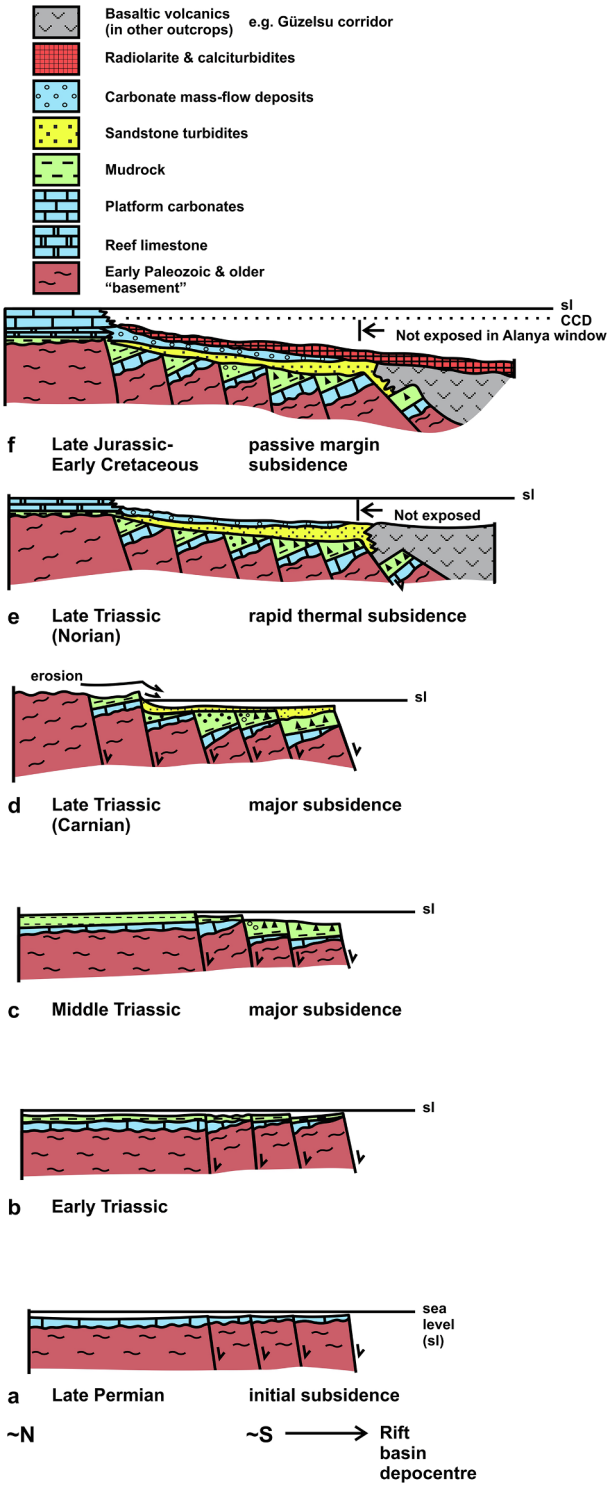

Fig. 20. Pulses of rifting inferred for the Early Palaeozoic-Late Cretaceous of the Alanya Window. **a,** Late Permian initial rifting (pulse 1) (Mid-Triassic in some adjacent areas); **b,** Early Triassic, continued subsidence; **c,** Middle Triassic rifting (pulse 2); **d,** Late Triassic (Carnian) rifting with regional uplift/erosion (pulse 3) and initial continental break-up; **e,** Late Triassic (Norian) continental break-up, subsidence and carbonate platform upgrowth (with collapse of distal margin); **f,** Late Jurassic-Early Cretaceous high-productivity of siliceous sediments (radiolarites) during continuing passive margin subsidence; mass-wasting of carbonate margin. The interpretation takes account of Late Triassic basic volcanic rock that are extensively developed in neighbouring outcrops of the Antalya Complex (e.g. Güzelsu outcrop to the NW and N of the Alanya Window).

dominated by radiolarian deposition (above the CCD), implying regional open-marine connectivity.

- The third phase of rifting during the Late Triassic (Carnian) was much more intense, associated with major regional-scale uplift and erosion, and also strong subsidence to create the accommodation space necessary for the accumulation of hundreds of metres of deep-marine terrigenous turbidites. This time period (mainly Carnian) corresponds to continental break-up to form, at least, some oceanic lithosphere in the Southern Neotethys.
- Detritus from the three rift phase was mainly locally derived from the underlying Cambrian-Permian continental succession, down to and including Cadomian basement.
- Tectonically deformed blocks and tectonic lenses (olistoliths) of pre-rift and early-rift lithologies within the Late Triassic deep-water rift basin in some areas are interpreted as collapsed rift fault blocks.
- Rift-related magmatism in the Antalya Complex in the Alanya Window is mainly restricted to rare intrusion of alkaline diabase-microgabbro sills. In contrast, Late Triassic, late-stage (Carnian) rifting in adjacent areas of the Antalya Complex (e.g. Güzelsu outcrop) was accompanied by voluminous eruptions of subaqueous alkaline basalt.
- Regional tectonic subsidence during the Norian was accompanied by marginal reef collapse (possibly influenced by eustatic sea-level fall).
- Jurassic to Late Cretaceous time was characterised by passive margin subsidence and background accumulation of radiolarian sediments beneath the CCD in distal areas.
- Carbonate drift deposits prograded, possibly from the Tauride carbonate platform to the north during Jurassic-Cretaceous.
- The basin was tectonically deformed during latest Cretaceous and Eocene times, mainly based on the evidence of regional comparisons. Initial large-scale, semi-ductile recumbent, nappe-like folding (c. E-W trending and generally south-verging), was followed by more upright, brittle-style folding on c. N-S axes and then strike-slip-influenced deformation.
- The overall driver of Late Cretaceous tectonic emplacement is interpreted as northward subduction of the Southern Neotethys, during which the Antalya Complex in the Alanya Window was located in the upper (Tauride) plate.

Declaration of Competing Interest

The authors declare that they have no known competing financial interests or personal relationships that could have appeared to influence the work reported in this paper.

Acknowledgements

We thank Ayhan Zenginoğlu for preparing thin sections and Güzide Önal for assistance with drawing the diagrams. The field and laboratory work were partly funded by the John Dixon Memorial Fund. The manuscript benefitted from constructive comments by Dov Avigad and an anonymous reviewer. Cemal Göncüoğlu kindly provided some information on the literature.

Appendix A. Supplementary material

Supplementary data to this article can be found online at https://doi.org/10.1016/j.jaesx.2020.100026.

References

Abbo, A., Avigad, D., Gerdes, A., Güngör, T., 2015. Cadomian basement and Paleozoic to Triassic siliciclastics of the Taurides (Karacahisar dome, south-central Turkey): Paleogeographic constraints from U-Pb–Hf in zircons. Lithos 227, 122–139.
Aksu, A.E., Calon, T.J., Hall, J., Mansfield, S., Yaşar, D., 2005. The Cilicia-Adana basin

complex, Eastern Mediterranean: Neogene evolution of an active fore-arc basin in an obliquely convergent margin. Mar. Geol. 221, 121–159.
Altıner, D. Özkan-Altıner, S. Koçyiğit,A., 2000. Late Permian foraminiferal biofacies belts in Turkey: paleogeographic and tectonic implication. In: Bozkurt, E., Winchester, J. A., Piper, J.D.A. (Eds.), Tectonics and Magmatism in Turkey and the Surrounding Area, Special Publication, Geological Society of London, 173, pp. 83–96.
Avigad, D., Abbo, A., Gerdes, A., 2016. Origin of the Eastern Mediterranean: Neotethys rifting along a cryptic Cadomian suture with Afro-Arabia. Geol. Soc. Am. Bull. 128, 1286–1296.
Bağcı, U., Parlak, O., Höck, V., 2008. Geochemistry and tectonic environment of diverse magma generations forming the crustal units of the Kızıldağ (Hatay) Ophiolite, Southern Turkey. Turk. J. Earth Sci. 17, 43–71.
Barrier, E., Vrielynck, B., Brouillet, J.F., Brunet, M.F., 2018. Paleotectonic Reconstruction of the Central Tethyan Realm. Tectono-Sedimentary-Palinspastic Maps from Late Permian to Pliocene: CCGM/CGMW, Paris. Atlas of 20 maps (scale: 1/15000000).
Betzler, C., Reijmer, J.J.G., Bernet, K., Eberli, G.P., Anselmetti, F., 1999. Sedimentary patterns and geometries of the Bahamian outer carbonate ramp (Miocene and Lower Pliocene, Great Bahama Bank). Sedimentology 46, 1127–1143.
Blumenthal, M., 1951. Récherches géologiques dans les Taurus occidental dans l'arrière pays d'Alanya. Maden Tetkik ve Arama, Report D 5.
Bosellini, A., Castellarin, A., Rossi, P.L., Simboli, G., Sommavilla, E., 1977. Schema sedimentologico e stratigrafico per il Trias medio della Val di Fassa ed aree circostanti (Dolomiti Centrali). Giornale di Geologia 42, 83–108.
Bosellini, A., Neri, C., Luciani, V., 1993. Platform margin collapses and sequence stratigraphic organization of carbonate slopes: Cretaceous-Eocene, Gargano Promontory, Southern Italy. Terra Nova 5, 282–297.
Bosworth, W., Stockli, D.F., 2016. Early magmatism in the greater Red Sea rift: timing and significance. Can. J. Earth Sci. 53, 1158–1176.
Bozkaya, Ö., Yalçın, H., 2004. New mineralogic data and implications for the tectono-metamorphic evolution of the Alanya Nappes, Central Tauride Belt, Turkey. Int. Geol. Rev. 46, 347–365.
Bozkaya, Ö., Yalçın, H., 2005. Diagenesis and very low-grade metamorphism of the Antalya unit: mineralogical evidence of Triassic rifting, Alanya-Gazipaşa, central Taurus belt, Turkey. J. Asian Earth Sci. 25, 109–119.
Buck, W.R., 2007. Dynamic processes in extensional and compressional settings: the dynamics of continental breakup and extension. In: Schubert, G. (Ed.), Treatise on Geophysics, Elsevier 6, pp. 335–376.
Brunn, H., 1974. Le problème de l'origine des nappes et leurs translations dans les Taurides occidentales. Bulletin de la Société Géologique de France 7, 101–106.
Brunn, J.H., de Graciansky, P.C., Gutnic, M., Juteau, T., Lefèvre, R., Marcoux, J., Monod, O., Poisson, A., 1970. Structures majeures et corrélations stratigraphiques dans les Taurides occidentales. Bulletin de la Société Géologique de France 12, 515–556.
Brunn, J.H., Dumont, J.H., de Graciansky, P.Ch., Gutnic, M., Juteau, Th., Marcoux, J., Monod, O., Poisson, A., 1971. Outline of the geology of the western Taurids. In: Geology and History of Turkey. Petroleum Exploration Society of Libya, Tripoli, pp. 225–255.
Çetinkaplan, M., 2018. Anamur (Alanya Masifi, Mersin) Bölgesinde yer alan Prekambriyen yaşlı kayaçların çok evreli P-T-t evrimi (Multi-Stage P-T-t evolution of Precambrian-aged rocks in Anamur (Alanya Massif, Mersin) Region). Geol. Bull. Turkey 61, 91–130 (in Turkish with English extended abstract).
Çetinkaplan, M., Pourteau, A., Candan, O., Koralay, O.E., Oberhänsli, R., Okay, A.İ., Chen, F., Kozlu, H., Şengün, F., 2014.P–T–t evolution of eclogite/blueschist facies metamorphism in Alanya Massif: time and space relations with HP event in Bitlis Massif, Turkey. Int. J. Earth Sci. 105, 1–35.
Çetinkaplan, M., Pourteau, A., Candan, O., Koralay, O.E., Oberhänsli, Okay, O.I., 2016b. P-T-t Evolution of eclogite/blueschist facies metamorphism in Alanya Massif: Time and space relations with HP Event in Bitlis Massif, Turkey. Int. J. Earth Sci. 105, 247–281.
Çetinkaplan, M., Candan, O., Koralay, O.E., Okay, A.İ., Oberhänsli, R., Chen, F., 2010. Alanya Masifin Petrolojisi, Jeokronolojisi ve Tektono-Metamorfik Evrimi (Petrology, geochronology and tectonic-metamorphic evolution of the Alanya Massif): Tübitak Projesi raporu, Project No: 107Y107, 226 pp. (unpublished).
Chen, G., Robertson, A.H.F., 2020. Interpretation of sandstones using major and trace element chemical data, exemplified by Triassic-Miocene sandstones from Cyprus. Sedimentary Geology, https://doi.org/10.1016/j.sedgeo.2020.105616.
Cochran, J.R., 2005. Northern Red Sea: nucleation of an oceanic spreading center within a continental rift. Geochem. Geophys. Geosyst. 6 doi.org/10.1029/2004GC000826.
Cooper, D.J.W., Toland, C., Ali, M.Y., Green, O., 2016. Evolution of the Arabian continental margin of the northern Dibba Zone, eastern United Arab Emirates and Oman. J. Asian Earth Sci. 129, 254–275.
Dean, W.T., Uyeno, T., Rickards, R.B., 1999. Ordovician and Silurian stratigraphy and trilobites, Taurus Mountains near Kemer, southwestern Turkey. Geol. Mag. 136, 373–393.
Delaune-Mayère, D., Marcoux, J., Parrot, J.-F., Poisson, A., 1977. Modèle d'évolution mésozoïque de la paléo-marge téthysienne au niveau des nappes radiolaritiques et ophiolitiques du Taurus Lycien d'Antalya et du Baër-Bassit. In: Biju-Duval, L. Montadert, L. (Eds.), Structural History of the Mediterranean Basins: Editions Technip, Paris, pp.79–94.
Demirtaşlı, E., 1983. Stratigraphy and tectonics of the area between Silifke and Anamur, Central Taurus Mountains, In: Tekeli O.,Göncüoğlu, M.C.(Eds.), International Symposium on the Geology of the Taurus Belt, Ankara-Turkey: Mineral Research and Exploration Institute (MTA), pp. 101–118p.
Demirtaşlı, E., 1987. Batı Toroslar'da Akseki-Manavgat ve Köprülü arasında kalan bölgenin jeoloji incelemesi (Geology of western Taurus in the region between Akseki-Manavgat and Köprülü): Mineral Research and Exploration Institute of Turkey (MTA) Report 8779 (unpublished).
De Wever, P., Azema, J., Fourcade, E., 1994. Radiolaires et radiolarites, production primaire, diagenèse et paléogéographie. Bull. Centre Recherches et Exploration-Production, Elf-Aquitaine 18, 1–63.
Dumont, J.-F., Gutnic, M., Marcoux, J., Monod, O., Poisson, A., 1972. Le Trias des Taurides occidentales (Turquie). Définition du bassin pamphylien: un nouveau domaine à ophiolites à la marge externe de la chaîne taurique. Zeitschrift der Deutschen Geologischen Gesellschaft 123, 385–409.
Eberli, G.P., Bernoulli, D., Vecsei, A., Sekti, R., Grasmueck, M., Lüdmann, T., Anselmetti, F.S., Mutti, M., Della Porta, G., 2019. A Cretaceous carbonate delta drift in the Montagna della Maiella, Italy. Sedimentology 66, 1266–1301.
Erwin, D.H., Bowring, S.A., Jin, Y., 2002. End-Permian mass extinctions: a review. In: Koeberl, C., MacLeod, K.G. (Eds.), Catastrophic Events and Mass Extinctions: Impacts and Beyond. Geological Society of America, Special Paper 356, 63–83.
Flecker, R., Poisson, A., Robertson, A.H.F., 2005. Facies and palaeogeographic evidence for the Miocene evolution of the Isparta Angle in its regional eastern Mediterranean context. Sed. Geol. 173, 277–314.
Flecker, R., Robertson, A.H.F., Poisson, A., Muller, C., 1995. Facies and tectonic significance of two contrasting Miocene basins in south coastal Turkey. Terra Nova 7, 221–232.
Franke, D., 2103. Rifting, lithosphere breakup and volcanism: comparison of magma-poor and volcanic rifted margins. Mar. Petrol. Geol. 43, 63–68.
Gardosh, M.A., Druckman, Y., 2006. Seismic stratigraphy, structure and tectonic evolution of the Levantine Basin, offshore Israel. In: Robertson, A.H.F., Mountrakis, D. (Eds.), Tectonic Development of the Eastern Mediterranean Region, Special Publication, Geological Society of London 260, pp. 201–227.
Gardosh, M.A., Garfunkel, Z., Druckman, Y., Buchbinder, B., 2010. Tethyan rifting in the Levant Region and its role in Early Mesozoic crustal evolution. In: Homberg, C., Bachmann, M. (Eds.), Evolution of the Levant Margin and Western Arabia Platform since the Mesozoic. Special Publication, Geological Society of London 341, pp. 9–36.
Garfunkel, Z., 1998. Constraints on the origin and history of the Eastern Mediterranean basin. Tectonophysics 298, 5–37.
Garfunkel, Z., 2004. Origin of the Eastern Mediterranean basin: a re-evaluation. Tectonophysics 39, 11–34.
Ghienne, J.F.T., Monod, O., Kozlu, O., Dean, H., 2010. Cambrian-Ordovician depositional sequences in the Middle East: a perspective from Turkey. Earth Sci. Rev. 101, 101–146.
Göncüoğlu, M.C., 2011. Geology of the Kütahya-Bolkardağ Belt. Miner. Res. Explor. Bull. 142, 223–277.
Göncüoğlu, M.C., Çapkınoğlu, Ş., Gürsu, S., Noble, P., Turhan, N., Tekin, U.K., Okuyucu, C., Göncüoğlu, Y., 2007. The Mississippian in the Central and Eastern Taurides (Turkey): constraints on the tectonic setting of the Tauride-Anatolide Platform. Geol. Carpath. 58, 427–442.
Göncüoğlu, M.C., Göncüoğlu, Y., Kozur, H.W., Kozlu, H., 2004. Paleozoic stratigraphy of the Geyik Dağı Unit in the Eastern Taurides (Turkey). New age data and implications for Gondwanan evolution: Geologica Carpathica 55, 433–447.
Göncüoğlu, M.C., Kozlu, H., 2000. Early Paleozoic evolution of the NW Gondwanaland: data from southern Turkey and surrounding regions. Gondwana Res. 3, 315–323.
Göncüoğlu, Y., Kozur, H.W., 2000a. Early Devonian transgression in the eastern Antalya Nappes: conodont data from the Tahtalıdağ Nappe, N of Alanya, southern Turkey. Records of Western Australian Museum, Supplement 58, 279–292.
Göncüoğlu, Y., Kozur, H.W., 2000b. Upper Cambrian and Lower Ordovicianconodonts from the Antalya Unit in the Alanya Tectonic Window, southern Turkey. Neus Jarbuch fur Geologie und Palaontologie-Monatshefe 1999, 593–604.
Göncüoğlu, Y., Kozur, H., 2000c. Early Silurian sea-level changes in southern Turkey: lower Telychian conodont data from the Kemer area, Western Taurides. Rec. Western Austral. Museum, Supplement 58, 293–303.
Groves, J.R., Altıner, D., 2005. Survival and recovery of calcareous foraminifera pursuant to the end-Permian mass extinction.Comptes. Rendus Palevo l4, 419–432.
Gutnic, M.F., Monod, O., Poisson, A., Dumont, J., 1979. Geologie des Taurides Occidentales (Turquie). Société Géologique de France, Mémoire 137, 1–112.
Haq, B.U., Hardenbol, J., Vail, P.R., 1988. Mesozoic and Cenozoic chronostratigraphy and cycles of sea-level change, In: Wilgus, C.K., Hastings, B.S., Kendall, C.G. St. C., Posamentier, H., Van Wagoner J., Ross, C.A. (Eds.), Sea-level changes: an integrated approach, Special Publication, Society of Economic Paleontologists and Mineralogists 42, pp.71–108.
Hayward, A., Robertson, A.H.F., 1982. Direction ofophiolite emplacement inferred from Cretaceous and Tertiary sediments of an adjacent autochthon, the Bey Dağları, S.W. Turkey. Bull. Geol. Soc. Am. 93, 68–75.
Huismans, R.S., Podladchikov, Y.Y., Cloetingh, S., 2001. Dynamic modeling of the transition from passive to active rifting, application to the Pannonian basin. Tectonics 20, 1021–1039.
Jenkyns, H.C., Winterer, E.L., 1982. Palaeoceanography of Mesozoic ribbon radiolarites. Earth Planet. Sci. Lett. 60, 351–376.
Joachimski, M.M., Lai, X.L., Shen, S.Z., Jiang, H.S., Luo, B., Chen, J., Chen, Y.D., Sun, Y.D., 2012. Climate warming in the latest Permian and the Permian-Triassic mass extinction. Geology 40, 195–198.
Johns, D.R., 1978. Mesozoic carbonate rudites, megabreccias and associated deposits from central Greece. Sedimentology 25, 561–573.
Large, R.R., Halpin, J.A., Lounejeva, E., Danyushevsy, L.V., Maslennikov, V., Gregory, D., Sack, P.J., Haines, P.W., Long, J.A., Makoundi, C., Stepanov, S., 2015. Cycles of nutrient trace elements in the Phanerozoic ocean. Gondwana Res. 28, 1282–1293.
Lefèvre, R., 1967. Un nouveau élément de la géologie du Taurus Lycien: les nappes d'Antalya (Turquie). Comptes Rendus de l'Académie des Sciences de Paris 165, 1365–1368.
Mackintosh, P.W., Robertson, A.H.F., 2012. Late Devonian-Late Triassic sedimentary development of the central Taurides, S Turkey: implications for the northern margin

of Gondwana. Gondwana Res. 21, 1089–1114.
Malpas, J., Calon, T., Squires, G., 1993. The development of a Late Cretaceous microplate suture zone in SW Cyprus. In: Prichard, H.M., Alabaster, T., Harris, N.B.W., Neary, C. R. (Eds.), Magmatic Processes and Plate Tectonics, London, Special Publication, Geological Society of London 76, pp. 177–195.
Marcoux, J., 1970. Age Carnien des termes effusifs du cortège ophiolitique des nappes d'Antalya (Taurus Lycien oriental, Turquie). Comptes Rendus Académie des Sciences de Paris 278, 285–287.
Marcoux, J., 1979. Antalya Naplarının genel yapısı ve Tetis güney paleocoğrafyasındaki yeri (General features of Antalya Nappes and their significance in the paleogeography of southern margin of Tethys). Geol. Soc. Turkey Bull. 14, 85–101.
Marcoux, J., 1995. Initiation of the south-Neotethys margin in the Antalya nappes (SW Turkey): Late Permian and Early Mid-Triassic rifting events, late Mid-Triassic oceanization. Eur. Union Geosci. Abstracts 7, 175.
Marcoux, J., Ricou, L.E., Burg, J.P., Brunn, J., 1989. Shear sense criteria in the Antalya and Alanya thrust system (southwestern Turkey): evidence for a southward emplacement. Tectonophysics 161, 81–91.
Maury, R.C., Lapierre, H., Maury, R.C., Lapierre, H., Bosch, D., Marcoux, J., Krystyn, L., Cotten, J., Bussy, F., Brunet, P., Sénebier, F., 2008. The alkaline intraplate volcanism of the Antalya nappes (Turkey): a Late Triassic remnant of the Neotethys. Bull. Société Géologique de France 179, 397–410.
Mohn, G., Manatschal, G., Müntener, O., Beltrando, M., Masini, E., 2010. Unravelling the interaction between tectonic and sedimentary processes during lithospheric thinning in the Alpine Tethys margins. Int. J. Earth Sci. 99, 75–101.
Moix, P., Gorican, S., Marcoux, J., 2009. First evidence of Campanian radiolarians in Turkey and implications for the tectonic setting of the Upper Antalya Nappes. Cretac. Res. 30, 952–960.
Monod, O., 1976. La "courbure d'Isparta"; une mosaïque de blocs autochtones surmontés de nappes composites à la jonction de l'arc hellénique et de l'arc taurique. Bulletin de la Société Géologique de France 18, 521–531.
Monod, O., 1977. Récherches Géologique dans les Taurus occidental au sud de Beyşehir (Turquie). Thèse de Doctorat de Science, Université de Paris-Sud, Orsay, France.
Monod, O., 1979. Carte Géologique du Taurus Occidental au sud de Beyşehir et Notice Explicative. Paris: CNRS Publications.
MTA, 2000. Geological Map of Turkey, 1:500,000, MadenTektik ve Arama Genel Müdürlüğü (General Directorate of Mineral Research and Exploration), Ankara.
Okay, A.İ., 1989. An exotic eclogite/blueschist slice in a Barrovian-style metamorphic terrain, Alanya Nappes, Southern Turkey. J. Petrol. 30, 107–132.
Okay, A.İ., Özgül, N., 1984. HP/LT metamorphism and structure of the Alanya Massif, Southern Turkey: an allochthonous composite tectonic sheet. In: Dixon, J.E, Robertson, A.H.F. (Eds.), The Geological Evolution of the Eastern Mediterranean, Special Publication, Geological Society of London 14, pp. 429–439p.
Özer, S., Kahrıman, H.H., 2019. Cenomanian canaliculate rudists (Bivalvia) from the Geyik DaÄŸÄ±-Hadim area (Central Taurides, S Turkey): systematic paleontology, stratigraphic importance and depositional environment. Cretaceous Research 103, 1–23.
Özgül, N., 1984. Stratigraphy and tectonic evolution of the Central Taurides. In: Tekeli, O., Göncüoğlu, M.C. (Eds.), International Symposium on the Geology of the Taurus Belt. Ankara, Turkey, pp. 77–90.
Özgül, N., 1984b. Alanya Tektonik Penceresi ve Bati Kesiminin Jeolojisi (Alanya tectonic window and geology of its western part). Geological Society of Turkey, Ketin Symposium, 1984, Ankara, pp. 97–120.
Parlak, O., Robertson, A.H.F., 2004. The ophiolite-related Mersin Melange, southern Turkey: its role in the tectono-sedimentary setting of Tethys in the Eastern Mediterranean region. Geol. Mag. 141, 257–286.
Parlak, O., Rızaoğlu, T., Bağcı, U., Karaoğlan, F., Höck, V., 2009. Tectonic significance of the geochemistry and petrology of ophiolites in southeast Anatolia, Turkey. Tectonophysics 473, 173–187.
Pearce, J.A., 1982. Trace element characteristics of lavas from destructive plate boundaries. In: Thorpe, R.S. (Ed.), Andesites. Wiley, New York, pp. 525–548.
Péron-Pinvidic, G., Manatschal, G., 2008. The final rifting evolution at deep magma-poor passive margins from Iberia-Newfoundland: a new point of view. Int. J. Earth Sci. 98, 1581–1597.
Poisson, A., 1977. Récherches Géologiques dans les Taurides Occidentales, Turquie. PhD thesis, University of Paris-Sud, Orsay, France.
Poisson, P., Yağmurlu, F., Bozcu, M., Şentürk, M., 2003. New insights on the tectonic setting and evolution around the apex of the Isparta Angle (SW Turkey). Geol. J. 38, 257–282.
Reston, T., Manatschal, G., 2011. Rifted margins: building blocks of later collision. In: Brown, D., Ryan, P.D. (Eds.), Arc-continent Collision. Springer, Berlin, pp. 3–22.
Ricou, L.E., Marcoux, J., Whitechurch, H., 1984. The Mesozoic organization of the Taurides: one or several ocean basins? In: Dixon, J.E., Robertson, A.H.F. (Eds.), The Geological Evolution of the Eastern Mediterranean, Special Publication, Geological Society of London 17, pp. 349–359.
Robertson, A.H.F., 1993. Mesozoic–Tertiary sedimentary and tectonic evolution of Neotethyan carbonate platforms, margins and small ocean basins in the Antalya Complex, S.W. Turkey. In: Frostick, L. E., Steel, R. (Eds.), Tectonic Controls and Signatures in Sedimentary Successions. Special Publications, International Association of Sedimentologists 20, pp. 415–465.
Robertson, A.H.F., 2000. Mesozoic–Tertiary tectonosedimentary evolution of a south-Tethyan oceanic basin and its margins in southern Turkey. In: Bozkurt, E., Winchester, J.A., Piper, J.D.A. (Eds.), Tectonics and Magmatism in Turkey and Surrounding Area, Special Publication, Geological Society of London 173, pp. 97–138.
Robertson, A.H.F., 2002. Overview of the genesis and emplacement of Mesozoic ophiolites in the eastern Mediterranean Tethyan region. Lithos 65, 1–67.
Robertson, A.H.F., 2007. Overview of tectonic settings related to the rifting and opening of Mesozoic ocean basins in the Eastern Tethys: Oman, Himalayas and Eastern Mediterranean regions. In: Karner, G., Manatschal, G., Pinheiro, L. M., (Eds.), Imaging, Mapping and Modelling Continental Lithosphere Extension and Breakup, Special Publication, Geological Society of London 282, pp. 325–389p.
Robertson, A.H.F., Clift, P.D., Degnan, P.J., Jones, G., 1991. Paleogeographic and paleotectonic evolution of the eastern Mediterranean Neotethys: palaeogeography. Palaeoclimatol. Palaeoecol. 87, 289–343.
Robertson, A.H.F., Degnan, P.J., 1993. Sedimentology and tectonic implications of the Lamayuru Complex: Deep-water facies of the Indian passive margin, Indus suture zone, Ladakh Himalaya, In: Treloar, P. J., Searle, M. P. (Eds.), Himalayan Tectonics, Special Publication, Geological Society of London 74 pp. 299–321.
Robertson, A.H.F., Parlak, O., Kinnaird, T., Taslı, K., Dumitrica, P., 2019. Rifting/passive margin development of the southern Neotethys: evidence from the Antalya Complex in the Alanya Window (Gazipaşa-Anamur area). 7. International Earth Science Colloquium on the Aegean region. IESCA 2019. Abstract Book, Program and Notebook. 7-11 October 2019, p. 5.
Robertson, A.H.F., Parlak, O., Ustaömer, T., 2009. Melange genesis and ophiolite emplacement related to subduction of the northern margin of the Tauride–Anatolide continent, central and western Turkey. In: van Hinsbergen, D.J.J., Edwards, M.A., Govers, R.J., (Eds.), Collision and Collapse at the Africa–Arabia–Eurasia Subduction Zone. Special Publication, Geological Society of London 311, pp. 9–66.
Robertson, A.H.F., Parlak, O., Ustaömer, T., 2012. Overview of the Palaeozoic-Neogene evolution of Neotethys in the Eastern Mediterranean region (southern Turkey, Cyprus, Syria). Pet. Geosci. 18, 381–404.
Robertson, A.H.F., Parlak, O., Ustaömer, T., 2013. Late Paleozoic-Early Cenozoic tectonic development of southern Turkey and the easternmost Mediterranean region: evidence from the inter-relations of continental and oceanic units. Spec. Publ. Geol. Soc. Lond. 372, 9–48.
Robertson, A.H.F., Parlak, O., Yıldırım, N., Dumitrica, P., Taslı, K., 2016. Late Triassic rifting and Jurassic-Cretaceous passive margin development of the Southern Neotethys: evidence from the Adıyaman area, SE Turkey. Int. J. Earth Sci. 105, 167–201.
Robertson, A.H.F., Poisson, A., Akıncı, Ö., 2003. Developments in research concerning Mesozoic–TertiaryTethys and neotectonics in the Isparta Angle, SW Turkey. Geol. J. 38, 195–234.
Robertson, A.H.F., Ustaömer, T., 2009. Formation of the upper Palaeozoic Konya Complex and comparable units in southern Turkey subduction–accretion processes: Implications for the tectonic development of Tethys in the Eastern Mediterranean region. Tectonophysics 473, 113–148.
Robertson, A.H.F., Waldron, J.W.F., 1990. Geochemistry and tectonic setting of Late Triassic and Late Jurassic–Early Cretaceous basaltic extrusives from the Antalya Complex, S. W. Turkey, In: Savaşçın, M.Y., Eronat, A. H. (Eds.), Proceedings International Earth Sciences Congress on Aegean Regions, Izmir, Turkey 2, pp. 279–299.
Robertson, A.H.F., Woodcock, N.H., 1981a. Alakır Çay Group, Antalya Complex S. W. Turkey: A deformed Mesozoic carbonate margin. Sedimentary Geology 30, 95–131.
Robertson, A.H.F., Woodcock, N.H., 1981b. Bileleyeri Group, Antalya Complex: deposition on a Mesozoic continental margin in S W. Turkey. Sedimentology 28, 381–401.
Robertson, A.H.F., Woodcock, N.H., 1981c. Gödene Zone, Antalya Complex, S.W. Turkey: volcanism and sedimentation on Mesozoic marginal ocean crust. Geologisches Rundschau 70, 1177–1214.
Robertson, A.H.F., Woodcock, N.H., 1982. Sedimentary history of the south-western segment of the Mesozoic-Tertiary Antalya continental margin, southwestern Turkey. Eclogae Geol. Helv. 75, 517–562.
Robertson, A.H.F., Woodcock, N.H., 1984.The SW segment of the Antalya Complex, Turkey as a Mesozoic–Tertiary Tethyan continental margin. In: Dixon J,E., Robertson, A.H.F (Eds.), The Geological Evolution of the Eastern Mediterranean, Special Publication, Geological Society of London 17, pp. 251–271.
Rygel, M.C., Fielding, C.R., Frank, T.D., Birgenheier, L.P., 2008. The magnitude of Late Paleozoic glacioeustatic fluctuations: a synthesis. J. Sediment. Res. 78, 500–511.
Şahin, N., Altıner, D., 2019. Testing of Permian-Lower Triassic stratigraphic data in a half-graben/tilt block system: evidence for the initial rifting phase in Antalya Nappes. Can. J. Earth Sci. 56, 1262–1283.
Şahin, N., Altıner, D., Ercengiz, M.B., 2014. Discovery of Middle Permian volcanism in the Antalya Nappes, southern Turkey: tectonic significance and global meaning. Geodin. Acta 25, 286–304.
Sarı, B., 2009. Planktonic foraminiferal biostratigraphy of the Coniacian-Maastrichtian sequences of the Bey Dağları Autochthon, Western Taurides, Turkey: thin section zonation. Cretac. Res. 30, 1103–1132.
Sarı, B., Özer, S., 2002. Upper Cretaceous stratigraphy of the Bey Dağları carbonate platform, Korkuteli area (Western Taurides, Turkey). Turk. J. Earth Sci. 11, 39–59.
Segev, A., Sass, E., Schattner, U., 2018. Age and structure of the Levant basin, Eastern Mediterranean. Earth Sci. Rev. 182, 233–250.
Şenel, M., 1980. Teke Torosları Güneydoğusunun Jeolojisi. Finike-Kumluca-Antalya. General Directorate of Mineral Research and Exploration (MTA) Report, 1980.
Şenel, M., Dalkılıç, H., Gedik, İ., Serdaroğlu, M., Bölükbaşı, A.S., Metin, S., Özgül, N., 1992. Eğirdir-Yenişarbademli-Gebiz ve Geriş-Köprülü (Isparta-Antalya) arasında kalan alanların jeolojisi (Geology of the region between Eğirdir-Yenişarbademli-Gebiz and Geriş-Köprülü (Isparta-Antalya)). Mineral Research and Exploration Institute of Turkey (MTA) Report, 9390 (unpublished).
Şenel, M., Dalkılıç, H., Gedik, İ., Serdaroğlu, M., Metin, S., Esentürk, K., Özgül, N., 1999. Orta Toroslar'da Güzelsu Koridoru ve kuzeyinin Jeolojisi (Geology of the Güzelsu Corridor and to the north in the Central Taurus). Bulletin of Geological Society of Turkey 2, 30–40.
Şenel, M., Dalkılıç, H., Gedik, İ., Serdaroğlu, M., Metin, S., Esentürk, K., Özgül, N., 1999.

Orta Toroslar'da Güzelsu Koridoru ve kuzeyinin Jeolojisi (Geology of the Güzelsu Corridor and to the north in the Central Taurus). Bull. Geol. Soc. Turkey 2, 30–40.
Şenel, M., Gedik, İ., Dalkılıç, H., Serdaroğlu, M., Bilgin, A.Z., Oğuz, M.F., Bölükbaşı, A.S., Koruçu, M., Özgül, N., 1996. Isparta büklümü doğusunda otokton ve allokton birimlerin stratigrafisi (Bat Toroslar) (Geology of autochthonous and allochthonous units (Western Taurides) at the east of Isparta Angle): General Directorate of Mineral Research and Exploration (MTA) Bulletin 118, 111–160.
Şenel, M., Göncüoğlu, Y., Kozur, H., 2000. Conodont dated Cambrian rocks from the Tahtalıdag Nappe (Antalya Nappes) of the Kemer Area, Western Taurides (Turkey). In: Proceeding 2nd Croatian Geological Congress, Cavtat-Dubrovnik, 17-20.5.2000, pp. 371–377.
Şenel, M., Bedi, Y., Usta, M. 2016. 1:100,000 ölçekli Türkiye jeoloji haritaları serisi (1:100,000-scale Geological Map of Turkey) Alanya-P 28 Paftası, No. 223. MadenTektik ve Arama Genel Müdürlüğü , Ankara (General Directorate of Mineral Research and Exploration , Ankara) (in Turkish with an English Abstract).
Şengör, A.M.C., Burke, K., 1978. Relative timing of rifting and volcanism on earth and its tectonic implications. Geophys. Res. Lett. 5, 419–421.
Şengör, A.M.C., Yılmaz, Y., 1981. Tethyan evolution of Turkey: a plate tectonic approach. Tectonophysics 75, 181–241.
Solak, C., Taslı, K., Özer, S., Koç, H., 2017. Biostratigraphy and facies analysis of the Upper Cretaceous-Danian? platform carbonate succession in the Kuyucak area, western Central Taurides, S Turkey. Cretac. Res. 79, 43–63.
Solak, C., Taslı, K., Özer, S., Koç, H., 2019. The Madenli (Central Taurides) Upper Cretaceous platform carbonate succession: benthic foraminiferal biostratigraphy and platform evolution. Geobios 52, 67–93.
Stampli, G.M., Borel, G.D., 2002. A plate tectonic model for the Paleozoic and Mesozoic constrained by dynamic plate boundaries and restored synthetic oceanic isochrons. Earth Planet. Sci. Lett. 196, 17–33.
Stern, R.J., Johnson, P., 2018. Constraining the opening of the Red Sea: evidence from the Neoproterozoic margins and Cenozoic magmatism for a Volcanic Rifted Margin. In: Rasul, N.M.A., Stewart, I.C.F. (Eds.), The Red Sea. Springer Earth System Sciences, Berlin, pp. 53–80.
Stockli, D.F., Bosworth, W., 2019. Timing of extensional faulting along the magma-poor central and northern Red Sea rift margin-transition from regional extension to necking along a hyperextended rifted margin. In: Rasul, N.M.A., Stewart, I.C.F., (Eds.), Geological Setting Palaeoenvironment and Archaeology of the Red Sea. Earth System Science Series, Springer Nature Switzerland AG, pp. 81–111.
Tekin, U.K., 1999. Biostratigraphy and systematics of late Middle to Late Triassic radiolarians from the Taurus Mountains and Ankara region, Turkey. Geologische-Paläontologische Mitteilungen Innsbruck. Sonderband 5, 1–296.
Tekin, U.K., 2002a. Late Triassic (Late Norian–Rhaetian) radiolarians from the Antalya Nappes, Central Taurides, Southern Turkey. Revista Italiana de Palaeotologia e Stratigrafia 108, 415–440.
Tekin, U.K., 2002b. Lower Jurassic (Hettangian–Sinemurian) radiolarians from the Antalya Nappes, Central Taurids, Southern Turkey. Micropaleontology 8, 177–205.
Tekin, U.K., Sönmez, I., 2010. Late Ladinian radiolarians from the Tahtalidag Nappe of the Antalya nappes, SW Turkey: Remarks on the late Middle and Late Triassic evolution of the Tahtalidag Nappe. Acta Geol. Pol. 60, 199–217.
Ulu, Ü., 1983. Sugözü-Gazipaşa (Antalya) alanının jeoloji incelemesi (Investigation of geological features around Sugözü-Gazipaşa (Antalya) region). Jeoloji Mühendisliği 9, 3–8 (in Turkish with English abstract).
Ulu, Ü., 1988.Gazipaşa (Antalya) bölgesinin jeolojisi (Geology of Gazipaşa region). PhD thesis, İstanbul University, 209pp. (in Turkish).
Ünal, E., Altıner, D., Yılmaz, I.Ö., Özkan-Altıner, S., 2003. Cyclic sedimentation across the Permian-Triassic boundary (Central Taurides Turkey). Riv. Ital. Paleontol. Stratigr. 109, 359–376.
Ustaömer, T., Ustaömer, P.A., Robertson, A.H.F., Gerdes, A., 2019. U-Pb-Hf isotopic data from detrital zircons in late Carboniferous and Mid-Late Triassic sandstones, and also Carboniferous granites from the Tauride and Anatolide continental units in S Turkey: implications for Tethyan palaeogeography. Int. Geol. Rev. https://doi.org/10.1080/00206814.2019.1636415.
Uzunçimen, S., Tekin, U.K., Bedi, Y., Perinçek, D., Varol, E., Soycan, H., 2011. Discovery of the Late Triassic (Middle Carnian–Rhaetian) radiolarians in the volcano-sedimentary sequences of the Koçali Complex, SE Turkey: correlation with the other Tauride units. J. Asian Earth Sci. 40, 180–200.
Varol, E., Tekin, U.K., Temel, A., 2007. Age and geochemistry of middle to late Carnian basalts from the Alakır Çay Nappe (Antalya Nappes, SW Turkey): implications for the evolution of the southern branch of Neotethys. Ofioliti 32, 163–176.
Vrielynck, B., Bonneau, M., Danelian, T., Cadet, J.-P., Poisson, A., 2003. New insights on the Antalya Nappes in the apex of the Isparta Angle: the Isparta Çay unit revisited. Geol. J. 38, 191–394.
Waldron, J.W.F., 1984a. Structural history of the Antalya Complex in the 'Isparta Angle', Southwest Turkey. In: Dixon, J.E., Robertson, A.H.F. (Eds.), Geological Evolution of the Eastern Mediterranean, Special Publication, Geological Society of London 17, pp. 273–286.
Waldron, J.W.F., 1984b. Evolution of carbonate platforms on a margin of the Neotethys ocean: Isparta Angle, south-western Turkey. Eclogae Geol. Helv. 77, 53–581.
Watts, K.F., Garrison, R.E., 1986. Sumeini Group, Oman-evolution of a Mesozoic carbonate slope on a South Tethyan continental margin. Sed. Geol. 48, 107–108.
Woodcock, N.H., Robertson, A.H.F., 1977. Imbricate thrust belt tectonics and sedimentation as a guide to the emplacement of part of the Antalya Complex, SW Turkey, in: İzdar, E., and Nakoman, E. (Eds.), 6th Colloquium on the Geology of Aegean Region, İzmir: Piri Reis International Contribution Series 2, 661–670.
Woodcock, N.H., Robertson, A.H.F., 1982.Wrench and thrust tectonics along a Mesozoic-Cenozoic continental margin; Antalya Complex, SW Turkey. Journal of the Geological Society of London 139, 147–163.
Yılmaz, P.O., 1984. Fossil and K–Ar data for the age of the Antalya Complex, S W Turkey, In: Dixon, J. E., and Roberson, A. H. F. (Eds.), The Geological Evolution of the Eastern Mediterranean Special Publication,Geological Society of London 17, pp. 335–348.
Yılmaz, P.O., Maxwell, J.C., 1984. An example of an obduction melange: the Alakır Cay unit, Antalya Complex, Southwest Turkey.Geological Society of America Special Paper 198, 139–152.
Zlatkin, O., Avigad, D., Gerdes, A., 2013. Evolution and provenance of Neoproterozoic basement and lower Paleozoic siliciclastic cover of the Menderes Massif (westernTaurides): Coupled U-Pb–Hf zircon isotope geochemistry. Gondwana Res. 23, 682–700.